REQ. NO. 1-9039

FINAL REPORT FOR EMR CONTRACT

OSU81-00232

on

Development of a Technique for Contact Angle Measurements on Irregularly Shaped Solid Particles

Phase III

Principal Investigator: Dr. A.W. Neumann

April 1982

JUL 28 1984
MICROMEDIA

University of Toronto
Department of Mechanical Engineering
5 King's College Road
Toronto, Ontario
M5S 1A4

123 pp

TABLE OF CONTENTS

	Page
INTRODUCTION	1
MATERIALS AND METHODS	3
A. MATERIALS	3
1. Solid Particles	3
1.1 Coal Samples	3
1.2 Gangue Materials, Clays	3
2. Matrix Materials	4
3. Surfactants	4
4. Oil Samples	5
B. METHODS	5
1. Freezing Front Experiments	5
2. Pretreatment of the Coal Samples	6
3. Surface tension, γ_{LV}, of Oils	6
4. Specific Heat, C_p, of the Powders	7
5. Neutron Activation Analysis (NAA)	7
EXPERIMENTAL RESULTS AND DISCUSSION	9
1. Freezing Front Experiments in Organic Matrix Materials	9
1.1 Surface Tension of Coal Particles	9
a) Effect of aging and drying	9
b) Coal G-1 sample	10
1.2 Surface Tension of Gangue Material and Clays	10
1.3 Carbon Lampblack	12
2. Freezing Front Experiments in Water/Ice with Coals	13

TABLE OF CONTENTS (cont'd)

	Page
3. Pretreatment of Coal	14
4. Liquid/Vapour, γ_{LV}, Surface Tension of Oils	15
5. Specific Heat of Coals and Clays	16
5.1 Coal No. 1, 2, 3 (see Appendix 2)	16
5.2 G-1 and Clays	16
6. Neutron Activation Analysis (NAA) of Trace Elements	17
CONCLUSIONS	19
TABLES 1-21	20-40
FIGURES 1-23	41-63
APPENDIX No. 1	
APPENDIX No. 2	
APPENDIX No. 3	

INTRODUCTION

This work is the continuation of the EMR Contract DSS 20SU-23440-0-9021. The purpose of this investigation was to develop a novel method, called freezing front technique, for the characterization of the surface properties of coal powders and to attempt to extend the application of this technique for the measurement of surface parameters of some gangue materials, clays or other solid particulate matter. The particle/vapour interfacial tension, γ_{PV}, as well as the contact angle, θ, with water on coal or on other solids can be used to characterize the hydrophobicity and hence the floatability of the various powders. To improve and refine the freezing front technique both the redesign of the experimental set up was completed and new matrix materials were introduced.

The liquid/vapour surface tension, γ_{LV}, of various oils used in coal processing was determined by means of a modified Wilhelmy technique. An attempt was made to modify the surface properties of some of the coal powders by a pretreatment with aqueous solutions of surfactants.

During the previous contract in 1979/80 (Phase I) and in 1980/81 (Phase 2) an investigation of six bituminous and one subbituminous freshly mined coal samples from different origins was initiated. During Phase 3 of the Contract (in 1981/82) the freezing front experiments were repeated with three of the bituminous and one subbituminous coals to study whether a longer storage (aging) of the coals do affect their surface properties and the hydrophobicity of the coal particles. The effect of the

preparation of the coal powders (wet and dry screening) and the influence of oven-drying on the surface properties of coal were also tested. Auxiliary measurements regarding the specific heat of coals and the other solid particles were also performed and the results are now publishable.

Two manuscripts containing this information are appended (Appendix No. 1 and No. 2). During the Contract period of 1981/82, two papers were published (CIM Bulletin, 74, 54, 1981; Fuel 61, 437, 1982). One paper is accepted for publication (Can. J. of Chemistry) and two more papers were submitted.

MATERIALS AND METHODS

A. MATERIALS

1. Solid Particles

1.1 Coal Samples

Six coal samples were studied during the present contract period. Four of them were medium volatile bituminous coal (No. 1, No. 2, CN-5A and G-1) while No. 3 wet as well as dry screened was a subbituminous coal. Five of the coal samples were aged (stored for different periods of time); sample G-1 was freshly mined. Each of the coal samples consisted of two fractions identified by a range of -60+100 and -200+325 mesh, respectively.

One portion of each sample was oven-dried at 105°C. All of the experiments were performed with both the non-dried and the oven-dried samples. The origin, rank, type of sizing and the condition of the coals are summarized in Table 1. The physical properties (density, ash and moisture content, surface area and specific heat) of these coals are given in Table 2.

1.2 Gangue Materials, Clays

We studied:

a) EMR subbituminous coal with high percentage of gangue material from Hot Creek Area, British Columbia, -100 mesh.

b) carbon lampblack (Fisher Scientific product)

c) three clay samples:

1. EMR bentonite commercial grade;

2. Ca-bentonite;

3. Ca-kaolinite.

One portion of each sample was oven-dried at 105°C and the experiments were performed with both the non-dried and the dried samples. The physical properties of the gangue materials are summarized in Table 3. All samples were provided by EMR, CANMET, Western Research Laboratory, Edmonton.

2. Matrix Materials

The matrix materials used were thymol, benzophenone and water/ice. For the earlier freezing front experiments, thymol has been used while benzophenone and water/ice were introduced as new matrices during Phase 3 of this Contract. The organic compounds were zone refined prior to the measurements. The physical and thermal properties of the matrix materials are summarized in Table 4.

3. Surfactants

For the pretreatment of the coal powders to modify their hydrophilic character, aqueous solutions of three different surfactants in two concentrations were used:

1. Sodium-dodecylsulfate, NaDS, $[CH_3 - (CH_2)_{11} - OSO_3]^-Na^+$, anionactive, in an aqueous solution of 0.01 and 0.05 M/l;

2. Hexadecyl trimethyl ammonium bromide, HTAB, $[CH_3 - (CH_2)_{15} - N(CH_3)_3]^+ Br^-$, cationactive, in a solution of 0.01 and 0.05 M/l;
3. Triton-X100, nonionic, in an aqueous solution of 0.5 and 2.5 wt%, respectively. (Triton-X100 is a trade name, neither the exact chemical composition nor the molecular weight is known).

4. Oil Samples

Six different oils were investigated. The oil samples: MIBC, Pine oil, Accoal 4433, Light oil No. 2, Heavy oil No. 6 and Cresylic acid were provided by EMR, CANMET, Western Research Laboratory, Edmonton, Alberta. The surface tension measurements were performed with the oil samples as received. The samples were stored at room temperature in well closed bottles.

B. METHODS

1. Freezing Front Experiments

The critical velocity of engulfment, V_c, was determined for the coal samples and gangue materials with thymol and in some cases with benzophenone and water/ice as matrix materials.

1. The critical velocity measurements with the two organic matrix materials were performed in the redesigned experimental set-up. The apparatus was redesigned to allow an improved control of the advance of the solidification front. For detailed information, see Appendices 1 and 2.

2. The freezing front experiments with water/ice were performed at 0°C using an ENDOCAL LT-50 type refrigerated circulating bath and transmitted light for the microscopic observation. The coal and clay powders suspended in water had to be degassed prior to the experiments because of the air bonded to the surface of the solid particles which led to bubble formation during the solidification front experiments.

2. Pretreatment of the Coal Samples

1.0 gram coal powder was shaken together with 10 ml surfactant solution of given concentration for 24 hours, then filtered through a glass fritt of medium pore size covered with a filter paper. The coal was then dried for two hours in an oven at 105°C. The treated samples were kept in well-closed bottles at room temperature. The critical velocity, V_c, was determined with both the untreated and the pretreated samples using thymol as matrix material.

3. Surface Tension, γ_{LV}, of Oils

The temperature dependence of the surface tension, γ_{LV}, of oils were determined by a modified Wilhelmy technique.

The oil sample was kept in a glass cell with a built-in waterjacket which was connected to an automatic temperature control device. The oil sample in the measuring cell was kept in an inert atmosphere of argon saturated with the vapour of the oil.

A Cahn R-100 electric balance was used to measure the mass of oil which was lifted above the flat liquid level. This mass is proportional to the surface tension of the oil, γ_{LV}. The measurements were performed within the temperature range from 20 to 90°C, increasing and decreasing the temperature by 1°C/min and in a separate set of measurements by 0.5°C/min.

4. Specific Heat, C_p, of the Powders

The specific heat, C_p, of the coal and clay samples was determined by Differential Scanning Calorimetry (DSC). The heating rate was chosen as 10 K/min., the chart speed as 20 mm/min., the chart range as 5 mV. The reference standard was a sapphire (α - Al_2O_3) disc. All measurements were carried out in an atmosphere of flowing dried N_2 gas over a temperature range of 283 to 363 K. The specific heat measurements were performed with both the non-dried and the oven-dried samples. For more details on specific heat measurements of coal powders see Appendix No. 2.

5. Neutron Activation Analysis (NAA) of Trace Elements in Coal

The mineral composition of the coal samples G-1, the subbituminous coal with clay and of carbon lampblack was determined by means of neutron activation analysis using the University of Toronto's SLOWPOKE reactor.

This analysis was performed at 5 kW and/or 2kW flux for 20, 21 and 21.5 minutes/gram, respectively. The coal standard

reference was SRM 1632 from the U.S. National Bureau of Standards, Washington, D.C. The concentration of the elements is given in percentage or ppm (part per million), respectively. The error given represents the 95 percent confidence limits.

EXPERIMENTAL RESULTS AND DISCUSSION

1. Freezing Front Experiments in Organic Matrix Materials

1.1 Surface Tension, γ_{PV}, of Coal Particles

a) The freezing front experiments were performed with five different coal samples: No. 1, 2, 3 wet screened and No. 3 and CN-5A dry screened; these samples were aged (stored for one or two years) a different aliquot also dried after aging. The critical velocity, V_c, of the particles was measured with thymol as matrix material. The results obtained were then compared with the results of the freshly mined "as obtained" coals from the earlier experiments (Phase 1 and 2). The effect of aging as well as the effect of oven-drying on the surface tension of the aged coals were established. The experimental details and results are summarized in Appendix 1.

b) One "as obtained", freshly mined coal, EMR G-1 was studied during the present Contract period. This coal is characterized as a high ash material, a medium volatile bituminous coal from Smoky River Area, Alberta. The critical velocity measurements were performed with both the "as obtained" and the as obtained/dried samples using thymol as matrix material.

The critical velocity, V_c, the free energy of adhesion, ΔF^{adh} and the particle surface tension, γ_{PV}, are summarized for both the non-dried and oven-dried G-1 samples in Table 5 and are given for 51.5°C (the melting temperature of thymol). The particle surface tension, γ_{PV}, and the contact angle, θ, with

water calculated for 20°C are given in Table 6. Both γ_{PV} and θ versus particle diameter, D, are plotted in Figure 1.

The critical velocity measurements have been repeated with the G-1 non-dried sample six months later. The results are shown in Figure 2. We concluded that neither the oven-drying of the as obtained coal (Fig. 1) nor the short-term storage (Fig. 2) caused changes in surface properties exceeding the error limits.

1.2 Surface Tension of Gangue Material and Clays

The critical velocity, V_c, of the EMR subbituminous coal with clay, -100 mesh and of the three different clay samples (EMR bentonite commercial grade, Ca-bentonite and Ca-kaolinite) was determined with thymol for both the as obtained and the as obtained/dried samples while the experiments with benzophenone were performed only for the as obtained powders.

a) Critical velocity measurements with a gangue material

Two main components of the EMR subbituminous coal with clay (-100 mesh) could be easily distinguished under the microscope: there were black coal particles with a particle size of 15 to approximately 180 μm in diameter and light brown, very small clay particles. The latter ones were present mainly in aggregated form and/or were adhering to the surface of the coal particles. The critical velocity, V_c, of the coal particles and the clay aggregates was measured simultaneously. For the as obtained sample the critical velocity, V_c, versus particle diameter, D (in

the case of clay D means the diameter of aggregates) is plotted in Figure 3. These results were obtained from the measurements with thymol as well as with benzophenone.

Although the V_c-D curves of the clay agglomerates (Fig. 3) are always above those of the coal particles, the difference in the critical velocities is relatively small considering the different chemical composition. The γ_{PV} of the coal versus particle diameter, D, at 20°C is plotted in Figure 4; the surface tension of the clay aggregates are not shown, the reason will be explained in the next paragraph. The γ_{PV} of the "as obtained" and the "as obtained/dried" coal particles were equal within the error limits (see Tables 7 and 8).

b) Critical velocity measurements with clay samples

The freezing front experiments performed with the clay powders gave rise to several problems. First, one cannot easily define the "particle" or rather the aggregate diameter because in some cases the aggregates changed their size by partial desintegration when the solidification front passed them.

Another problem was to find the correct thermal conductivity, k_p, of the clay minerals for the calculation of the free energy of adhesion, ΔF^{adh} (see Final Reports of Phase I and II, and Appendix 1). In the literature, one can find k_p values from 0.15 to 1.05 J/m.s.K usually without any specification as to the condition of the clay mineral.

During the experimental work, benzophenone seemed to be a more suitable matrix material for clay particles than thymol because its higher γ_{LV} value is closer to the surface tension of the hydrophilic clay minerals. The critical velocities, V_c, versus aggregate's size, D*, are given in Figures 5, 6 and 7 for the clay samples. An approximation was made for the calculation of γ_{PV} of the clay aggregates from the V_c data obtained with benzophenone using for the thermal conductivity k_p = 0.5 J/m.s.K. The results are plotted in Figure 8 and summarized in Table 9. The γ_{PV} of the various clays ranges from 43 to 46 mJ/m^2, somewhat higher than the particle surface tension, γ_{PV}, of the coal particles in the gangue material.

For the measurement of the critical velocity of a single (not aggregated) clay particle the freezing front technique is not suitable as the particle size of the clays is too small (approximately 1 μm or less).

1.3 Critical Velocity Measurements with Carbon Lampblack

The freezing front experiments in thymol did not give information on the critical velocity, V_c, for single particles of carbon lampblack. The powder was aggregated in liquid thymol; the size of the aggregates varied between 7 to 210 μm in diameter. When the solidification front of thymol passed the aggregates they desintegrated similarly as the clays, forming smaller aggregates or single, very small particles. The mass meridan size of carbon lampblack (determined by disc centrifuge)

was given as 0.4 μm in diameter by EMR. Particle of this size cannot be studied by means of the freezing front technique.

The V_c measurements were also attempted for carbon lampblack with water/ice as matrix material. Again desintegration of the aggregates was observed.

To characterize the surface properties of solid particles with diameters near 1 μm or less other experimental approach possibly sedimentation volume measurements or certain adhesion strategies, developed in the laboratory of the principal investigator for biological cells, should be explored.

2. Freezing Front Experiments in Water/Ice with Coals

Preliminary freezing front experiments were performed in water/ice with two coal samples; No. 2 wet screened and CN-5A dry screened, both bituminous, in one particle size (-200 + 325 mesh). For the calculation of ΔF^{adh} an average particle diameter of 50 μm was used.

The critical velocity, V_c, the energy of adhesion, ΔF^{adh}, and the particle/vapour interfacial tension, γ_{pv}, obtained from the measurements in water/ice at 0^oC are summarized in Table 10. These results indicate that the γ_{pv} of coal suspended in water is very high (75.0 mJ/m^2), the surface of the particles is apparently not hydrophobic any more. The particle/vapour interfacial tension, γ_{pv}, and the contact angle, θ, data obtained from different (organic matrices and water/ice) systems given for 20^oC are compared in Table 11.

The difference between the γ_{pv} values obtained from water and from the organic matrix materials for the same coal sample is more than 30 mJ/m^2.

In organic materials, coal particles proved to be of intermediate hydrophobicity, whereas in water, the coal particles appeared to be very hydrophilic. This pattern of behavior suggests that for practical applications coal has two effective surface tensions, a lower one when the coal in interacting with hydrocarbons and a higher one when it interacts with an aqueous phase. We shall attempt to clarify these phenomena by sedimentation experiments.

Some experiments with clays were also performed in water/ice, but the difficulties previously mentioned were enhanced by swelling of the clay particles in water.

3. Pretreatment of Coal

The pretreatment of two coal powders (coal No. 3 wet as well as dry screened) in two fractions (-60+100 and -200+325 mesh) were performed using aqueous solutions of the anionactive NaDS, the cationactive HTAB and the non-ionic TRITON-X100 surfactants in two concentrations. The critical velocity of the pretreated coals were measured with thymol at 51.5°C, then the particle surface tension, γ_{pv}, and the contact angle, θ, were calculated. The γ_{pv} versus particle diameter, D for coal No. 3 wet screened are plotted in Figures 9, 10 and 11, the same plots for coal No. 3 dry screened are given in Figures 12, 13 and 14. All these γ_{pv} values refer to the melting temperature of thymol (51.5°C). The

surface tension, γ_{PV}, and the contact angle, θ, given for 20°C are summarized in Tables 12 and 13 for coal No. 3 wet screened and in Tables 14 and 15 for coal No. 3 dry screened.

The results show that in the case of coal No. 3 wet screened none of the surfactants made the particles more hydrophobic. The difference between the γ_{PV} of the untreated and pretreated samples remained within the error limits. In the case of coal No. 3 dry screened the cationactive HTAB made the surface of the particles even more hydrophilic and the nonionic TRITON-X100 provided a slightly more hydrophobic surface than the untreated sample. Both surfactants were effective in the higher concentration (0.05 M/l and 2.5 wt%, respectively).

Our efforts to change the surface properties of coal by pretreatment of various surface active materials turned out to have only a minor effect in all cases. It is therefore suggested to conduct a fundamental study of the adsorption of water soluble polymeric compounds on coal particles.

4. Liquid/Vapour Surface Tension, γ_{LV}, of Oils

The surface tension, γ_{LV}, of different oil samples was measured by means of a modified Wilhelmy technique in the temperature range from 20 to 90°C. We studied six oil samples: MIBC, Pine Oil, Accoal 4433, Light oil No. 2, Heavy oil No. 6 and Cresylic acid X-700 provided by EMR, CANMET, Western Research Laboratory, Edmonton, Alberta. The upper temperature bound depended on the vapour pressure and thermal stability of the oil

samples. The surface tension, γ_{LV}, was measured at least three times for each sample.

Plots of γ_{LV} versus temperature for the six oil samples are given in Figures 15 - 20. The surface tension values at different termperatures are summarized in Table 16; the temperature coefficients, $\frac{d\gamma_{LV}}{dT}$ are given in Table 17.

5. Specific Heat of Coal and Clay Samples

The specific heat measurements were performed both with the as obtained and with the oven-dried coal and clay samples, carbon lampblack and gangue material.

5.1 The specific heats of the coal samples No. 1, No. 2 and No. 3 are discussed in detail in Appendix 2.

5.2 The specific heat of coal EMR G-1 for both fractions, of the clay and of gangue materials are summarized in Tables 18, 19 and 20, respectively. The C_p versus temperature of coal EMR G-1, of coal with gangue material, of carbon lampblack and of the clay samples are plotted in Figures 21, 22 and 23.

The difference in C_p between the as "obtained" and "dried" coal G-1 samples does not exceed the experimental error limit (Fig. 21). The moisture contents of these coal fractions are low (<1 wt%) (see Table 2). The specific heats of the "as obtained" gangue material (EMR subbituminous coal with clay) as well as the carbon lampblack are higher than those of the corresponding dried

samples (Fig. 22). In the case of carbon lampblack, this difference cannot be explained by high moisture content because the water content of carbon lampblack is less than 1 wt% (Table 3).

The specific heats of the clay samples versus temperature are plotted in Figure 23. With exception of Ca-kaolinite (moisture <1 wt%), the as obtained clays had higher C_p values than the corresponding oven-dried samples because of their higher water content (Table 3). No difference was found in the specific heats of the two "as obtained" bentonites (EMR commercial and Ca-bentonite) but there was a difference between the same dried samples: the commercial grade had lower C_p value. This bentonite might be a mixture of various clay minerals (illite, kaolinite) which probably loses the bonded water easier than the three-layered Ca-bentonite.

6. Neutron Activation Analysis (NAA) of Trace Elements

The concentration of some trace elements in coal G-1, in the gangue material as well as in carbon lampblack was determined by neutron activation analysis. The results are summarized and compared with the analysis data of a standard coal in Table 21. The concentration of the elements is given in percentage or ppm, respectively, and the error given represents the 95 percent confidence limit.

No differences were found between the two fractions of coal G-1 neither for the "as obtained" nor the "oven-dried" portions. The concentration of the trace elements of the carbon lampblack,

as expected, was very low, and in the subbituminous coal with clay very high.

CONCLUSIONS

1. The effect of aging (storage) as well as oven-drying on the surface properties of coal particles can be monitored by means of the freezing front technique.

2. Aging of coal samples changes the hydrophobicity of the surface of coal particles. The change depends on the type of sizing (wet or dry screening) more than on the rank of the coal.

3. Solidification front experiments with various coal particles indicated that the particle surface tension, γ_{pv}, depends on the matrix material (hydrocarbon or water/ice).

4. At very small particle size, of the order of 1 μm, Brownian motion and thermophoretic flows make freezing front measurements impossible.

5. The pretreatment with surface active materials had only a minor effect on the surface properties of coal.

6. The improved design of the freezing front set-up improved the sensitivity and reproductibility of the critical velocity measurements considerably.

Table 1

Coal Samples by Origin, Rank,

Type of Screening and Age

Coal Sample	Origin (Locality)	Rank	Type of Sizing	Condition of Sample
No.1	Quintette Area, Northeastern British Columbia	medium volatile, bituminous	wet screened	aged
No.2	Mountain Park Area, Alberta	medium volatile, bituminous	wet screened	aged
No.3	Judy Creek Area, Northern Alberta	subbituminous	wet screened	aged
No.3	Judy Creek Area, Northern Alberta	subbituminous	dry screened	aged
CN-5A	Crownest Pass Area, Alberta - British Columbia border	medium volatile, bituminous	dry screened	aged
G-1	Smoky River Area, Alberta	medium volatile, bituminous	dry screened	"as obtained"

Table 2

Physical Properties of Coal Samples

Physical Property	-60+100 mesh fraction						-200+325 mesh fraction					
	wet screened			dry screened			wet screened			dry screened		
	No.1	No.2	No.3	No.3	CN-5A	G-1	No.1	No.2	No.3	No.3	CN-5A	G-1
Density* (kg/m^3)	1520	1470	1630	1630	1410	1680	1430	1430	1640	1640	1460	1610
Ash Content (wt %)*	19.38	23.33	28.96	31.03	14.70	36.51	10.78	17.03	31.71	39.11	14.89	30.27
Moisture Content (wt %)	0.10	0.47	2.33	10.43	0.71	0.10	1.45	0.64	2.40	9.47	0.51	0.34
Surface Area* (m^2/kg)	550	620	10430	10430	900	730	720	890	12150	12150	1090	1050
Specific Heat+ (kJ/kg·K) at 51.5°C	1.08	1.12	1.14	1.18	1.14	1.04	1.18	1.19	1.13	1.11	1.25	1.02
at 0°C	0.87	0.93	0.96	1.05	1.04	0.76	0.94	0.99	0.92	0.90	0.98	0.77

* These data were obtained from EMR, CANMET, Western Research Laboratory, Edmonton, Alberta, courtesy of Dr. H.A. Hamza.

\+ The specific heat data are given for dried coal samples.

Table 3

Physical Properties of Gangue Materials and Clays

Physical Properties \ Sample	EMR subbituminous coal with clay -100 mesh	Carbon lampblack	EMR bentonite commercial grade	Ca-bentonite	Ca-kaolinite
Density* (kg/m^3)	2040	1610	2570	2280	2460
Ash Content* (wt %)	78.45	-	-	-	-
Moisture Content (wt %)	5.14	0.82	9.76	7.12	0.51
Surface Area* (m^2/kg)	-	30100	-	31900	20700
Specific heat+ kJ/kg·K) at 51.5°C	1.02	0.81	0.93	1.15	1.02
at 0°C	0.88	0.66	0.78	1.01	0.85

* These data were obtained from EMR, CANMET, Western Reserach Laboratory, Edmonton, Alberta.

\+ The specific heat data are given for dried samples.

Table 4

Physical Properties of the Matrix Materials

Substance	Density ρ_L (kg/m^3)	Viscosity μ ($N \cdot s/m^2$)	Specific Heat C_p ($kJ/kg \cdot K$)	Thermal Conductivity k_p ($J/m \cdot s \cdot K$)	Surface Tension, γ_{LV} at melting point (mJ/m^2)	Surface Tension, γ_{SV} at melting point (mJ/m^2)
Thymol	925	0.00397	2.370	0.1298	29.9 at 51.5°C	29.4 at 51.5°C
Benzophenone	1146	0.00516	1.856	-	39.9 at 48.0°C	34.5 at 48.0°C
Water/ice	999.8	0.001787	4.2177	0.5610	75.6 at 0°C	80.2 at 0°C

Table 5

Critical Velocity, ΔF^{adh} and γ_{PV} Values for EMR G-1 Coal Sample in Thymol at 51.5°C

Particle Diameter	EMR G-1 Coal					
	as obtained			as obtained/dried		
D (μm)	Critical Velocity V_c (μm/sec)	ΔF^{adh} (mJ/m²)	γ_{PV} at 51.5°C (mJ/m²)	Critical Velocity V_c (μm/sec)	ΔF^{adh} (mJ/m²)	γ_{PV} (mJ/m²)
30	6.35±1.55	0.0740±0.0124	35.2±0.89	8.3 ±1.3	0.0882±0.0095	36.2±0.68
45	6.05±1.55	0.0869±0.0153	36.1±1.09	7.7 ±1.4	0.102 ±0.0127	37.2±0.91
60	5.75±1.55	0.0964±0.0178	36.8±1.27	7.1 ±1.4	0.111 ±0.0150	37.8±1.07
75	5.55±1.55	0.1050±0.0200	37.4±1.43	6.6 ±1.4	0.117 ±0.0170	38.2±1.21
180	4.50±1.20	0.139 ±0.0254	39.9±1.81	4.30±1.15	0.135 ±0.0247	39.5±1.76
210	4.35±1.15	0.146 ±0.0265	40.4±1.89	3.90±1.05	0.136 ±0.0251	39.6±1.79
240	4.18±1.07	0.152 ±0.0267	40.7±1.91	3.75±0.95	0.142 ±0.0247	40.0±1.76
270	4.00±1.00	0.156 ±0.0267	41.0±1.91	3.58±0.88	0.145 ±0.0244	40.2±1.74
300	3.83±0.97	0.159 ±0.0276	41.2±1.97	3.45±0.85	0.149±0.0252	40.5±1.80
330	3.65±0.95	0.162 ±0.0289	41.4±2.06	3.35±0.85	0.153±0.0266	40.8±1.80

Table 6

Particle/Vapour Interfacial Tension, γ_{PV}, and Contact Angle, θ, of Coal EMR G-1 Sample at 20°C

Particle Diameter D (μm)	EMR G-1 Coal as obtained γ_{PV} at 20°C (mJ/m²)	as obtained θ at 20°C (degree)	as obtained/dried γ_{PV} at 20°C (mJ/m²)	as obtained/dried θ at 20°C (degree)
30	37.3±0.89	76.9±1.49	38.3±0.68	75.2±1.08
45	38.2±1.09	75.4±1.79	39.3±0.91	73.6±1.51
60	38.9±1.27	74.2±2.04	40.0±1.07	72.4±1.73
75	39.5±1.43	73.3±2.40	40.3±1.21	71.9±1.97
180	42.0±1.81	69.1±3.07	41.6±1.76	69.8±3.00
210	42.5±1.89	68.3±3.27	41.7±1.79	69.6±3.03
240	42.8±1.91	67.8±3.32	42.1±1.76	68.9±2.96
270	43.1±1.91	67.2±3.23	42.3±1.74	68.6±2.97
300	43.3±1.97	66.9±3.37	42.6±1.80	68.1±3.09
330	43.5±2.06	66.6±3.57	42.9±1.90	67.6±3.27

Table 7

Critical Velocity, ΔF^{adh} and γ_{PV} Values for EMR Subbituminous Coal with Clay at 51.5°C

Particle Diameter	EMR Subbituminous Coal with Clay					
	as obtained			as obtained/dried		
D (μm)	Critical Velocity V_c (μm/sec)	ΔF^{adh} (mJ/m²)	γ_{PV} at 51.5°C (mJ/m²)	Critical Velocity V_c (μm/sec)	ΔF^{adh} (mJ/m²)	γ_{PV} at 51.5°C (mJ/m²)
15	8.65±1.90	0.061±0.009	34.2±0.7	11.15±3.05	0.074±0.014	35.2±1.0
30	7.60±1.70	0.078±0.012	35.4±0.8	9.40±2.80	0.093±0.019	36.5±1.4
45	6.70±1.60	0.087±0.014	36.1±1.0	8.10±2.50	0.102±0.022	37.2±1.5
60	6.00±1.50	0.092±0.016	36.5±1.1	7.10±2.15	0.107±0.022	37.5±1.6
75	5.35±1.45	0.095±0.018	36.7±1.3	6.40±2.00	0.111±0.024	37.6±1.7
90	4.80±1.30	0.096±0.018	36.8±1.3	5.80±1.80	0.113±0.024	38.0±1.7
105	4.40±1.30	0.098±0.020	36.9±1.4	5.40±1.70	0.116±0.025	38.2±1.8
120	3.90±1.05	0.096±0.018	36.8±1.3	5.10±1.60	0.119±0.026	38.4±1.8
135	3.60±0.95	0.096±0.017	36.8±1.2	4.85±1.55	0.122±0.027	38.6±1.9
150	3.40±0.90	0.097±0.018	36.9±1.3	4.70±1.50	0.126±0.027	38.9±2.0
175	3.25±0.80	0.102±0.017	37.2±1.2	4.60±1.50	0.133±0.030	39.4±2.1

Table 8

Particle/Vapour Interfacial Tension, γ_{PV}, and Contact Angle, θ, of EMR Subbituminous Coal with Clay

Particle Diameter	EMR Subbituminous Coal with Clay			
	as obtained		as obtained/dried	
D (μm)	γ_{PV} at 20°C (mJ/m²)	θ (degree)	γ_{PV} at 20°C (mJ/m²)	θ (degree)
15	36.3±0.7	78.4±1.0	37.3±1.0	76.8±1.6
30	37.5±0.8	76.5±1.4	38.6±1.4	74.7±2.2
45	38.2±1.0	75.4±1.7	39.3±1.5	73.6±2.5
60	38.6±1.1	74.8±1.9	39.6±1.6	73.0±2.6
75	38.8±1.3	74.4±2.1	39.9±1.7	72.6±2.8
90	38.9±1.3	74.3±2.1	40.1±1.7	72.3±2.9
105	39.0±1.4	74.1±2.3	40.3±1.8	71.9±3.0
120	38.9±1.3	74.3±2.1	40.5±1.8	71.6±3.1
135	38.9±1.2	74.3±2.0	40.7±1.9	71.3±3.2
150	39.0±1.3	74.2±2.1	41.0±2.0	70.8±3.3
175	39.3±1.2	73.6±2.0	41.5±2.1	69.9±3.6

Table 9

γ_{PV} of Clay Aggregates at 20°C

Matrix Material: Benzophenone

Aggregates D (μm)	γ_{PV} (mJ/m²) at 20°C		
	EMR Bentonite Commerical Grade	Ca-Bentonite	Ca-Kaolinite
15	43.6±0.2	43.7±0.3	44.8±0.2
30	43.9±0.3	44.1±0.3	45.5±0.3
45	43.9±0.4	44.2±0.4	45.9±0.4
60	43.7±0.4	44.3±0.5	46.1±0.4
75	43.6±0.5	44.3±0.6	46.2±0.5
90		44.4±0.6	46.3±0.6
105		44.4±0.7	46.4±0.5
120		44.6±0.7	46.5±0.6
135		44.7±0.7	46.6±0.6
150		44.8±0.7	46.7±0.7

Table 10

Critical Velocity, ΔF^{adh} and γ_{PV} Data from Experimental Observations with Water/Ice System for D = 50 μm at 0°C

Samples -200+325 mesh	Critical Velocity V_c (μm/sec)	ΔF^{adh} (mJ/m²)	γ_{PV} (mJ/m²)	θ (degree)
Coal No.2	4.4±1.0	0.085±0.013	75.0±0.3	7.2±1.3
CN-5A	5.6±0.5	0.096±0.006	74.8±0.1	8.2±1.0

Table 11

Particle/Vapour Interfacial Tension and Contact Angle Data of Coal Samples for D = 50 μm at 20°C

Matrix Material	Coal No.2 -200+325 mesh		CN-5A -200+325 mesh	
	γ_{PV} (mJ/m^2)	θ (degree)	γ_{PV} (mJ/m^2)	θ (degree)
Water	73.7±0.3	13.1±1.3	73.5±0.1	13.8±1.0
Thymol	40.5±1.9	71.6±3.1	45.4±1.3	63.3±2.2
Biphenyl	38.9±0.2	74.3±0.3	-	-
Naphthalene	39.4±0.4	73.4±0.6	-	-

Table 12

Particle Surface Tension, γ_{PV}, for Untreated and Pretreated Coal No.3 Wet Screened

D (μm)	γ_{PV} at 20°C (mJ/m^2)						
	untreated	NaDS		HTAB		TRITON X-100	
		0.01 M/l	0.05 M/l	0.01 M/l	0.05 M/l	0.5 wt %	2.5 wt %
15	-	-	-	-	-	-	-
30	37.6±0.4	-	38.7±0.6	37.7±0.5	39.0±0.5	37.7±0.5	37.6±0.4
45	38.0±0.5	-	39.6±0.7	38.7±0.6	39.7±0.6	38.7±0.6	38.2±0.5
60	38.2±0.5	41.6±0.8	40.3±0.8	39.4±0.7	40.1±0.8	39.6±0.7	38.6±0.5
75	38.5±0.6	41.8±0.9	40.8±0.9	39.9±0.8	40.4±0.9	40.2±0.8	38.7±0.6
90	39.1±0.6	41.8±0.9	41.2±0.9	40.4±0.9	40.7±0.9	40.8±0.8	38.9±0.5
120	40.0±0.7	41.5±1.1	41.6±1.1	41.1±1.0	41.2±1.0	41.6±0.9	39.5±0.8
150	40.8±0.8	41.8±1.2	42.0±1.2	41.8±1.0	41.9±1.2	42.2±0.9	39.9±0.9
180	41.6±0.9	42.5±1.1	42.0±1.2	42.6±1.1	42.5±1.3	42.7±1.0	40.4±0.8
210	42.2±1.0	43.1±1.2	42.2±1.1	43.3±1.2	43.1±1.4	43.3±1.1	40.7±0.9
240	42.7±1.0	-	42.1±1.1	44.0±1.3	43.9±1.5	43.9±1.2	40.7±1.0
270	43.2±1.1	-	-	-	-	-	40.8±1.0

Table 13

Contact Angle, θ, for Untreated and Pretreated Coal No.3 Wet Screened

D (μm)	untreated	θ at 20°C (degree) NaDS 0.01 M/l	NaDS 0.05 M/l	HTAB 0.01 M/l	HTAB 0.05 M/l	TRITON X-100 0.5 wt %	TRITON X-100 2.5 wt %
15	-	-	-	-	-	-	-
30	76.3±0.6	-	74.5±1.0	76.2±0.8	74.0±0.8	76.2±0.8	76.4±0.7
45	75.7±0.8	-	73.0±1.2	74.6±1.0	72.9±1.1	74.5±1.0	75.4±0.8
60	75.3±0.8	69.9±1.3	72.0±1.3	73.5±1.2	72.2±1.4	73.1±1.1	74.8±0.8
75	74.9±0.9	69.5±1.5	71.1±1.5	72.5±1.3	71.8±1.4	72.1±1.3	74.6±0.9
90	74.0±1.0	69.4±1.5	70.5±1.6	71.8±1.5	71.3±1.4	71.2±1.3	74.3±0.9
120	72.4±1.2	69.9±1.9	69.7±1.9	70.7±1.7	70.5±1.7	69.7±1.5	73.2±1.2
150	71.0±1.4	69.4±2.0	69.2±2.0	69.4±1.8	69.4±2.0	68.7±1.5	72.5±1.4
180	69.8±1.5	68.3±2.0	69.1±2.0	68.1±1.9	68.3±2.2	67.8±1.7	71.8±1.3
210	68.8±1.7	67.2±2.1	68.8±1.9	67.0±2.1	67.2±2.4	67.0±1.9	71.3±1.5
240	68.0±1.8	-	68.9±1.8	65.7±2.3	65.9±2.6	65.9±2.0	71.3±1.6
270	67.1±1.9	-	-	-	-	-	71.2±1.7

Table 14

Particle Surface Tension, γ_{PV}, for Untreated and Pretreated Coal No.3 Dry Screened

D (μm)	γ_{PV} at 20°C (mJ/m^2) untreated	NaDS 0.01 M/l	NaDS 0.05 M/l	HTAB 0.01 M/l	HTAB 0.05 M/l	TRITON X-100 0.5 wt %	TRITON X-100 2.5 wt %
15	36.6±0.4	-	35.9±0.4	-	40.5±0.7	36.2±0.4	35.3±0.2
30	37.8±0.5	37.3±0.6	36.9±0.6	37.6±0.6	42.4±0.8	37.1±0.6	35.8±0.3
45	38.5±0.6	37.9±0.7	37.3±0.7	37.9±0.6	43.4±0.9	37.7±0.6	35.8±0.3
60	39.2±0.5	38.4±0.7	37.7±0.8	38.3±0.7	44.2±1.0	38.3±0.7	35.6±0.4
75	39.9±0.5	39.0±0.6	37.9±0.9	38.8±0.8	44.8±1.0	38.9±0.8	35.5±0.4
90	40.5±0.6	39.5±0.6	38.1±0.9	39.2±0.8	45.4±0.9	39.4±0.7	35.6±0.6
120	-	40.4±0.7	-	-	46.3±1.0	40.4±0.7	35.8±0.7
150	42.4±0.6	41.2±0.8	39.4±1.2	41.0±0.9	46.8±1.1	41.4±0.8	36.8±0.7
180	43.1±0.7	41.8±0.9	40.1±1.3	41.8±1.0	47.2±1.2	42.2±0.9	38.0±0.7
210	43.7±0.8	42.4±1.0	40.7±1.4	42.6±1.1	47.6±1.3	43.0±0.9	39.8±0.7
240	44.3±0.8	42.9±1.0	41.2±1.5	43.3±1.2	48.1±1.5	43.6±1.0	-
270	44.6±0.7	43.4±1.1	-	-	48.6±1.6	44.3±1.1	-

Table 15

Contact Angle, θ, for Untreated and Pretreated Coal No.3 Dry Screened

D (μm)	θ at 20°C (degree) untreated	NaDS 0.01 M/l	NaDS 0.05 M/l	HTAB 0.01 M/l	HTAB 0.05 M/l	TRITON X-100 0.5 wt %	TRITON X-100 2.5 wt %
15	78.0±0.6	-	79.0±0.7	-	71.6±1.2	78.7±0.6	80.0±0.3
30	76.0±0.9	76.8±0.9	77.5±0.9	76.3±1.0	68.5±1.4	77.1±0.9	79.3±0.4
45	74.9±1.0	75.8±1.1	76.9±1.2	75.9±0.9	66.7±1.5	76.1±0.9	79.3±0.6
60	73.[illegible]0.8	75.0±1.1	76.3±1.3	75.2±1.1	65.4±1.7	75.2±1.1	79.5±0.7
75	72.6±0.9	74.1±0.9	75.9±1.5	74.4±1.2	64.3±1.7	74.3±1.2	79.7±0.8
90	71.6±1.0	73.2±1.0	75.5±1.5	73.8±1.4	63.3±1.6	73.4±1.2	79.6±0.9
120	-	71.8±1.2	-	-	61.8±1.8	71.8±1.2	79.3±1.1
150	68.4±1.1	70.4±1.3	73.4±1.9	70.8±1.6	60.9±1.8	70.2±1.3	77.7±1.2
180	67.3±1.2	69.4±1.5	72.2±2.1	69.4±1.7	60.2±2.1	68.8±1.5	75.7±1.2
210	66.2±1.3	68.4±1.6	71.3±2.3	68.2±1.9	59.5±2.3	67.5±1.6	72.8±1.2
240	65.3±1.4	67.5±1.8	70.5±2.5	67.0±2.0	58.7±2.5	66.4±1.7	-
270	64.6±1.2	66.7±1.9	-	-	57.9±2.6	65.2±1.8	-

Table 16

Temperature Dependence of the Surface Tensions, γ_{LV}, of Oils

Temperature	γ_{LV} (mJ/m^2)					
^oC	MIBC	Pine Oil	Accoal 4433	Light Oil No.2	Heavy Oil No.6	Cresylic Acid X-700
20	24.43±0.87	25.80±0.81	27.05±0.65	31.57±0.45	32.69±0.48	37.50±1.50
30	23.56±0.80	25.16±1.22	26.34±0.56	30.75±0.89	31.97±0.45	36.52±1.51
40	22.56±0.79	24.44±0.67	25.52±0.42	29.87±0.51	31.18±0.57	35.48±1.17
50	21.67±0.90	23.89±0.93	24.71±0.33	29.03±0.45	30.41±0.60	34.57±1.03
60	20.73±0.84	23.35±0.97	24.01±0.10	28.17±0.45	29.64±0.68	33.51±1.02
70	19.74±1.02	22.76±1.26	23.14±0.18	27.22±0.89	28.86±0.85	32.48±0.92
80	18.79±1.23	22.08±1.14	22.29±0.48	26.42±1.52	28.08±0.92	31.50±0.85
90	17.90±1.25	21.37±1.46	21.44±0.55	25.52±0.89	27.32±1.07	30.46±0.88

Table 17

Temperature Coefficients of the Surface Tension, $\frac{d\gamma_{LV}}{dT}$, of Oils

Oil Sample	$\frac{d\gamma_{LV}}{dT}$ ($mJ/m^2 \cdot {}^{o}C$)
MIBC	-0.093 ± 0.017
Pine Oil	-0.064 ± 0.006
Accoal 4433	-0.077 ± 0.014
Light Oil No.2	-0.086 ± 0.013
Heavy Oil No.6	-0.077 ± 0.014
Cresylic Acid	-0.100 ± 0.018

Table 18

Specific Heat of Coal Samples EMR G-1 for

-60+100 and -200+325 mesh Fractions

Temperature (K)	Specific Heat C_p (kJ/kg·K)			
	-60+100 mesh		-200+325 mesh	
	as obtained	dried	as obtained	dried
290	0.840±0.055	0.843±0.013	0.859±0.031	0.849±0.032
300	0.898±0.046	0.890±0.038	0.913±0.010	0.891±0.050
310	0.926±0.042	0.946±0.070	0.964±0.004	0.935±0.040
320	0.999±0.050	1.014±0.079	1.028±0.035	1.002±0.040
330	1.027±0.075	1.068±0.077	1.071±0.050	1.048±0.031
340	1.092±0.045	1.125±0.070	1.134±0.037	1.089±0.021
350	1.122±0.051	1.152±0.012	1.179±0.066	1.144±0.030
360	1.152±0.048	1.171±0.027	1.246±0.022	1.184±0.020

Table 19

Specific Heat of Gangue Materials

Temperature (K)	Specific Heat C_p (kJ/kg·K)			
	EMR Subbituminous Coal with Clay, -100 mesh		Carbon Lampblack	
	as obtained	dried	as obtained	dried
290	1.059±0.053	0.927±0.043	0.754±0.059	0.722±0.021
300	1.087±0.050	0.943±0.071	0.805±0.070	0.732±0.013
310	1.130±0.042	0.973±0.036	0.866±0.082	0.771±0.022
320	1.178±0.037	1.015±0.056	0.870±0.082	0.777±0.019
330	1.230±0.023	1.034±0.052	0.924±0.041	0.849±0.007
340	1.262±0.019	1.067±0.069	0.985±0.074	0.852±0.002
350	1.298±0.058	1.102±0.050	1.045±0.095	0.889±0.017
360	1.322±0.054	1.131±0.077	1.098±0.078	0.946±0.022

Table 20

Specific Heats of Clay Samples

Temperature (K)	Specific Heat C_p (kJ/kg·K)					
	EMR Bentonite Commercial Grade		Ca-bentonite		Ca-kaolinite	
	as obtained	dried	as obtained	dried	as obtained	dried
290	1.177±0.060	0.857±0.049	1.170±0.060	1.111±0.056	0.944±0.026	0.959±0.033
300	1.171±0.045	0.859±0.052	1.150±0.070	1.087±0.098	0.937±0.037	0.954±0.036
310	1.204±0.085	0.875±0.084	1.186±0.085	1.131±0.050	0.968±0.053	0.984±0.074
320	1.226±0.045	0.921±0.036	1.200±0.060	1.137±0.050	1.013±0.047	1.013±0.066
330	1.246±0.080	0.945±0.057	1.238±0.040	1.156±0.066	1.031±0.025	1.036±0.066
340	1.286±0.038	0.963±0.060	1.277±0.077	1.204±0.095	1.089±0.029	1.099±0.062
350	1.314±0.042	1.007±0.085	1.309±0.083	1.249±0.042	1.134±0.042	1.141±0.027
360	1.330±0.049	1.040±0.027	1.360±0.056	1.273±0.030	1.160±0.061	1.178±0.045

Table 21

Neutron Activation Analysis (NAA) of Trace Elements

Element concentration	Coal G-1 dried		Coal subbituminous +clay -100 mesh		Carbon Lampblack	NBS-SRM standard coal
	-60+100	-200+325	as obtained	dried	as obtained	
Si %	10.14±2.02	10.34±5.74	16.07±4.01	18.1±2.8	0	0
Al %	4.85±0.31	4.39±0.08	7.94±0.43	8.12±0.09	4.78±0.29	1.51±0.08
Ca %	0.56±0.07	0.47±0.02	0.98±0.07	1.04±0.04	0.05±0.01	0.37±0.04
Mg %	1.02±0.07	0.88±0.16	2.02±0.16	2.10±0.14	0.03±0.01	0.19±0.04
Na %	0.070±0.013	0.069±0.006	0.173±0.008	0.173±0.010	0.011±0.004	0.036±0.002
Ba ppm	477±31	470±12	791±13	789±56	3.9±7.4	320±20
Ti ppm	2761±126	2833±112	2973±85	2970±180	18.7±1.1	920±50
V ppm	50.2±3.6	45.8±3.8	83.2±5.8	84.2±11.1	32.5±6.3	32.3±1.5
Mn ppm	33.8±3.0	28.8±0.9	57.2±3.7	58.1±1.8	5.8±0.8	41±2
U ppm	3.86±0.05	3.96±0.14	2.17±0.24	2.25±0.29	0.037±0.031	1.6±0.2
Dy ppm	2.04±0.09	2.04±0.09	2.68±0.07	2.66±0.17	0.012±0.010	0.57±0.04
Cl ppm	171±19	218±45	53.5±39.2	76.5±30.6	114±20	920±30
Br ppm	3.6±1.4	4.8±2.2	0	0	0	16.6±0.6

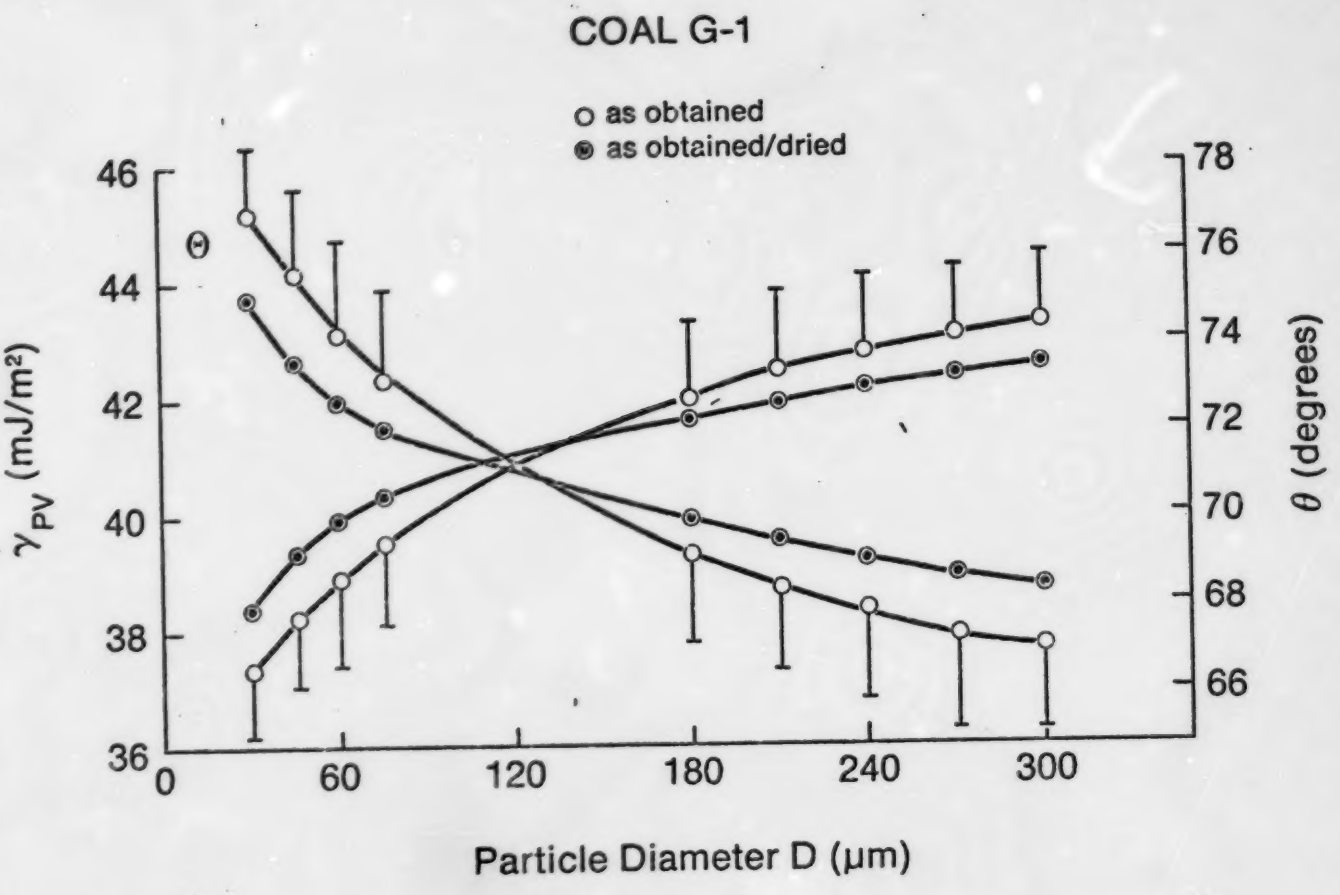

Figure 1

Particle surface tension, γ_{PV}, and contact angle, θ, versus particle diameter, D, for the "as obtained" as well as the "obtained/dried coal G-1 samples at 20°C

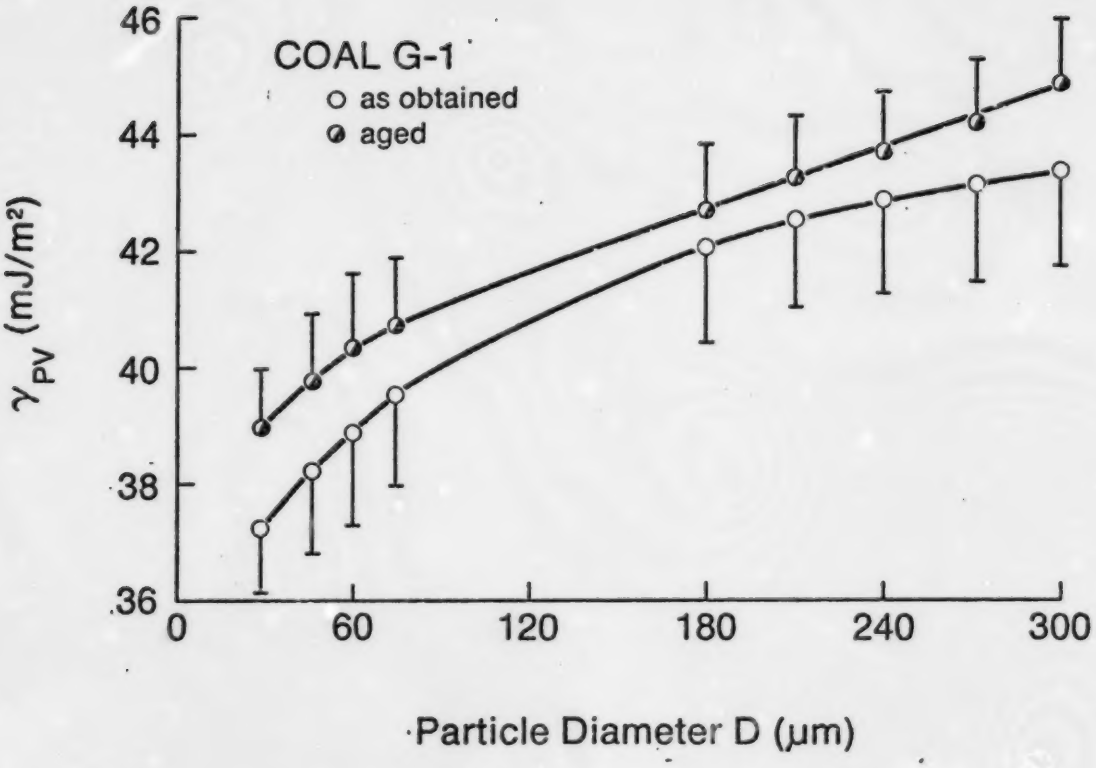

Figure 2

Particle surface tension, γ_{PV}, versus particle diameter, D, for "as obtained" and "aged" coal G-1 samples at 20°C

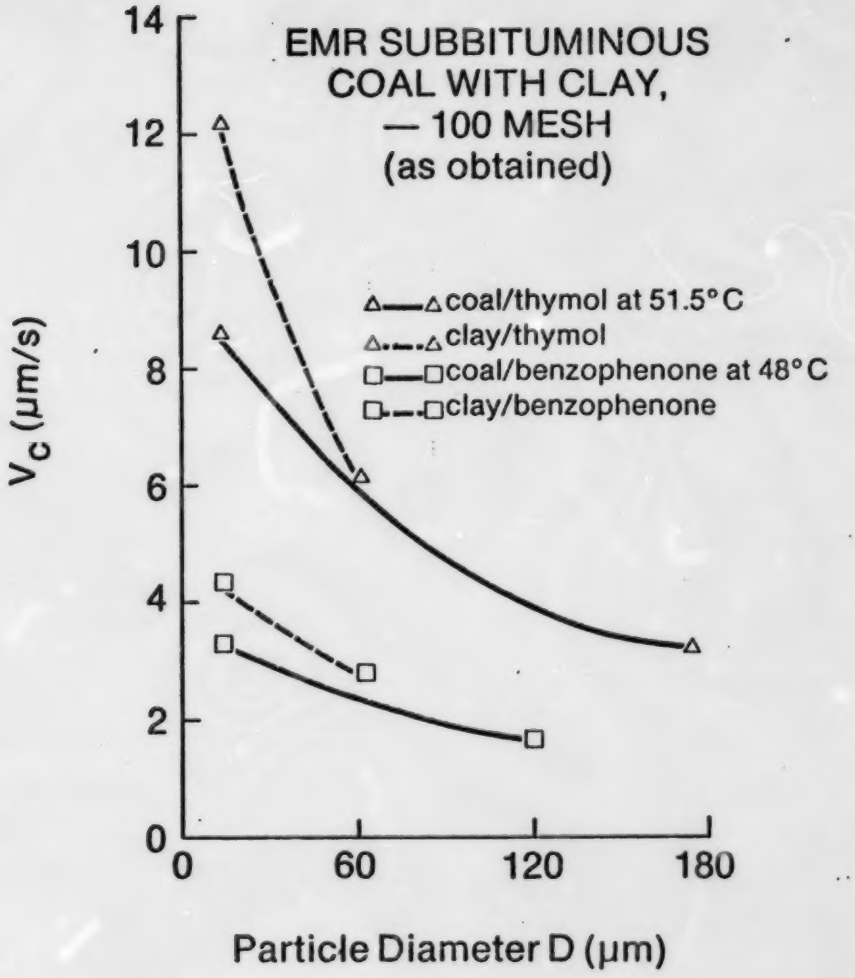

Figure 3

Critical velocity V_c, versus particle diameter, D, for for the gangue material in two orgainic matrix materials

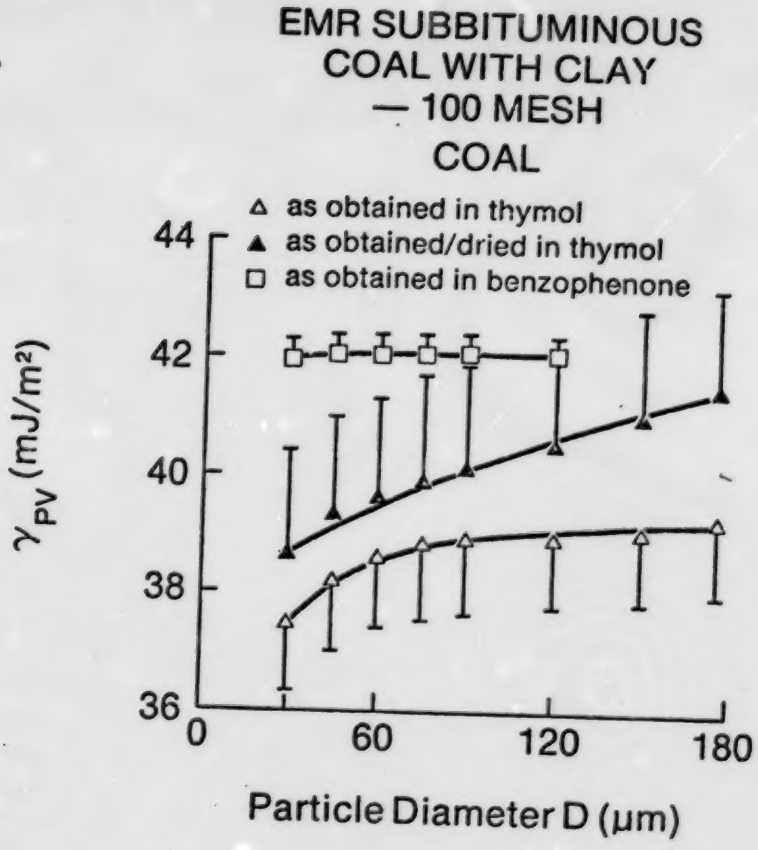

Figure 4

Particle surface tension, γ_{PV}, of coal in the gangue material versus particle diameter, D, for three different systems

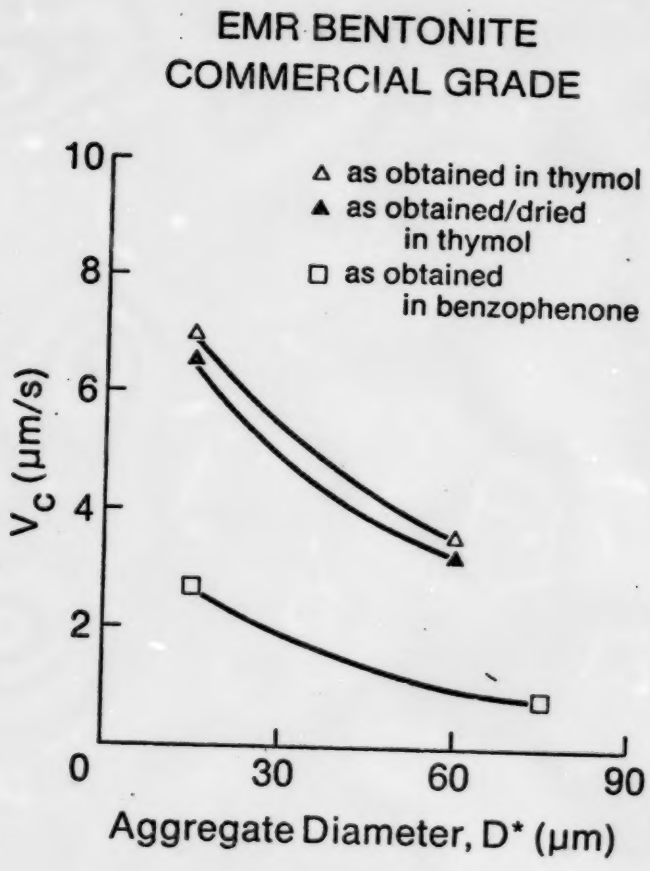

Figure 5

Critical velocity, V_c, versus aggregate diameter, D*, for EMR bentonite commercial grade

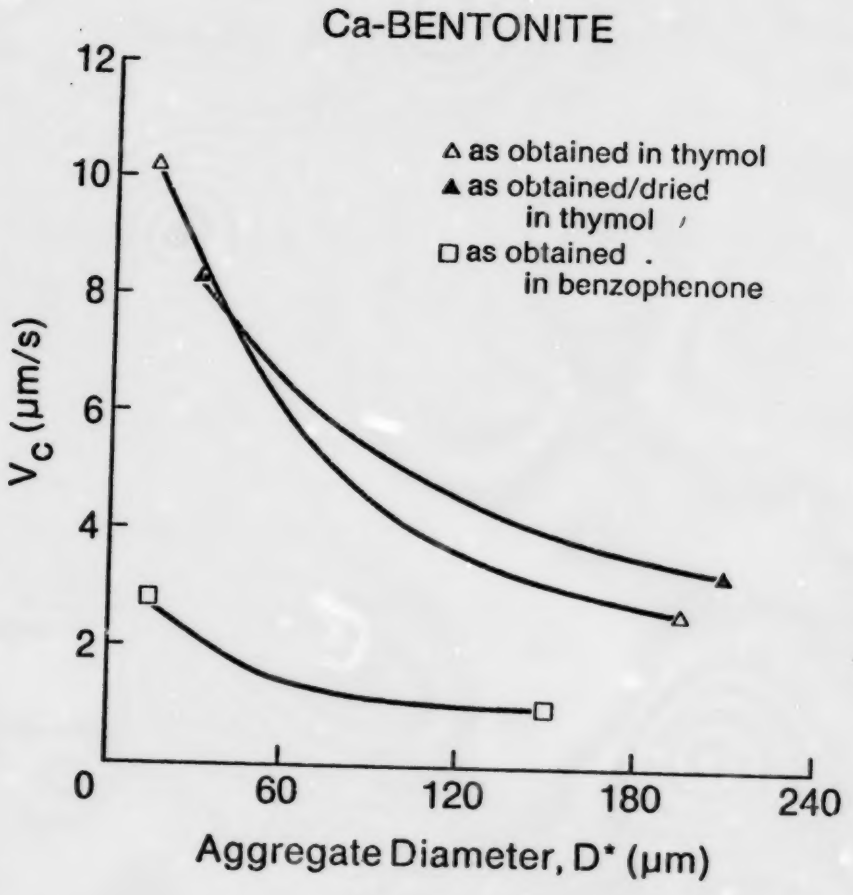

Figure 6

Critical velocity, V_c, versus aggregate diameter, D*, for Ca-bentonite

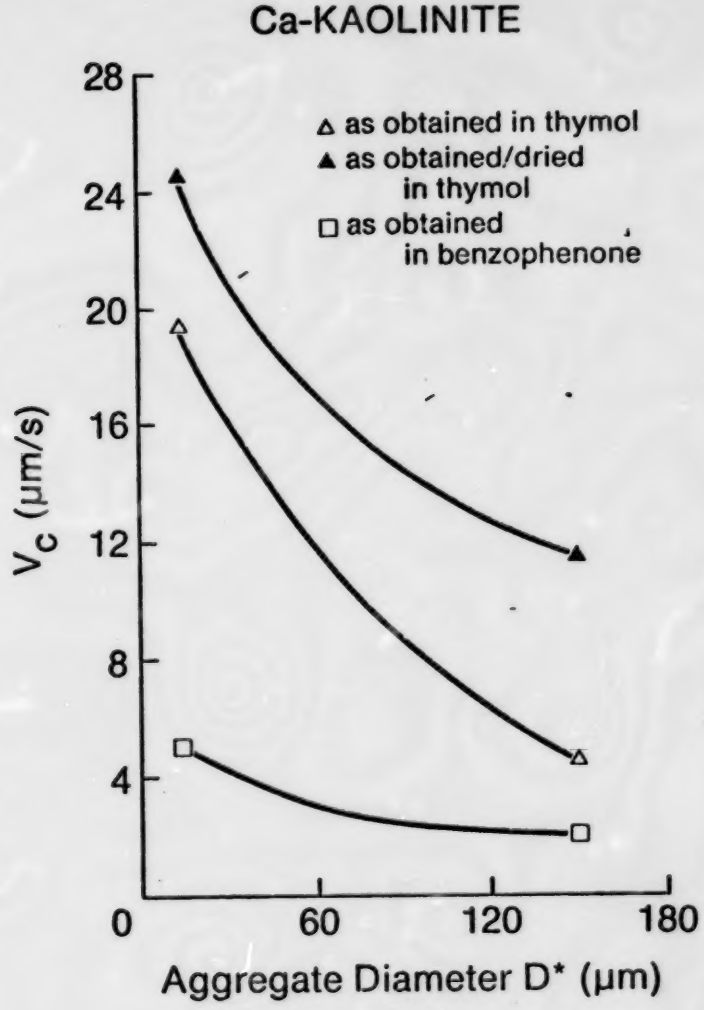

Figure 7

Critical velocity, V_c, versus aggregate diameter, D*, for Ca-kaolinite

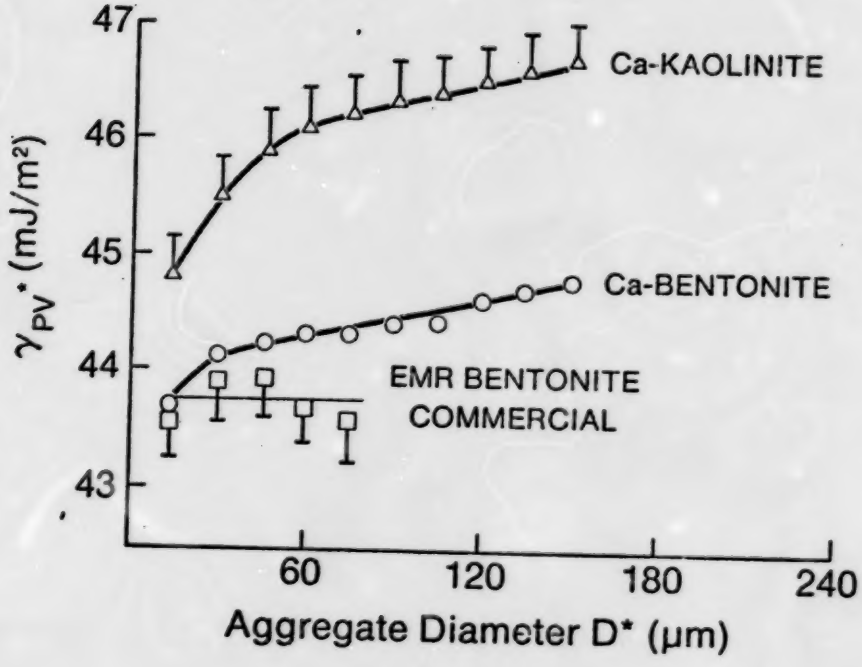

Figure 8

Aggregate surface tension, γ_{PV}*, versus aggregate diameter, D*, for different clays in benzophenone

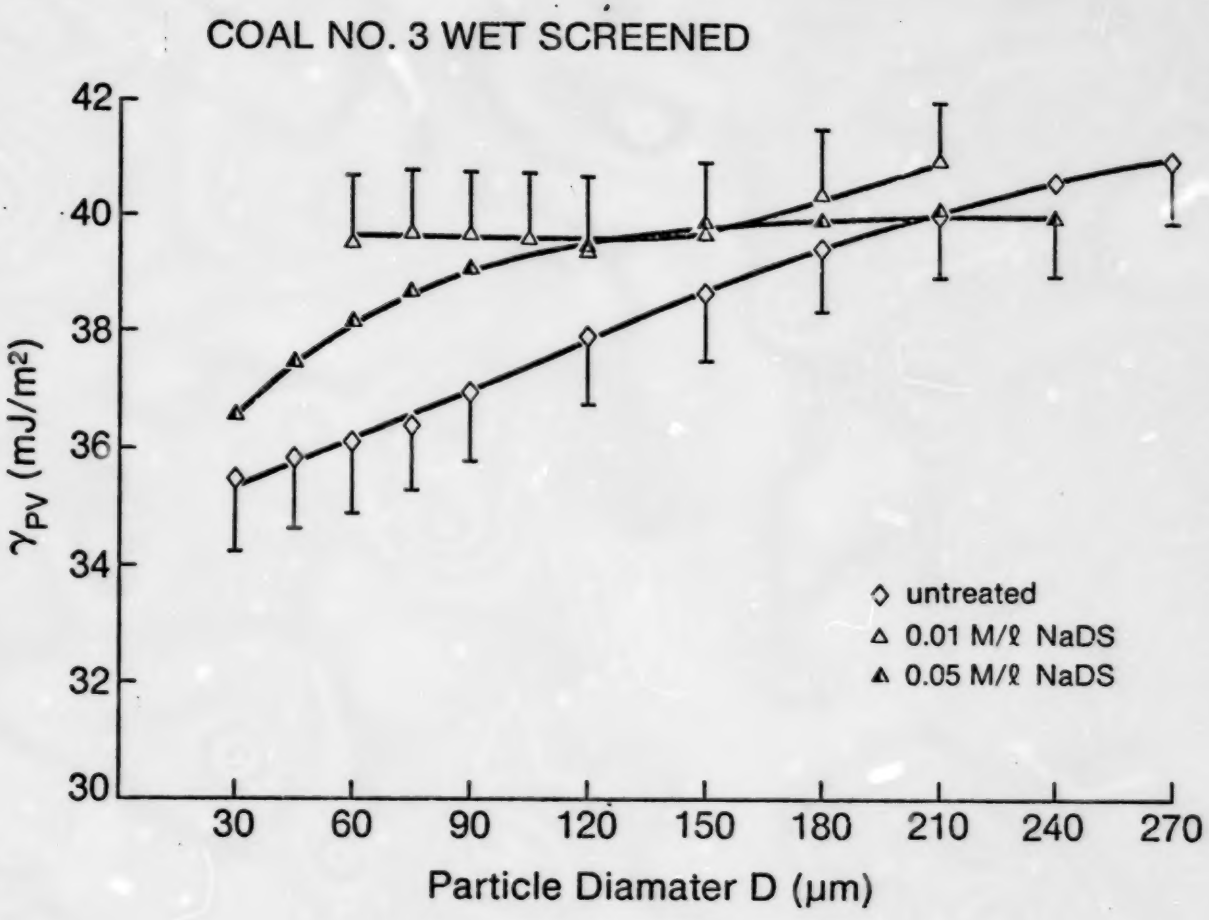

Figure 9

Particle surface tension, γ_{PV}, versus particle diameter, D, for pretreated coal No. 3 wet screened. Pretreatment with NaDS

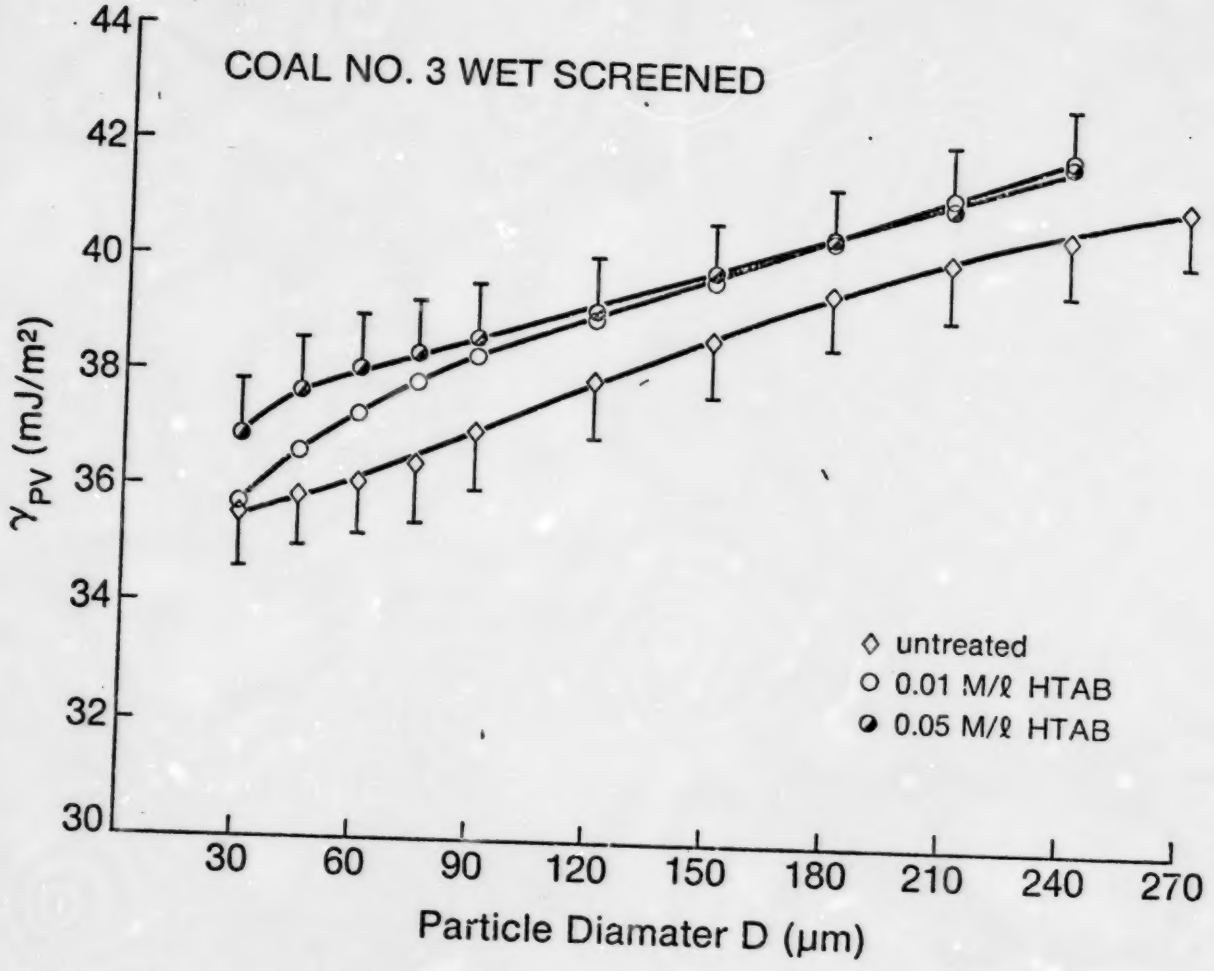

Figure 10

Particle surface tension, γ_{PV}, versus particle diameter, D, for pretreated coal No. 3 wet screened. Pretreatment with HTAB

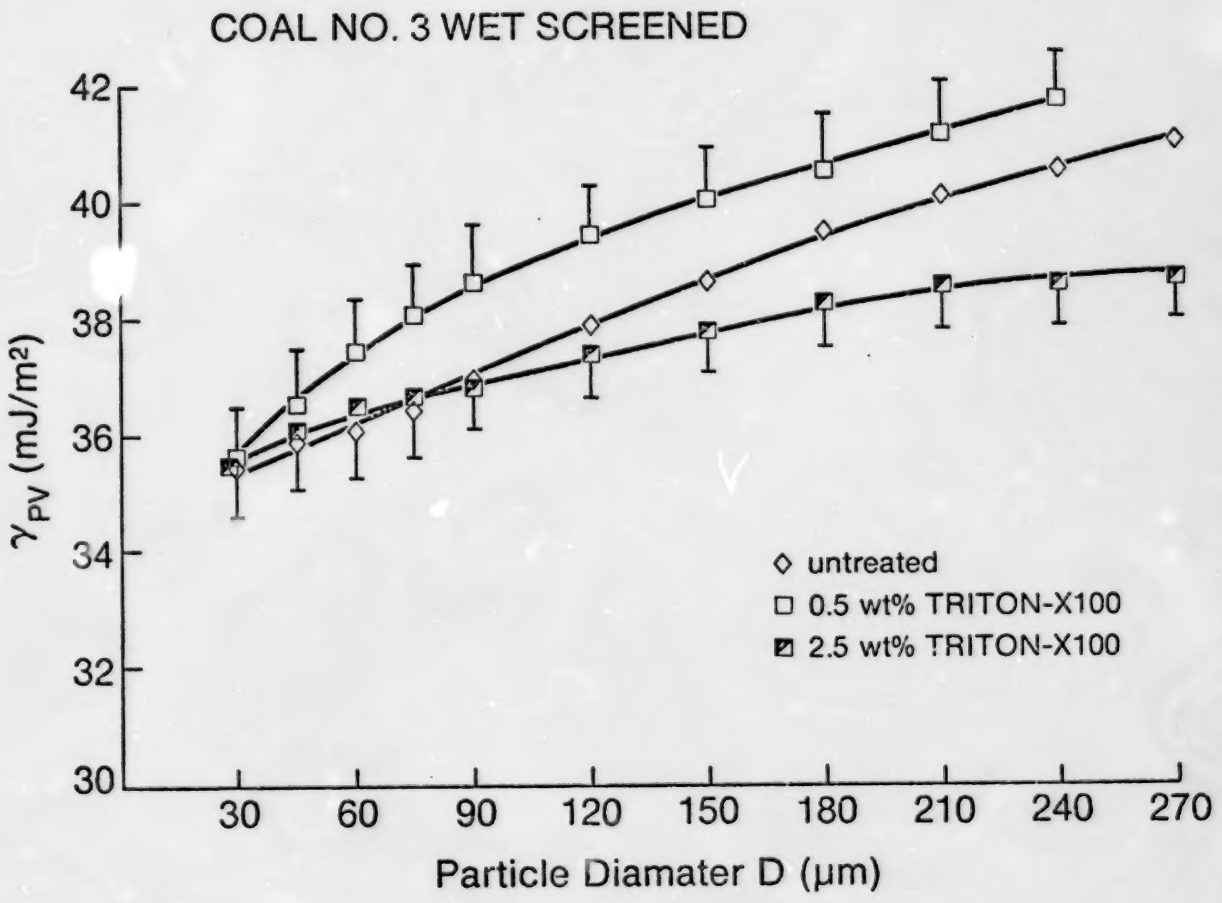

Figure 11

Particle surface tension, γ_{PV}, versus particle diameter, D, for pretreaed coal No. 3 wet screened. Pretreatment with Triton-X100

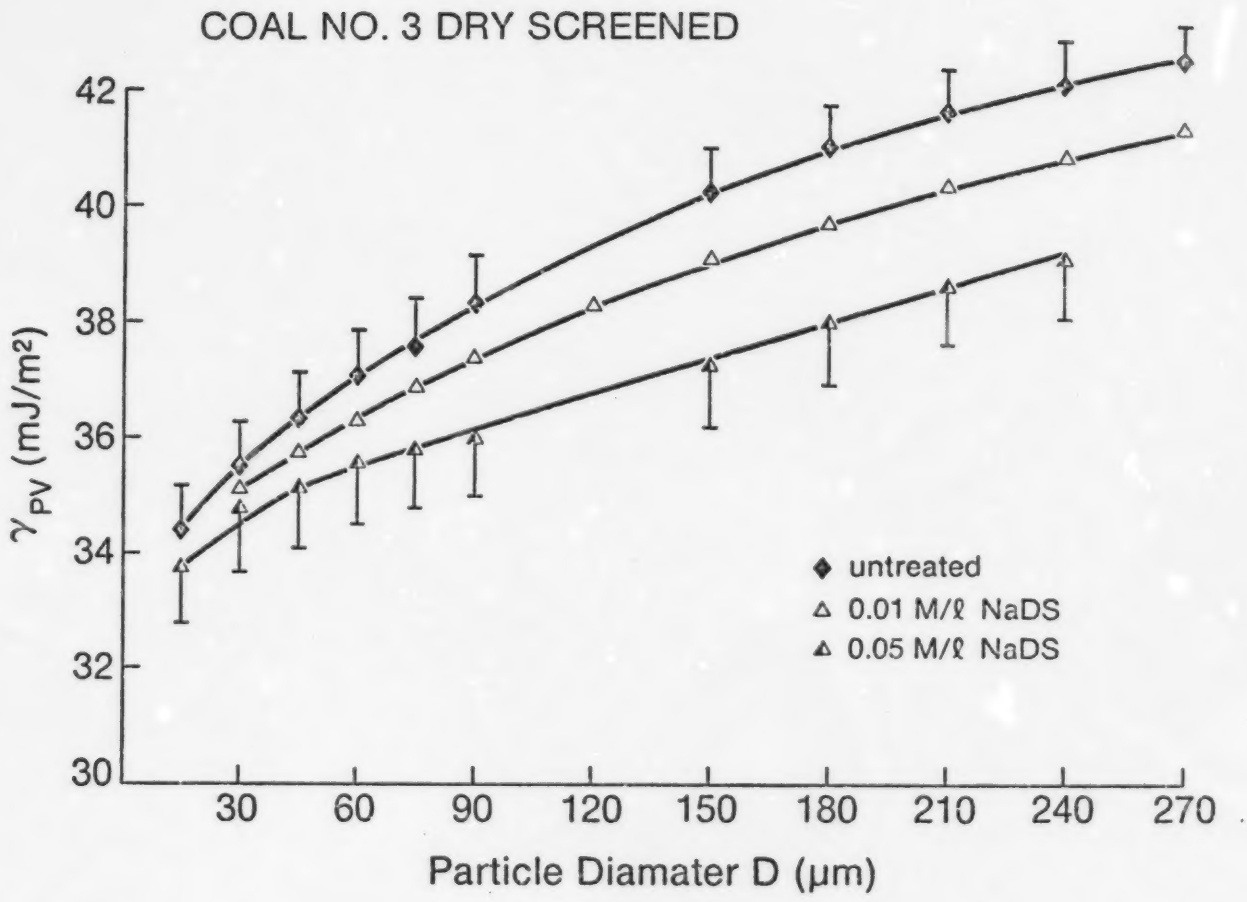

Figure 12

Particle surface tension, γ_{PV}, versus particle diameter, D, for pretreated coal No. 3 dry screened. Pretreated with NaDS

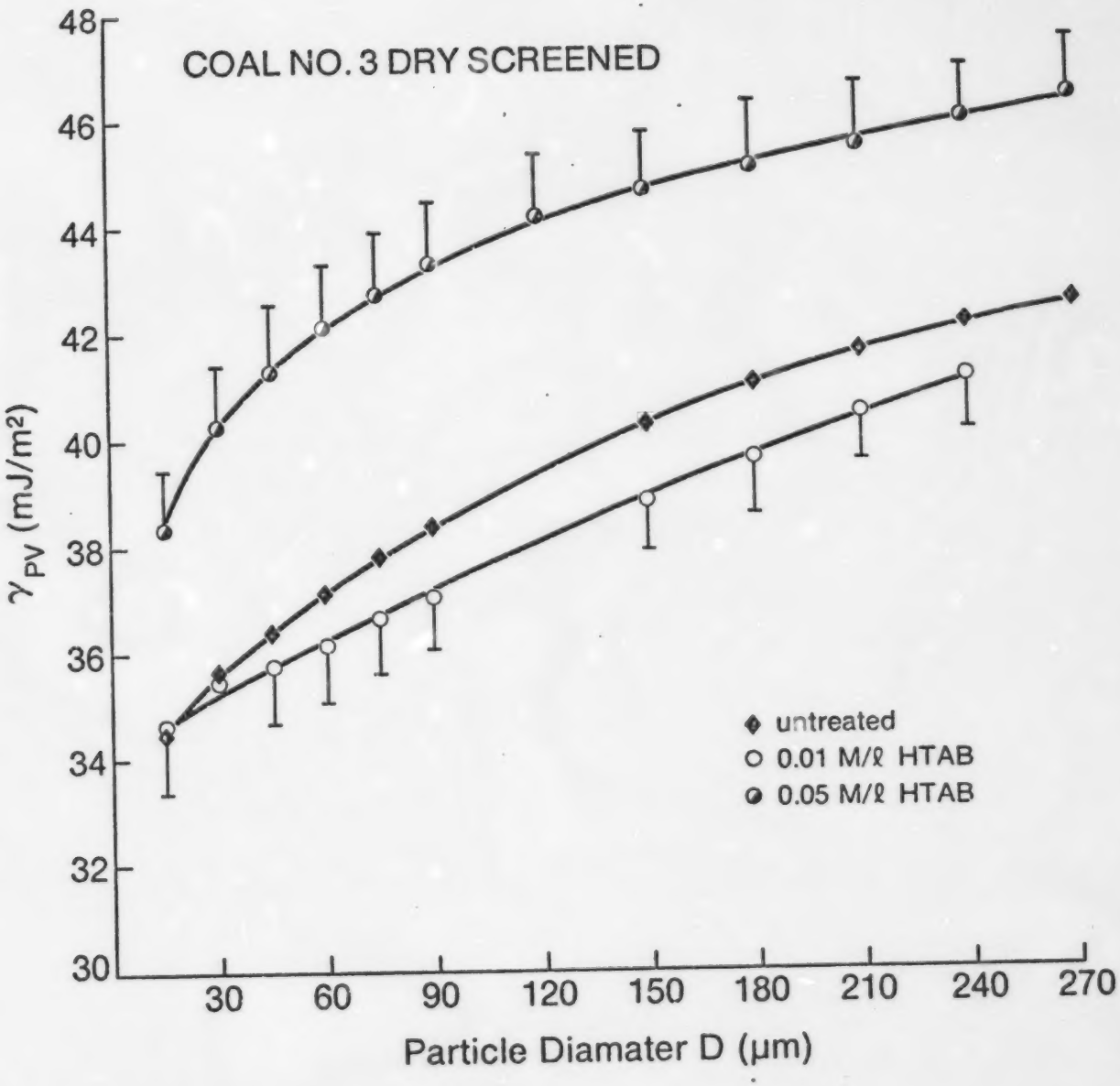

Figure 13

Particle surface tension, γ_{pv}, versus particle diameter, D, for pretreated coal No. 3 dry screened.
Pretreated with HTAB

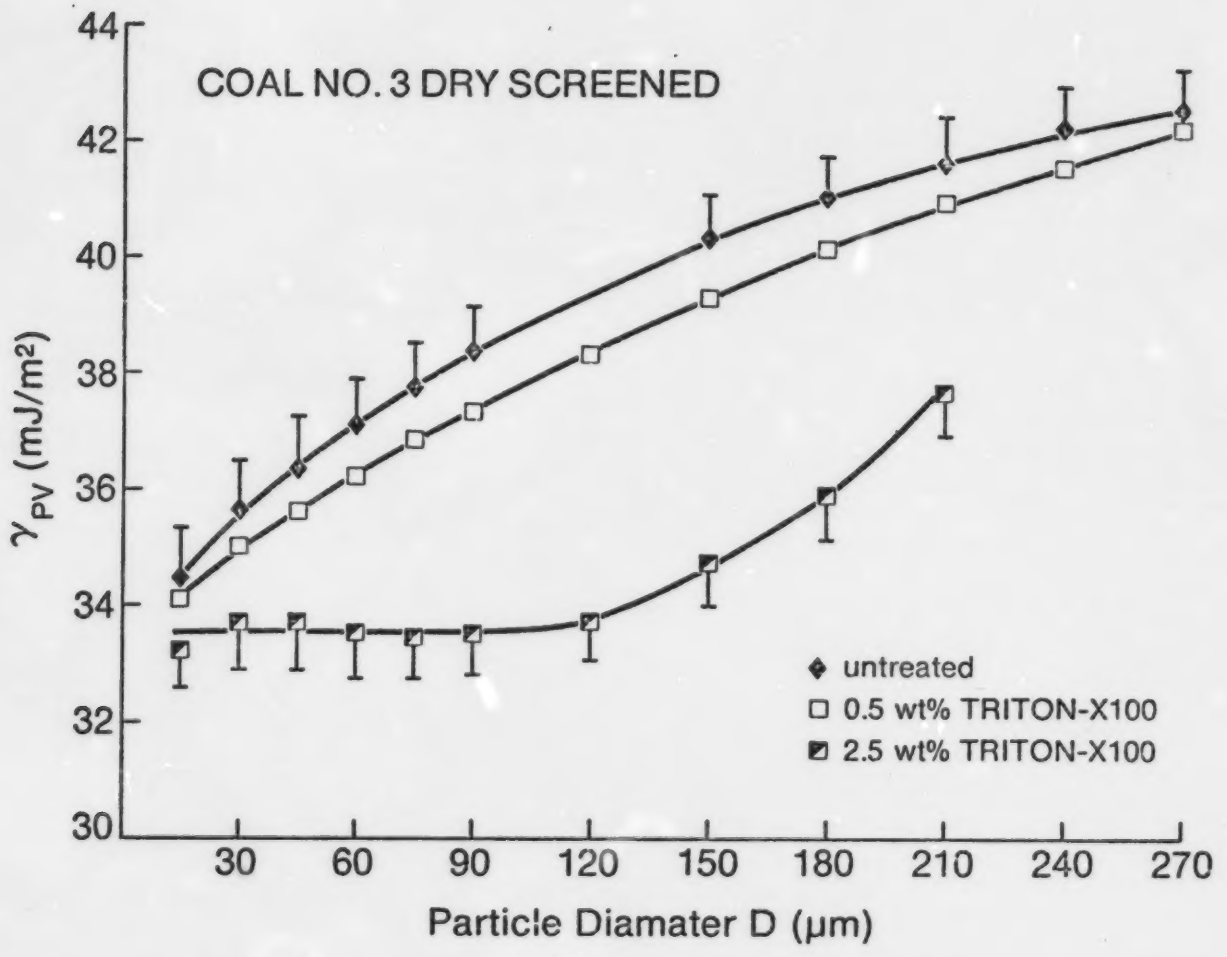

Figure 14

Particle surface tension, γ_{PV}, versus particle diameter, D, for pretreated coal No. 3 dry screened. Pretreated with Triton-X100

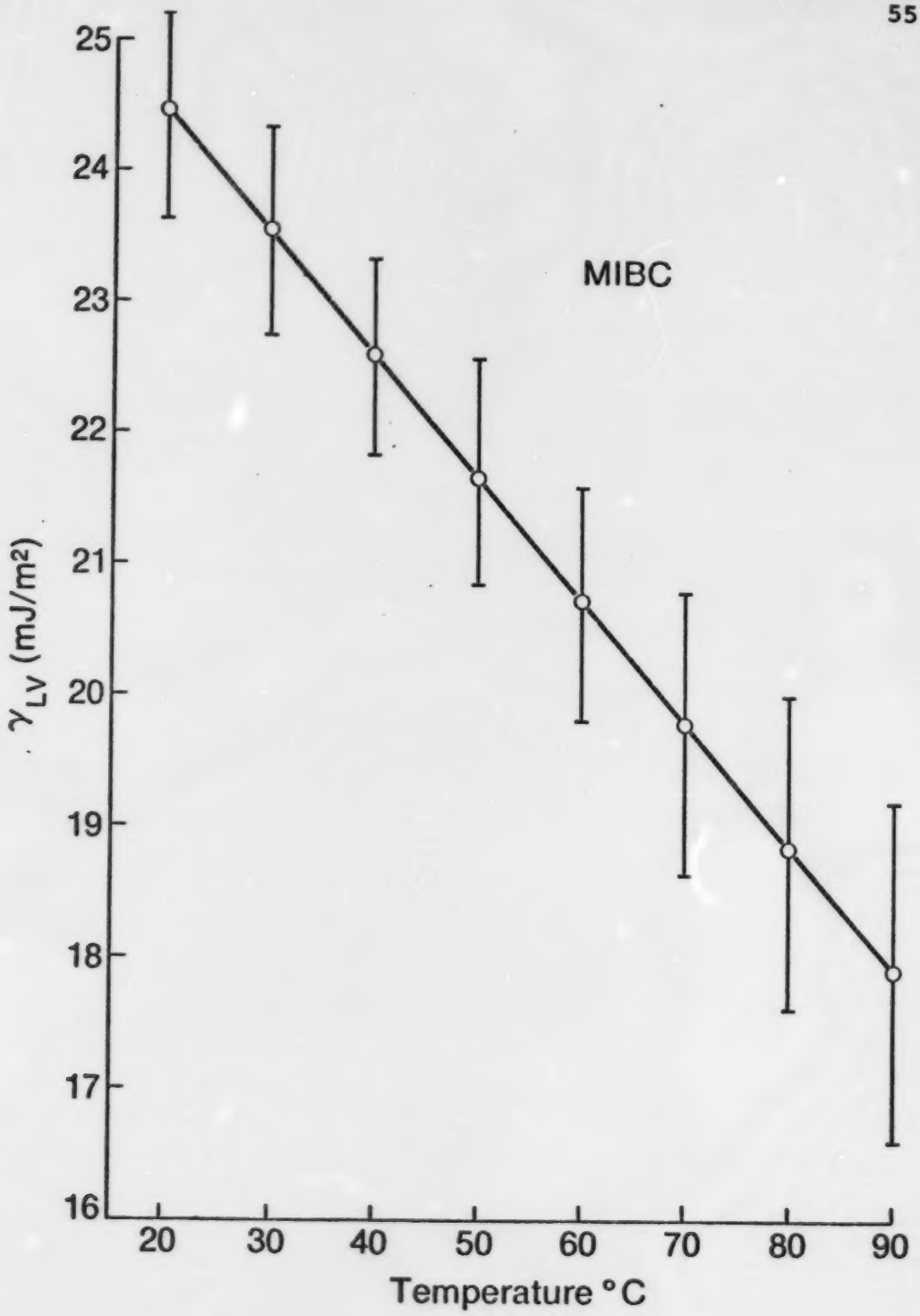

Figure 15

Liquid/vapour interfacial tension, γ_{LV}, versus temperature, t, for MIBC oil

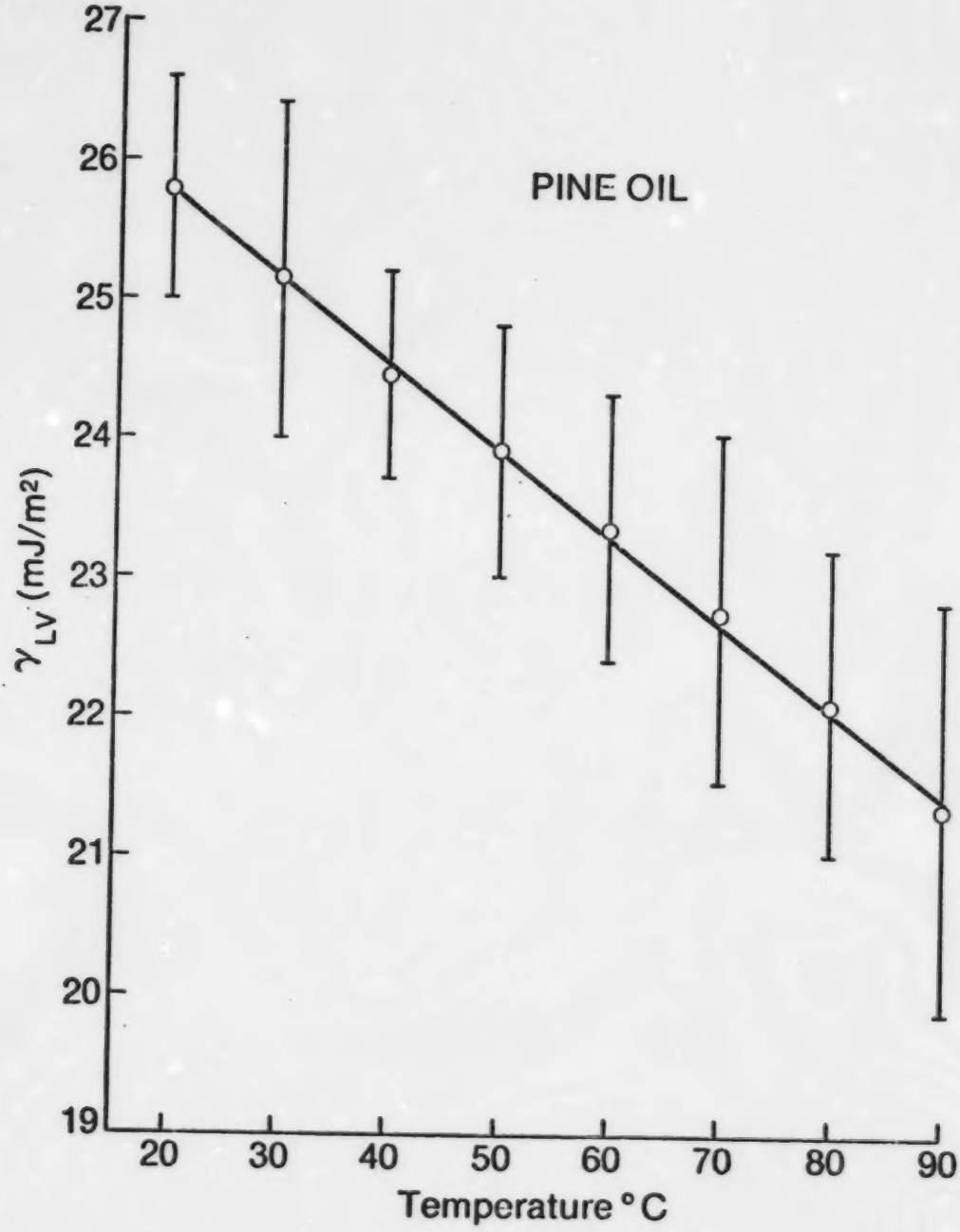

Figure 16

Liquid/vapour interfacial tension, γ_{LV}, versus temperature, t, for Pine oil

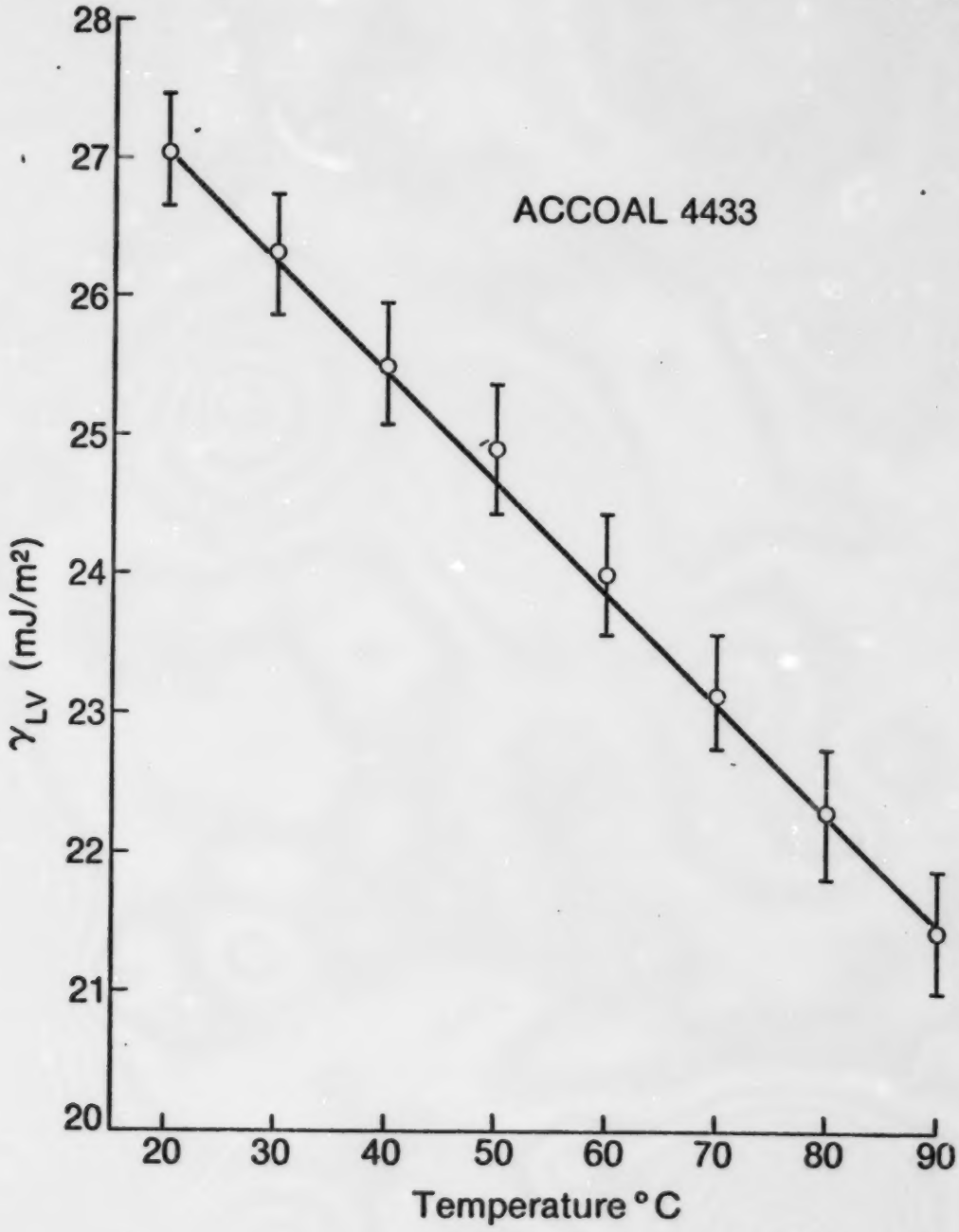

Figure 17

Liquid/vapour interfacial tension, γ_{LV}, versus temperature, t, for Accoal 4433 oil

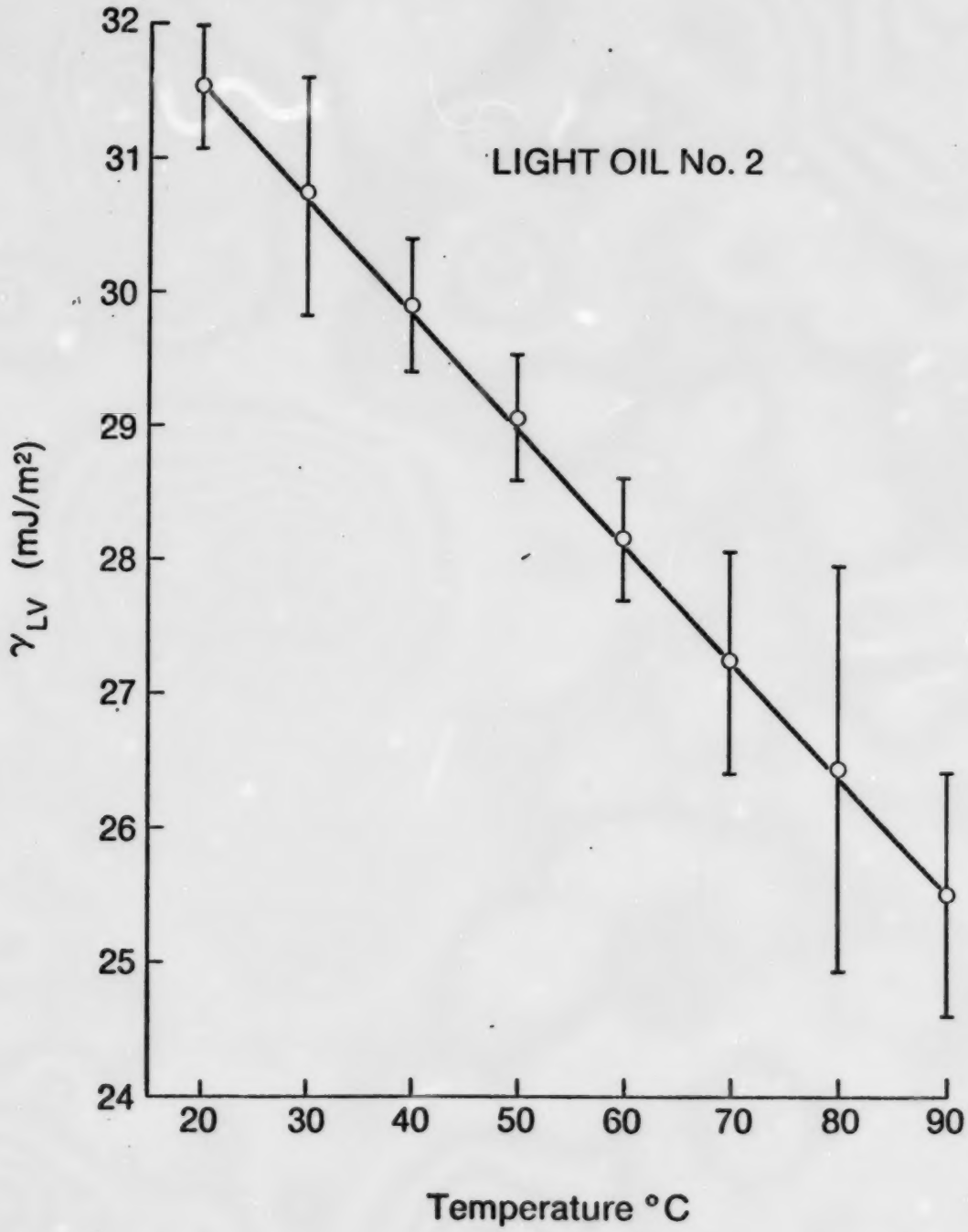

Figure 18

Liquid/vapour interfacial tension, γ_{LV}, versus temperature, t, for Light oil No. 2

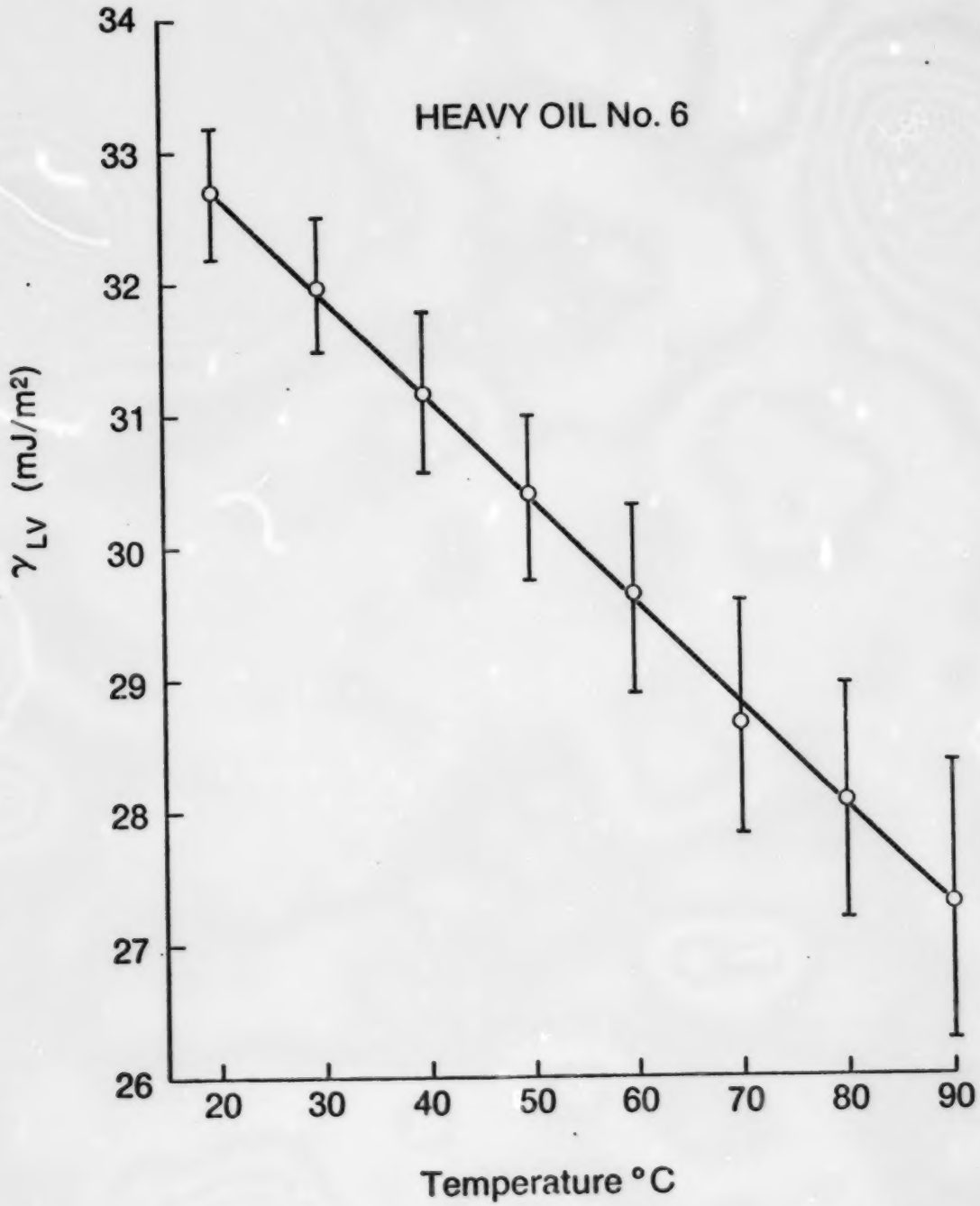

Figure 19

Liquid/vapour interfacial tension, γ_{PV}, versus temperature, t, for Heavy oil No. 6

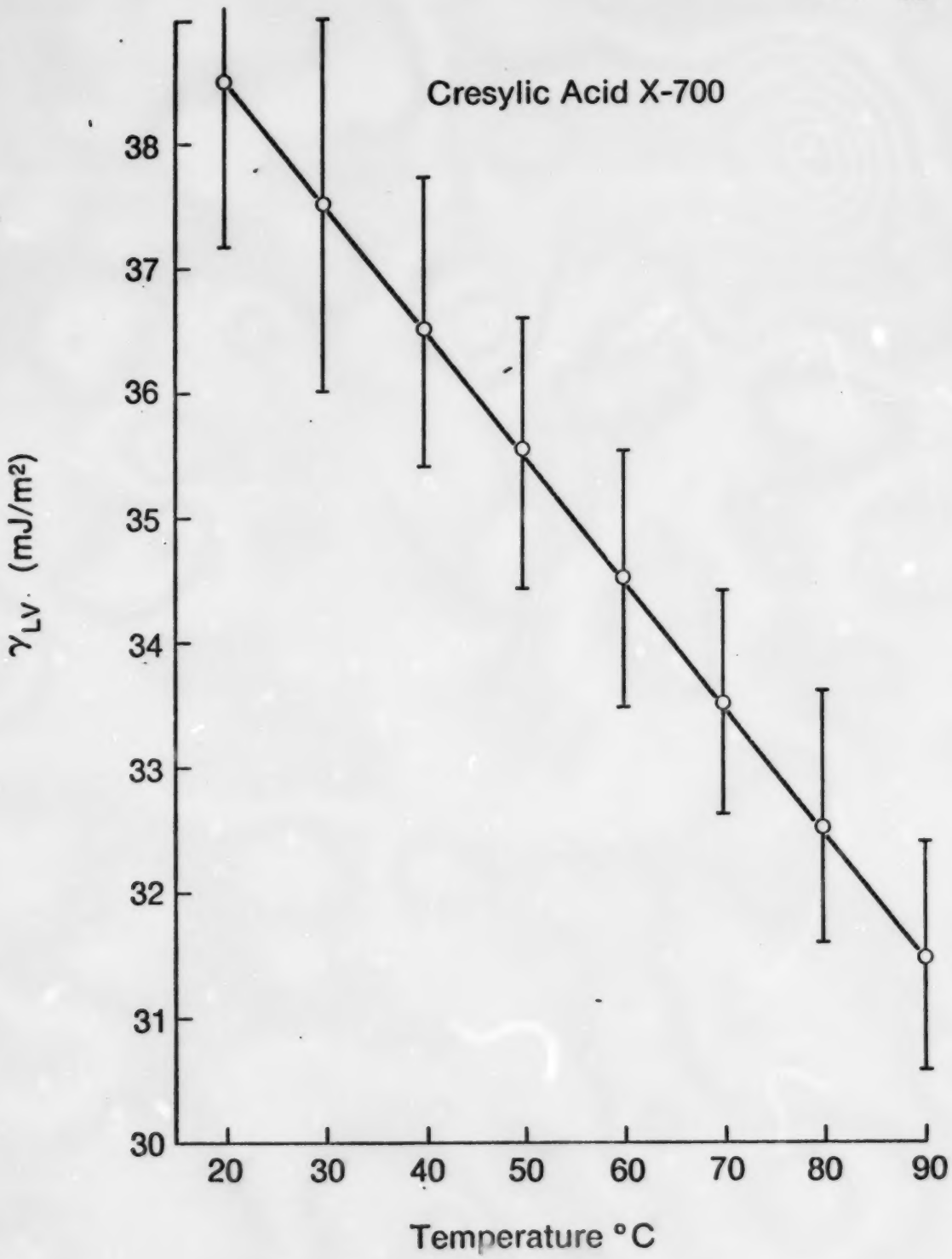

Figure 20

Liquid/vapour interfacial tension, γ_{LV}, versus temperature, t, for Cresylic acid X-700

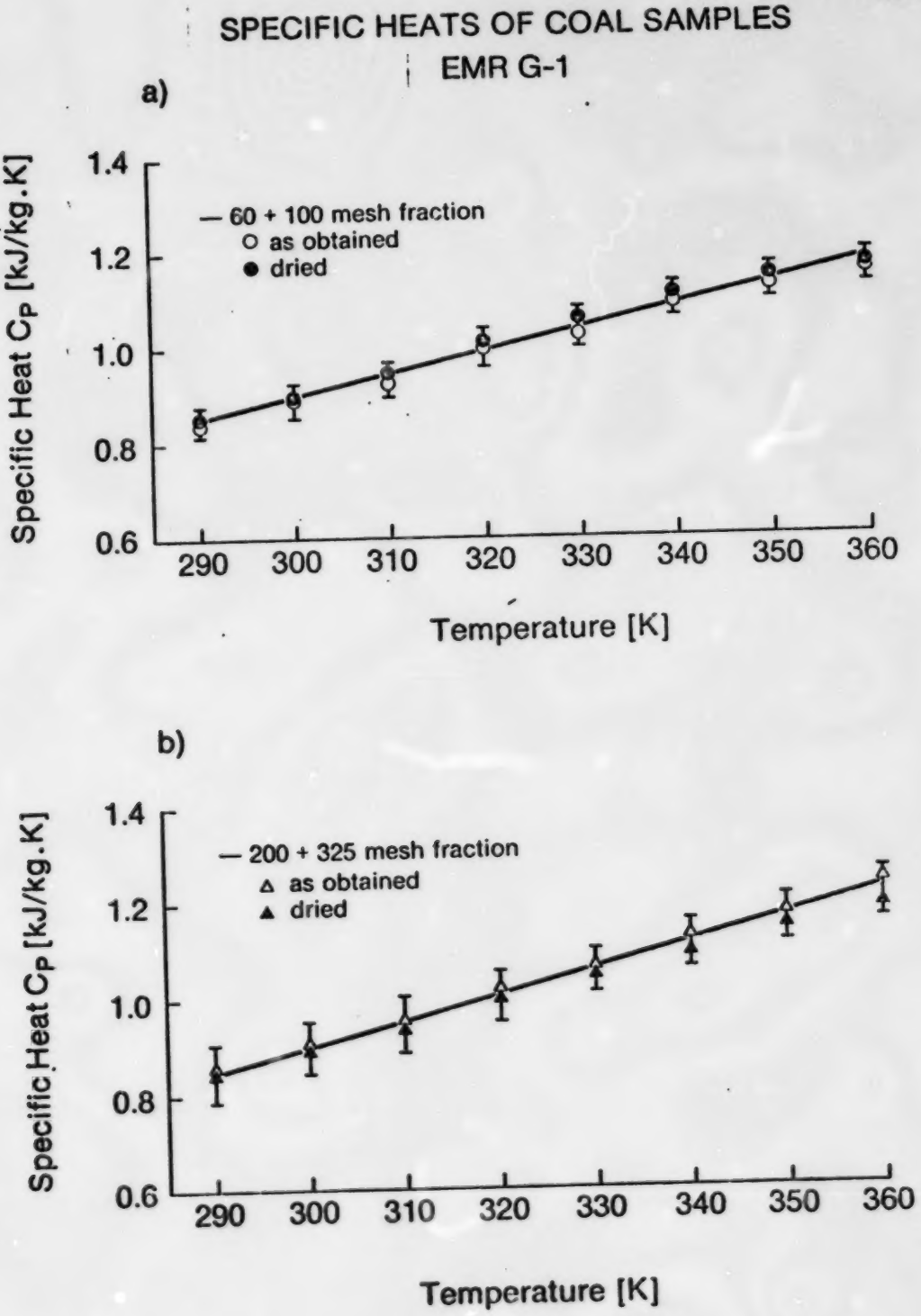

Figure 21

Specific heat, C_p, versus temperature, T, for EMR G-1 coal; a) -60+100 mesh fraction, b) -200+325 mesh fraction

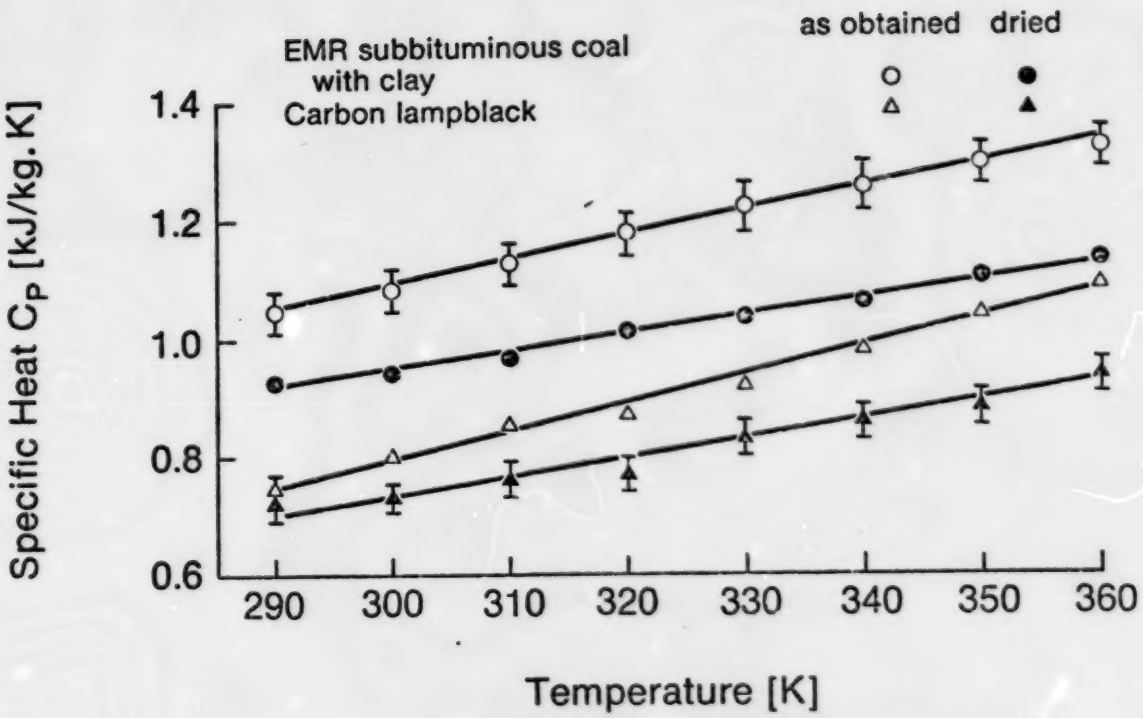

Figure 22

Specific heat C_p, versus temperature, T, for EMR subbituminous coal with clay and carbon lampblack

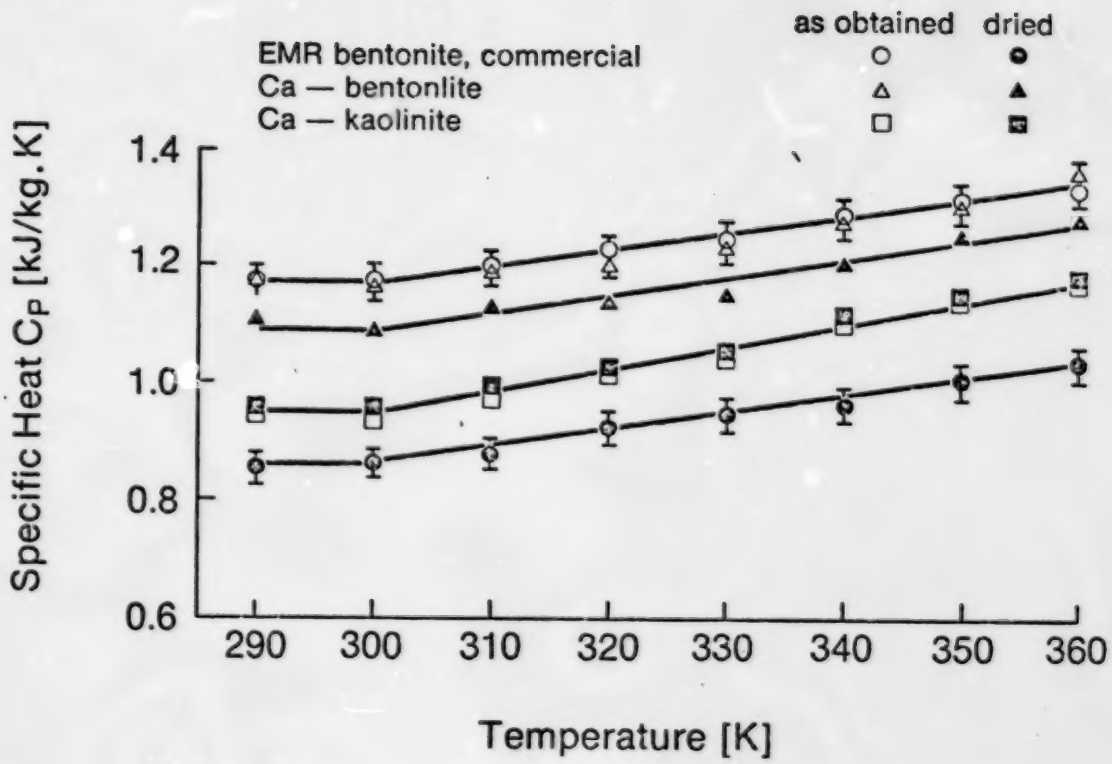

Figure 23

Specific heat, C_p, versus temperature, T, for different clays

APPENDIX No. 1

EFFECT OF AGING ON THE SURFACE CHARACTERISTICS OF COAL POWDERS

E.I. Vargha-Butler[+], T.K. Zubovits[+], R.P. Smith[+], I.H.L. Tsim[+], H.A. Hamza* and A.W. Neumann[+]

[+] Department of Mechanical Engineering
University of Toronto, Toronto, Ontario
M5S 1A4 (Canada)

* Western Research Laboratory, CANMET,
Energy, Mines and Resources, Canada
Edmonton, Alberta, T6G 2C2 (Canada)

ABSTRACT

The particle/vapour interfacial tension, γ_{pv}, of coal powders of different origins was determined by means of the freezing front technique. Both bituminous and subbituminous coals from Western Canada were examined. The experiments were performed with size fractions of -60+100 and -200+325 mesh of freshly mined and aged coal powders. The effect of the preparation of the coal powders (wet and dry screening) and the influence of oven-drying on the surface properties of aged coal were also tested.

The surface tension of coal, γ_{pv}, was found to change with particle size, D. Storage (aging) and preparation of powdered coal has a greater effect on the surface tension than the rank. The presence of water, e.g. in wet screening makes the coal surface less amenable to further oxidation, especially in the case of high ash coal. Bituminous coal with lower ash content becomes more hydrophilic after storage for prolonged times. Dry screened coal was found to have become more hydrophobic due to aging. Oven-drying affects the surface tension of only the dry screened samples of all coals.

INTRODUCTION

Beneficiation and utilization of coal powders involves processes such as froth flotation and mixing the coal powders with oil or water. In these processes, the wettability of the coal powders by various liquids will therefore play an important role. To characterize the wettability of coal powders, one has to determine the surface tension, γ_{pv}, of the coal particles. Methods for the measurement of the surface properties of small solid particles have not been available in the past. However, a novel technique has been developed in our laboratory for the determination of the surface parameters of solid particulate matter such as polymer particles [1,2,3,4]. This method, called freezing front technique, interprets quantitatively the engulfment or rejection of the particles, embedded in the melt of a matrix material, by a solidification front. The technique, which depends on microscopic observation of the interaction of the particles with the solidification front, was recently extended to determine the surface tension of powdered coal [5,6] and oil sand residues [7].

The freezing front technique proved to be a powerful method to characterize the wettability of coals from different origins and to detect differences and changes in the hydrophobicity of coal powders which could play a role in flotation [5,6].

As the coal fines are rarely utilized immediately after mining, the bulk and surface properties of the powdered coal might change during storage. The particle size, porosity, the surface area, rank, mineral and water content and the preparation

technique (temperature of grinding, wet and dry screening) may all contribute to its final properties.

The possibility of autogenous oxidation of stored coal powders is widely known. To prevent the oxidative deterioration of coal during transport and storage, current techniques seek to control loss of moisture from coal and access of water and oxygen to it [8]. But the access of water might change the surface and/or bulk properties. As Karr [9] pointed out, in the case of sizing of pulverized coal the main problem encountered is the possible interaction of the coal with the fluid medium used. Robin and Rouxhet [10] surmised that the molecular water in coal is not simply physically adsorbed but it can be retained by chemical interaction with the surface. It means that partly the moisture content of the raw coal and partly the water added during the sizing process or storage might be responsible for changes in the hydrophobicity of the powdered coal.

The storage of lower rank coal, particularly of coal with higher volatile matter content, may result in oxidation even at ambient temperatures [8,11]. The literature on coal oxidation is contradictory. Berkowitz [8] pointed out that overall oxidation rates become dependent on coal porosity and tend to decrease with increasing rank or particle size. Below 70^{o}C and for low-rank coal, specific chemical composition and moisture will lead to spontaneous oxidation forming acid functional groups and peroxides. But further oxidation, leading to formation of humic acids, is very slow at ambient temperature. Chamberlain et al. [12], Ohochi et al. [13] and Dugan et al. [14] agreed that the

dry oxidation of coal proceeds even at ambient temperature and the degree of oxidation depends on the rank, volatile matter and moisture. On the other hand, Jensen et al. [15] found little or no reaction below 180°C when subbituminous coal was oxidized.

Low rank coals are usually contaminated by clay and other minerals. Painter and Coleman [16] found that clay minerals in coal are relatively uneffected by low temperature oxidation.

In view of the apparent complexity of the changes of the properties of coal under various influences, it was decided to study the change in the wettability of coal powders with time. To this end, the surface tension of various coal powders was studied at intervals of up to two years. Both bituminous and subbituminous coal was examined. While the earlier results [5,6] showed a particle size dependence of the surface tension of coal powders we wanted to ascertain that this dependence is not an artefact of the freezing front method but a feature of the heterogeneity of the coal powders. Therefore, measurements with a chemically homogeneous polymer will also be reported.

It was not clear whether wet or dry screening of coal has any influence on the surface properties of coal powder after subsequent aging. For this reason, the effect of the preparation was studied. Finally, the influence of oven-drying on the surface parameters of coal particles was also examined.

All of the coal powders originated from Western Canada and were provided by EMR, CANMET, Western Research Laboratory, Edmonton, Alberta, Canada.

MATERIALS

1. Matrix materials

The freezing front experiments were performed using thymol as matrix material with the exception of the measurements with polymer powders, where salol (phenyl salicilate) and benzophenone (diphenyl ketone) were also used. Thymol and benzophenone were supplied by Fisher Scientific and salol was an Eastman product. All matrix materials were zone refined prior to the measurements. The thermal and physical properties of the matrix materials are given in Table 1.

2. Polymer particles

Three polymers were chosen: poly(vinyl chloride), PVC, poly(acetal) resine, acetal and poly(methyl methacrylate), PMMA. They were Polysciences Inc. products. The particle size varied from 20 to 60 μm in diameter for PVC and PMMA and from 30 to 150 μm for acetal. The physical properties of the polymer samples are summarised in Table 2.

3. Coal samples

Four types of coal were studied:

Coal No.1: Quintette Area, Northeastern British Columbia,

Coal No.2: Mountain Park Area, Alberta,

Coal No.3: Judy Creek Area, Northern Alberta, and

CN-5A: Crownest Pass Area, Alberta-British Columbia border.

Coal No.1, No.2 and CN-5A were medium volatile bituminous samples, while No.3 was a subbituminous coal with high ash

content. Three of the samples were dry ground and wet screened (No.1, 2 and 3). Coal CN-5A and one portion of No.3 were dry screened after grinding. Samples of two size fractions of -60+100 and -200+325 mesh were used for the experiments. The coal powders were stored at room temperature in well-closed bottles without being exposed to either light or heat until use. A portion of each of the aged samples was dried in an oven at 105°C for six hours and then kept in a desiccator prior to the measurements.

The physical properties of the coal samples "as obtained" are given in Table 3. The density of the coal samples was determined by means of sample volume measurements using a null pycnometer, the surface area by the BET method (helium - nitrogen) and the specific heat was determined by means of differential scanning calorimetry. The ash content was determined according to ASTM #D 3174. Finally, the moisture content was obtained by measuring the loss of weight after drying in an oven at 105°C. The moisture content determination was repeated after storage (aged samples) for each sample fraction.

FREEZING FRONT EXPERIMENTS

1. Method

At low solidification rates, particles embedded in a melt may be either rejected or engulfed when encountered by the solidification front. The freezing front experiment involves the determination of the critical velocity, V_c, of engulfment. At low solidification rates, all particles in the melt will be

rejected by the solidification front, if the particle/vapour interfacial tension, γ_{PV}, is higher than the liquid/vapour surface tension, γ_{LV}, of the matrix material, i.e. $\gamma_{PV} > \gamma_{LV}$. (If $\gamma_{PV} < \gamma_{LV}$, the particles will be engulfed even at low solidification rate). As the rate of solidification increases, the hydrodynamic drag force opposing the particle motion will increase. At a certain rate, called critical velocity, V_c, the two forces become equal and engulfment occurs. V_c can be determined experimentally by microscopic measurements and correlated with the free energy of adhesion (ΔF^{adh}) by means of a scheme of dimensional analysis [2,4]. If the various physical properties both of matrix material and particles are all known, ΔF^{adh} can be calculated using the following expression [5]:

$$\Delta F^{adh} = 6070 \left[\frac{\rho_L^{0.6854}\ T^{0.3995}}{\mu^{0.0849}}\right]\left[\frac{k_P^{0.6005}}{(\rho_P\ C_P)^{0.2009}}\right] D^{0.4844}\ V_c^{0.6854} \quad (1)$$

where

ΔF^{adh} = free energy of adhesion (mJ/m^2);

ρ_L = density of matrix material (kg/m^3);

T = melting point of matrix material (K);

μ = viscosity of matrix material ($N.s/m^2$);

ρ_P = density of particle (kg/m^3);

k_P = thermal conductivity of particle (J/m.s.K);

C_P = specific heat of particle (J/kg.K);

D = particle diameter (m);

V_c = critical velocity (m/s).

The next step is the determination of the particle/vapour interfacial tension, γ_{PV}, from the ΔF^{adh} value. Calibration curves of γ_{PV} versus ΔF^{adh} are available for each matrix material considered here. For more details see References [2,3,4,6,17,18].

2. Apparatus

Particle interaction with the solidification front is studied in a copper chamber. The matrix material and particles are placed in the cell and covered by a glass slide. Freezing is initiated by establishing a temperature gradient along the solidification cell and then lowering the overall temperature. This is accomplished by heating or cooling each end of the copper cell by means of thermoelectric devices. The amount of heat transfer by each thermoelectric device is determined by a feedback controller. The temperature at each end is measured by a thermistor. This temperature is compared with the programmed value, producing an error signal which is amplified by the bipolar controller which in turn powers the thermoelectric device. This is done independently for each end of the copper cell. Water circulating through the aluminum heat sink removes heat from the thermoelectric devices. The maximum temperature gradient is $10^{o}C/cm$ in the cell. The maximum rate of cooling is $0.1^{o}C/sec$.

With this apparatus, the velocity and the profile of the solidification front can be controlled easily. This particular freezing front cell set-up was designed [19] for organic matrix

materials for temperatures ranging from ambient up to approximately 100°C.

The interaction between the particle and the solidification front is observed through a reflected light microscope.

RESULTS

1. Surface tension of polymer particles

In order to establish a basis for comparing the subsequent results for coal with results for more homogeneous particles, we first present typical results obtained for acetal, PMMA and PVC particles.

The solidification front velocity, V, versus particle diameter, D, for acetal/benzophenone, is shown in Fig.1. There are three modes of particle interaction distinguished by different symbols and referred to as "rejection", "transition" and "engulfment". The existence of these three modes reflects the fact that the transition from "rejection" to "engulfing" is not sharp. The two broken curves separate "transition" from "engulfment" and "rejection". The central solid line represents the critical velocity, V_c. The critical velocity curve for two other polymers, PMMA and PVC, both measured in thymol as a function of particle diameter, D, is given in Fig.2. The free energy of adhesion, ΔF^{adh}, was calculated from the V_c data using equation (1). The particle surface tension, γ_{PV}, was then obtained from the calibration curves of γ_{PV} versus ΔF^{adh} given for the different matrix materials (see Method). All these data

for the four polymer/matrix systems at the melting temperature of the matrix materials are summarized in Table 4.

From the results given in Table 4 it is evident that within the particle size range measured, the surface tension of the polymer particles is independent of particle size, as expected.

The surface tensions of PMMA (the last two systems in Table 4) measured with thymol and salol are in good agreement when we consider that due to the difference in the melting points of the two matrix materials, the particle surface tension in salol should be approximately 0.5 mJ/m^2 higher than in thymol.

2. Surface tension of coal particles

The freezing front experiments were performed with 15 different coal powders. These consisted of five intrinsically different coal samples, which were studied in three different conditions:

a. freshly mined ("as obtained")

b. aged

c. aged and dried

The rank, the type of the preparation, the age (storage time) and the condition of the sample are summarized in Table 5. The critical velocity, V_c, of the coal particles was measured with thymol as matrix material for all of the samples. The results given below for coal are obtained at the melting temperature of thymol ($51.5^{o}C$).

The critical velocity, V_c, versus particle diameter, D, for the "as obtained" No.2 and No.3 wet screened as well as No.3 dry screened samples (#4,7,10, Table 5) are plotted in Fig.3. These

results were obtained in 1979 from experiments with freshly mined and sized coal powders. Coal No.1 was initially so hydrophobic that all the particles were engulfed even by thymol at very low solidification rates. Thymol has the lowest surface tension (γ_{LV} = 29.9 mJ/m^2 at 51.5^{o}C), among the matrix materials available at this time. The significance of this finding is that particles with a surface tension γ_{PV} less than γ_{LV} of the matrix material are engulfed, i.e. all that could be established at that time was that the surface tension of coal No.1 was less than 29.9 mJ/m^2. Coal sample CN-5A was originally measured as fresh coal powder (#13, Table 5) in 1980, but the particle size dependence was not investigated in detail. Instead, V_c was determined for the two size fractions (-200+325 and -60+100 mesh). These results are also indicated in Fig.3, by using the average particle sizes for these two mesh fractions.

The surface tensions, γ_{PV}, of the coal particles were calculated from the data of Fig.3 as explained above. The results are plotted in Fig.4. Similar plots for the aged coal powders No.1, No.2 and No.3 wet screened as well as for No.3 and CN-5A dry screened are given in Figs. 5 and 6. Fig.5 represents data for the aged powders (#2,5,8,11 and 14, Table 5) and Fig.6, the results for the corresponding aged/dried samples (#3,6,9,12 and 15, Table 5). The errors given in the Figures are 95 percent confidence limits; only the upper or lower segments of the error bars are shown for the upper and lower curves, respectively, to avoid graphical overlap. The errors are similar for those cases where no error bars are shown.

The results for one wet screened (coal No.2) and for one dry screened (coal No.3) are summarized in Tables 6 and 7, as examples. It is apparent that γ_{PV} changes with particle size, in contradistinction to polymer particles, see Table 4.

DISCUSSION

a) Effect of aging on the surface tension of coal particles

In order to evaluate the effect of aging on the surface properties of the coals investigated, Fig.5 has to be compared with Fig.4.

The results for two wet screened samples, No.2 and No.3 are within the error limits, i.e., the surface tension is unchanged after two years of aging. However, coal No.1, which was so hydrophobic in 1979 that we could only establish that its surface tension γ_{PV} was less than 29.9 mJ/m^2 at 51.5^{o}C, had become significantly more hydrophilic. For small particles the surface tension has increased to 36 mJ/m^2 and for the largest particles to 43 mJ/m^2, see Fig.5.

Dry screened coals became more hydrophobic due to aging. The effect seems to be less dependent on particle size than in the case of the wet screened sample. The decrease in γ_{PV} is particularly large in the case of coal CN-5A, i.e. approximately 8 mJ/m^2. It was assumed that average particle diameters of 75 µm and 210 µm could be assigned to the two mesh sizes -200+325 and -60+100, respectively. The results of the aging measurements with the various coals for these two size fractions are summarized in Table 8.

b) Effect of oven-drying on the surface tension of aged coal

To evaluate the effect of oven-drying on the surface properties of the aged coal, the data of Figs.5 and 6 have to be compared, see Fig.7. We infer from Fig.7a that drying of wet-screened coal has no effect on the surface tension, γ_{PV}, at all. In the case of the dry-screened coals (Fig.7b), oven-drying renders both coals (No.3 and CN-5A) more hydrophilic, but not at small particle sizes. The results of the oven-drying for the two average particle sizes are also summarised in Table 8.

Thus, in summary, we infer that neither aging nor drying after aging has a significant effect on the wet screened coal samples, with the exception of No.1, which shows a considerable change due to aging (but not due to drying). It is interesting to note that aging imparts identical surface tensions to the two bitumenous coals, No.1 and 2, whereas the surface tension of the subbitumenous coal No.3 remains quite different.

Dry screened coal samples, on the other hand, show a very different response to aging and subsequent drying. Aging causes the surface tension, γ_{PV}, both of No.3 and CN-5A to decrease. Subsequent drying causes γ_{PV} to increase again, in the case of No.3 to exactly the initial value prior to aging.

While conclusive reasons for these patterns of behaviour cannot be given at this time, one might speculate as follows: In the wet screening process, the coal samples No.2 and No.3 acquire a protective water layer, the sorption of which is induced by their relatively high content of inorganic matter. This layer might subsequently prevent further oxidation. Coal No.1, on the

other hand, because of its low content of inorganic material, would not adsorb water significantly and would therefore remain amenable to further oxidation. Drying after the aging might or might not remove any adsorbed water. If adsorbed water was removed, then the coal might not have had sufficient time for further oxidation.

In the case of dry screening, diffusion of low molecular weight hydrocarbons to the surface might have rendered the coal more hydrophobic during the aging process. Subsequent drying might have removed these hydrocarbons from the surface, making the coal samples again about as hydrophilic as they were originally.

SUMMARY OF FINDINGS

1. A variation of the surface tension of coal with particle size was found.
2. Aging of powdered coal may cause changes in the surface properties.
3. The preparation (wet screening versus dry screening) of coal powders plays a more important role than the rank of the coal.
4. For coal with higher ash content, wet screening makes the surface of coal powder less susceptible to further change in hydrophobicity.
5. Wet screened coal with low ash content, which is originally hydrophobic, is more hydrophilic after storage.

6. Dry screened coal was found to have become more hydrophobic due to aging. This effect is only observed for larger particle sizes.
7. Drying after storage does not affect the surface tension of the wet screened samples, but makes the dry screened coal more hydrophilic.

ACKNOWLEDGEMENTS

This work was supported by EMR, CANMET Contract No. OSU 81-00232.

REFERENCES

1. S.N. OMENYI and A.W. NEUMANN, J. Appl. Phys., 47 (1976) 3956.

2. S.N. OMENYI, Ph.D. Thesis, University of Toronto, Toronto, Canada, 1978.

3. S.N. OMENYI, R.P. SMITH and A.W. NEUMANN, J. Colloid Interface Sci., 75 (1980) 117.

4. S.N. OMENYI, A.W. NEUMANN, W.W. MARTIN, G.M. LESPINARD and R.P. SMITH, J. Appl. Phys., 52 (1981) 796.

5. M.R. SOULARD, M.A.Sc. Thesis, University of Toronto, Toronto, Canada, 1980.

6. E.I. VARGHA-BUTLER, M.R. SOULARD, A.W. NEUMANN and H.A. HAMZA, CIM Bulletin, 74 (1981) 54.

7. E.I. VARGHA-BUTLER, T.K. ZUBOVITS, Z.M. POTOCZNY and A.W. NEUMANN, (in preparation).

8. N. BERKOWITZ, An Introduction to Coal Technology, Academic Press, New York, 1979, pp. 95-98; 189-194.

9. C. KARR, Jr. (Ed.), Analytical Methods for Coal and Coal Products, Academic Press, New York, 1978, Vol.1 pp. 112-117.

10. P.L. ROBIN and P.G. ROUXHET, Fuel, 55 (1976) 177.

11. G.J. PITT and G.R. MILLWARD (Eds.), Coal and Modern Coal Processing: An Introduction, Academic Press, London, 1979, pp. 63.

12. E.A.C. CHAMBERLAIN, G. BARASS and J.T. THIRLAWAY, Fuel, 55 (1976) 217.

13. H. OHOCHI, M. SHIOTANI and J. SOHMA, Fuel, 48 (1969) 167.

14. P.DUGAN and V.J. MORAN, Fuel, 49 (1970) 415.

15. E.J. JENSEN, N. MELNYK, J.C. WOOD and N. BERKOWITZ, Coal Science; Advances in Chemistry Series No.55, Am. Chem. Soc., New York, 1966, pp. 621-634.

16. P.C. PAINTER and M.M. COLEMAN, American Laboratory, 12 (1980) 28.

17. S.N. OMENYI, A.W. NEUMANN and C.J. VAN OSS, J. Appl. Phys., 52 (1981) 789.

18. R.P. SMITH., M.A.Sc. Thesis, University of Toronto, Toronto, Canada, 1981.

19. D.W. FRANCIS, private communication.

Table 1

PHYSICAL PROPERTIES OF THE ORGANIC MATRIX MATERIALS

SUBSTANCE	DENSITY ρ_L (kg/m³)	VISCOSITY μ (N.s/m²)	SPECIFIC HEAT C_P (kJ/kg.K)	THERMAL CONDUCTIVITY k_P (J/m.s.K)	SURFACE TENSION, γ_{LV} at melting point (mJ/m²)	SURFACE TENSION, γ_{SV} at melting point (mJ/m²)
Thymol	925	0.00397	2.370	0.1298	29.9 at 51.5°C	29.4 at 51.5°C
Salol	1200	0.00889	1.637	0.0837	35.3 at 43.0°C	34.5 at 43.0°C
Benzophenone	1146	0.00516	1.856		39.9 at 48.0°C	34.5 at 48.0°C

Table 2

PHYSICAL PROPERTIES OF THE POLYMER SAMPLES

SUBSTANCE	DENSITY (kg/m^3)	SPECIFIC HEAT (kJ/kg.K)	THERMAL CONDUCTIVITY (J/m.s.K)
PMMA	1250	1.380	0.188
PVC	1400	1.250	0.163
Acetal	1410	1.465	0.230

Table 3

PHYSICAL PROPERTIES OF THE COAL SAMPLES

PHYSICAL PROPERTIES	COAL SAMPLES									
	-60 + 100 mesh					-200 + 325 mesh				
	wet screened			dry screened		wet screened			dry screened	
	No.1	No.2	No.3	No.3	CN-5A	No.1	No.2	No.3	No.3	CN-5A
Density (kg/m^3)	1520	1470	1630	1630	1410	1430	1430	1640	1640	1460
Surface Area (m^2/kg)	550	620	10430	10430	900	720	890	12150	12150	1090
Specific Heat at 51.5°C (J/kg.K)	1078	1118	1144	1188	1158	1182	1193	1128	1108	1212
Ash Content (wt %)	19.38	23.33	28.96	31.03	14.70	10.78	17.03	31.71	39.11	14.89
Moisture Content (wt %) "as obtained"	0.10	0.47	2.33	10.43	0.71	0.45	0.64	2.40	9.47	0.51
Moisture Content (wt %) aged	0.10	0.59	3.34	10.57	0.47	0.51	0.51	3.50	9.10	0.64

Table 4

SURFACE CHARACTERISTICS OF POLYMERS AT THE MELTING TEMPERATURES OF MATRIX MATERIALS

PARTICLE MATERIAL	DIAMETER D (μm)	CRITICAL VELOCITY V_c (μm/sec)	ΔF^{adh} (mJ/m²)	γ_{PV} (mJ/m²)
		in benzophenone at 48.0°C		
Acetal	30	14.0 ± 2.4	0.753 ± 0.090	45.2 ± 0.6
	60	9.5 ± 2.4	0.860 ± 0.150	45.9 ± 1.0
	90	7.3 ± 2.4	0.874 ± 0.200	46.0 ± 1.4
	120	6.5 ± 2.4	0.871 ± 0.220	46.0 ± 1.5
	150	5.7 ± 2.4	0.887 ± 0.260	46.1 ± 1.8
		in thymol at 51.5°C		
PVC	20	1.10 ± 0.17	0.086 ± 0.009	36.1 ± 0.7
	30	0.74 ± 0.11	0.080 ± 0.008	35.6 ± 0.6
	45	0.56 ± 0.09	0.080 ± 0.009	35.6 ± 0.6
	60	0.45 ± 0.07	0.080 ± 0.008	35.6 ± 0.6
PMMA	20	2.20 ± 0.30	0.152 ± 0.014	40.7 ± 1.0
	30	1.50 ± 0.19	0.140 ± 0.012	40.0 ± 0.9
	45	1.10 ± 0.14	0.140 ± 0.012	40.0 ± 0.9
		in salol at 43.0°C		
PMMA	20	1.28 ± 0.14	0.116 ± 0.009	41.0 ± 0.4
	30	0.88 ± 0.16	0.109 ± 0.008	40.7 ± 0.4
	45	0.63 ± 0.10	0.106 ± 0.008	40.6 ± 0.4
	60	0.46 ± 0.80	0.098 ± 0.012	40.2 ± 0.6

Table 5

VARIATION OF COAL SAMPLES INVESTIGATED BY RANK, TYPE OF SIZING, AGE AND CONDITION

TYPE OF SAMPLE	RANK	TYPE OF SIZING	DATE OF MEASUREMENT	No. and SYMBOL OF SAMPLE	CONDITION OF SAMPLE
Coal No.1	bituminous	wet screened	1979	1 ○	"as obtained"
			1981	2 ◐	aged
				3 ◘	aged/dried
Coal No.2	bituminous	wet screened	1979	4 □	"as obtained"
			1981	5 ◪	aged
				6 ▣	aged/dried
Coal No.3	subbituminous	wet screened	1979	7 △	"as obtained"
			1981	8 ◭	aged
				9 ▲	aged/dried
Coal No.3	subbituminous	dry screened	1979	10 ◇	"as obtained"
			1981	11 ◈	aged
				12 ◆	aged/dried
Coal CN-5A	bituminous	dry screened	1980	13 ▽	"as obtained"
			1981	14 ▼	aged
				15 ▼	aged/dried

Table 6

SURFACE CHARACTERISTICS OF COAL No.2
WET SCREENED SAMPLE AT 51.5°C

MATRIX: THYMOL

COAL SAMPLE	DIAMETER D (μm)	CRITICAL VELOCITY V_c (μm/sec)	ΔF^{adh} (mJ/m²)	γ_{PV} (mJ/m²)
	30	10.2 ± 3.2	0.102 ± 0.022	37.2 ± 1.6
Coal No.2	60	8.7 ± 2.9	0.128 ± 0.029	39.0 ± 2.1
"as obtained"	90	7.5 ± 2.4	0.141 ± 0.030	39.9 ± 2.2
1979	150	6.2 ± 1.7	0.159 ± 0.030	41.3 ± 2.1
(#4)	180	5.8 ± 1.6	0.166 ± 0.031	41.8 ± 2.2
	240	5.3 ± 1.6	0.180 ± 0.036	42.7 ± 2.6
	30	9.0 ± 1.3	0.094 ± 0.009	36.6 ± 0.7
Coal No.2	60	6.5 ± 0.9	0.105 ± 0.010	37.4 ± 0.7
aged	90	6.2 ± 0.8	0.123 ± 0.011	38.7 ± 0.8
1981	150	5.8 ± 0.8	0.152 ± 0.014	40.8 ± 1.0
(#5)	180	5.6 ± 0.8	0.162 ± 0.016	41.5 ± 1.1
	240	5.3 ± 0.8	0.180 ± 0.019	42.7 ± 1.3
	30	7.5 ± 0.8	0.083 ± 0.006	35.8 ± 0.4
Coal No.2	60	6.7 ± 0.7	0.107 ± 0.008	37.5 ± 0.5
aged/dried	90	6.5 ± 0.7	0.128 ± 0.009	39.0 ± 0.7
1981	150	6.1 ± 0.6	0.158 ± 0.011	41.2 ± 0.8
(#6)	180	5.9 ± 0.7	0.167 ± 0.012	41.8 ± 0.8
	240	5.5 ± 0.7	0.184 ± 0.016	43.1 ± 1.1

Table 7

SURFACE CHARACTERISTICS OF COAL No.3
DRY SCREENED SAMPLE AT 51.5°C

MATRIX: THYMOL

COAL SAMPLE	DIAMETER D (μm)	CRITICAL VELOCITY V_c (μm/sec)	ΔF^{adh} (mJ/m²)	γ_{PV} (mJ/m²)
	30	7.6 ± 1.7	0.082 ± 0.013	35.8 ± 0.9
Coal No.3	60	6.7 ± 1.7	0.106 ± 0.018	37.4 ± 1.3
"as obtained"	90	6.1 ± 1.7	0.121 ± 0.023	38.5 ± 1.6
1979	150	5.5 ± 1.6	0.141 ± 0.028	40.0 ± 2.0
(#10)	180	5.2 ± 1.6	0.149 ± 0.031	40.6 ± 2.2
	240	4.9 ± 1.6	0.165 ± 0.036	41.7 ± 2.6
	30	7.5 ± 0.8	0.082 ± 0.006	35.7 ± 0.4
Coal No.3	60	5.4 ± 0.8	0.091 ± 0.009	36.4 ± 0.6
aged	90	-	-	-
1981	150	3.4 ± 0.7	0.102 ± 0.014	37.2 ± 1.0
(#11)	180	3.0 ± 0.6	0.104 ± 0.014	37.3 ± 1.0
	240	2.5 ± 0.6	0.105 ± 0.017	37.4 ± 1.0
	30	7.5 ± 1.0	0.082 ± 0.007	35.7 ± 0.5
Coal No.3	60	6.2 ± 0.6	0.100 ± 0.007	37.1 ± 0.5
aged/dried	90	6.0 ± 0.6	0.119 ± 0.008	38.4 ± 0.6
1981	150	5.7 ± 0.5	0.146 ± 0.009	40.3 ± 0.6
(#12)	180	5.5 ± 0.5	0.155 ± 0.010	41.0 ± 0.7
	240	5.2 ± 0.5	0.172 ± 0.011	42.2 ± 0.8

Table 8

PARTICLE/VAPOUR INTERFACIAL TENSION, $_{o}^{C}\gamma_{PV}$, OF DIFFERENT COAL SAMPLES AT 51.5°C

	COAL SAMPLE	DIAMETER D (μm)	γ_{PV} at 51.5°C (mJ/m²) "as obtained" 1979	aged 1981	aged/dried 1981
wet screened	Coal No.1	75	<29.9	37.9 ± 0.6	38.8 ± 0.9
		210	<29.9	42.6 ± 1.1	42.6 ± 1.2
	Coal No.2	75	39.5 ± 2.1	38.0 ± 0.8	38.3 ± 0.6
		210	42.7 ± 2.6	42.2 ± 1.2	42.5 ± 1.1
	Coal No.3	75	37.7 ± 1.3	38.0 ± 0.7	37.5 ± 1.6
		210	40.3 ± 1.3	39.1 ± 1.0	38.4 ± 2.3
dry screened	Coal No.3	75	38.0 ± 1.5	36.6 ± 0.6	37.8 ± 0.5
		210	41.1 ± 2.4	37.4 ± 1.2	41.6 ± 0.8
	Coal CN-5A	75	1980 43.3 ± 1.3	38.4 ± 1.2	38.5 ± 0.7
		210	47.5 ± 1.6	39.1 ± 1.4	43.3 ± 1.0

FIGURE CAPTIONS

Figure 1. Solidification front velocity, V, versus particle diameter, D, for acetal/benzophenone system.

Figure 2. Critical velocity, V_c, versus particle diameter, D:

- ○ PVC/thymol;
- △ PMMA/thymol

Figure 3. Critical velocity, V_c, versus particle diameter, D, for "as obtained" (freshly mined and processed) samples:

- □ coal No.2 wet screened (#4 in Table 5);
- △ coal No.3 wet screened (#7);
- ◇ coal No.3 dry screened (#10);
- ▽ coal CN-5A dry screened (#13).

Figure 4. Particle surface tension, γ_{PV}, versus particle diameter, D, for "as obtained" samples:

- □ coal No.2 wet screened (#4 in Table 5);
- △ coal No.3 wet screened (#7);
- ◇ coal No.3 dry screened (#10);
- ▽ coal CN-5A dry screened (#13).

Figure 5. Particle surface tension, γ_{PV}, versus particle diameter, D, for aged samples:

- ◐ coal No.1 wet screened (#2 in Table 5);
- ◩ coal No.2 wet screened (#5);
- ◭ coal No.3 wet screened (#8);
- ◆ coal No.3 dry screened (#11);
- ▼ coal CN-5A dry screened (#14).

Figure 6. Particle surface tension, γ_{PV}, versus particle diameter, D, for the aged/dried samples:

- ● coal No.1 wet screened (#3 in Table 5);
- ■ coal No.2 wet screened (#6);
- ▲ coal No.3 wet screened (#9);
- ◆ coal No.3 dry screened (#12);
- ▼ coal CN-5A dry screened (#15).

Figure 7. Effect of the drying process. Particle/vapour interfacial tension, γ_{PV}, versus particle diameter, D, for aged samples before and after drying.

a) wet screened samples:

- ⊘ coal No.1 aged (#2 in Table 5)
- ● coal No.1 aged/dried (#3)
- ◪ coal No.2 aged (#5)
- ■ coal No.2 aged/dried (#6)
- ◭ coal No.3 aged (#8)
- ▲ coal No.3 aged/dried (#9)

b) dry screened samples:

- ◈ coal No.3 aged (#11)
- ◆ coal No.3 aged/dried (#12)
- ▽ coal CN-5A aged (#14)
- ▼ coal CN-5A aged/dried (#15)

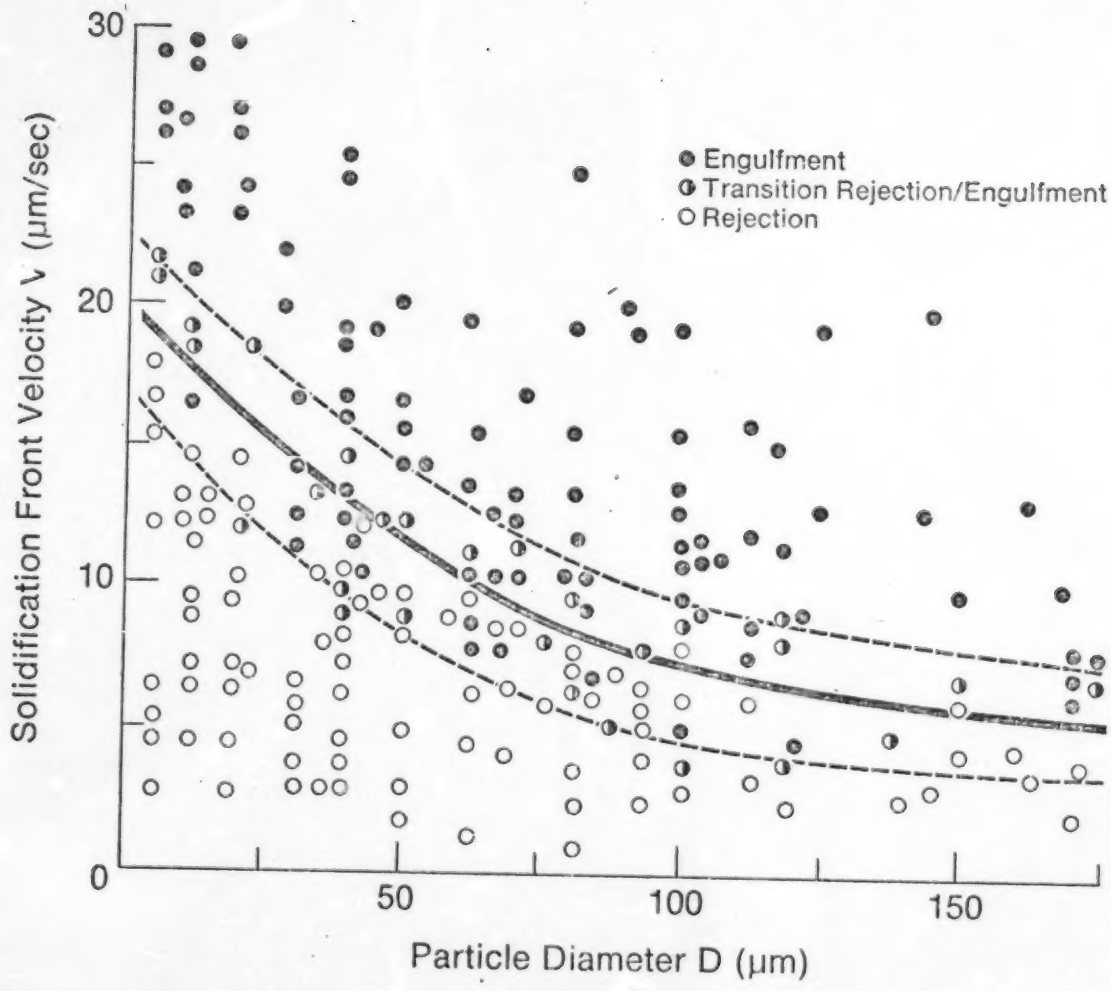
30
20
10
0
50
100
150
Solidification Front Velocity v (μm/sec)
Particle Diameter D (μm)
Engulfment
Transition Rejection/Engulfment
Rejection

Figure 1

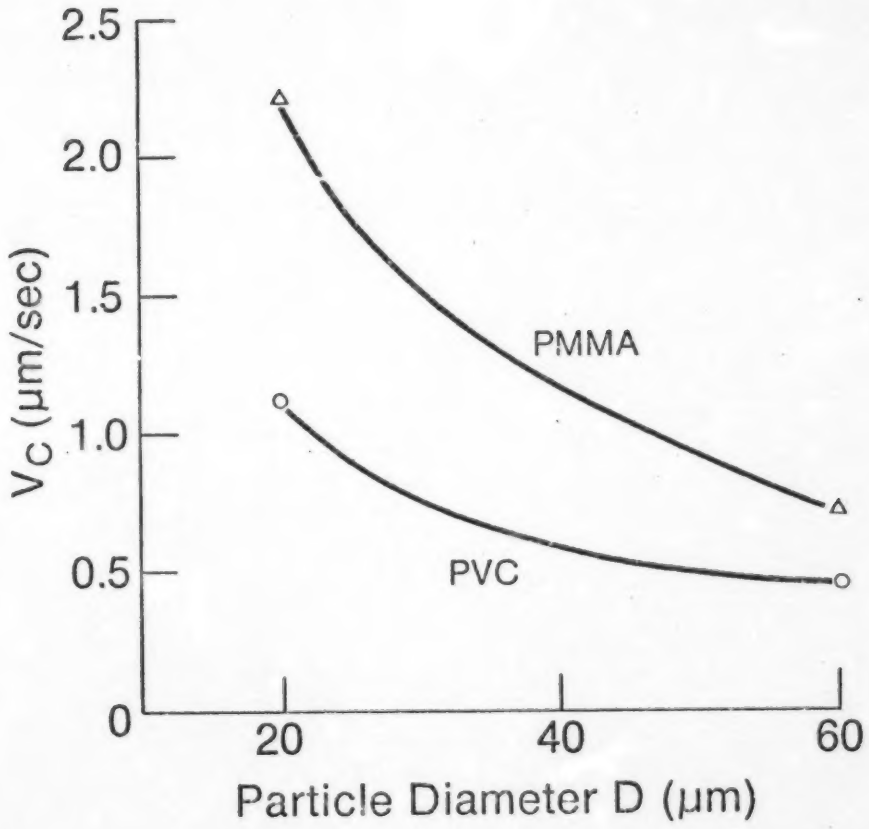
2.5
2.0
1.5
1.0
0.5
0
V_C (μm/sec)
PMMA
PVC
20
40
60
Particle Diameter D (μm)

Figure 2

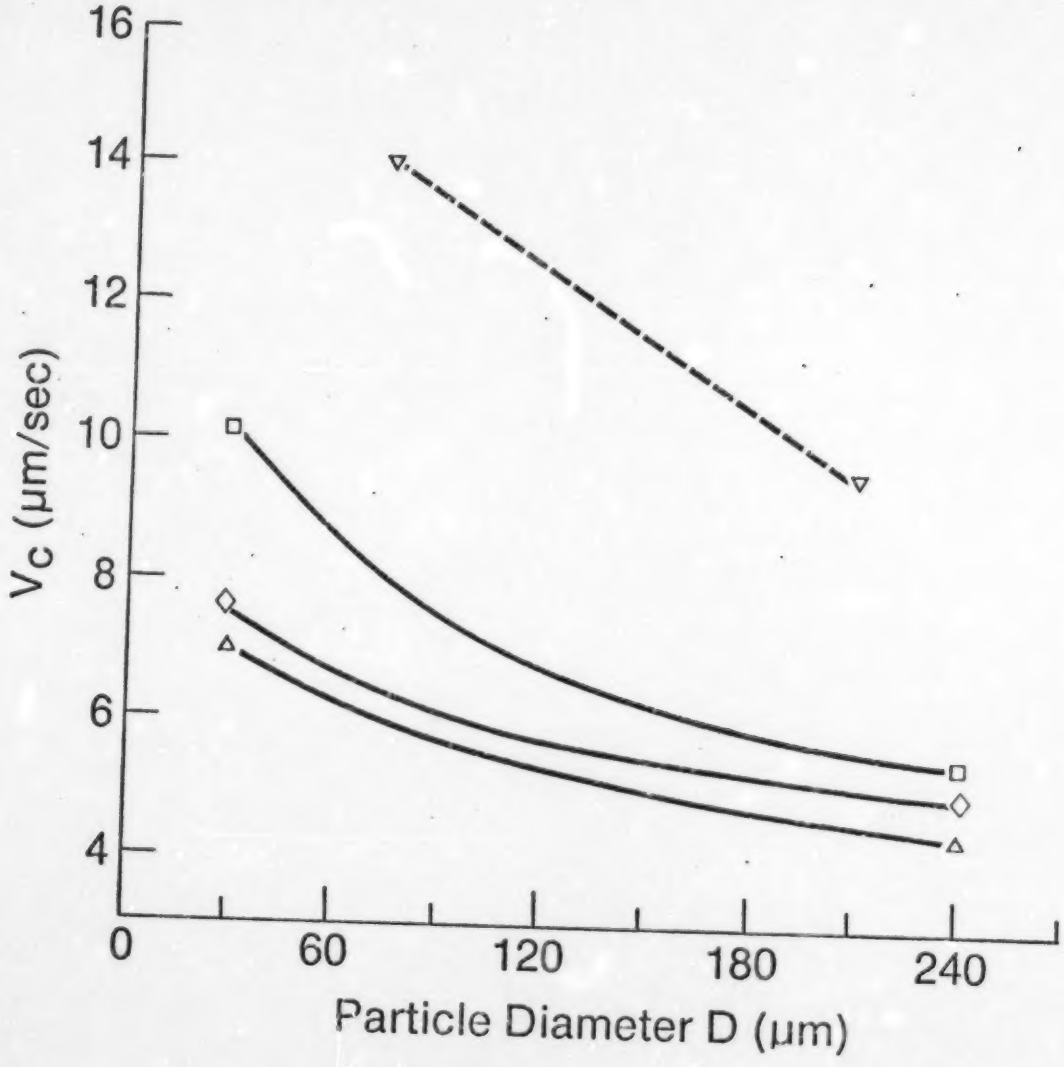

Figure 3

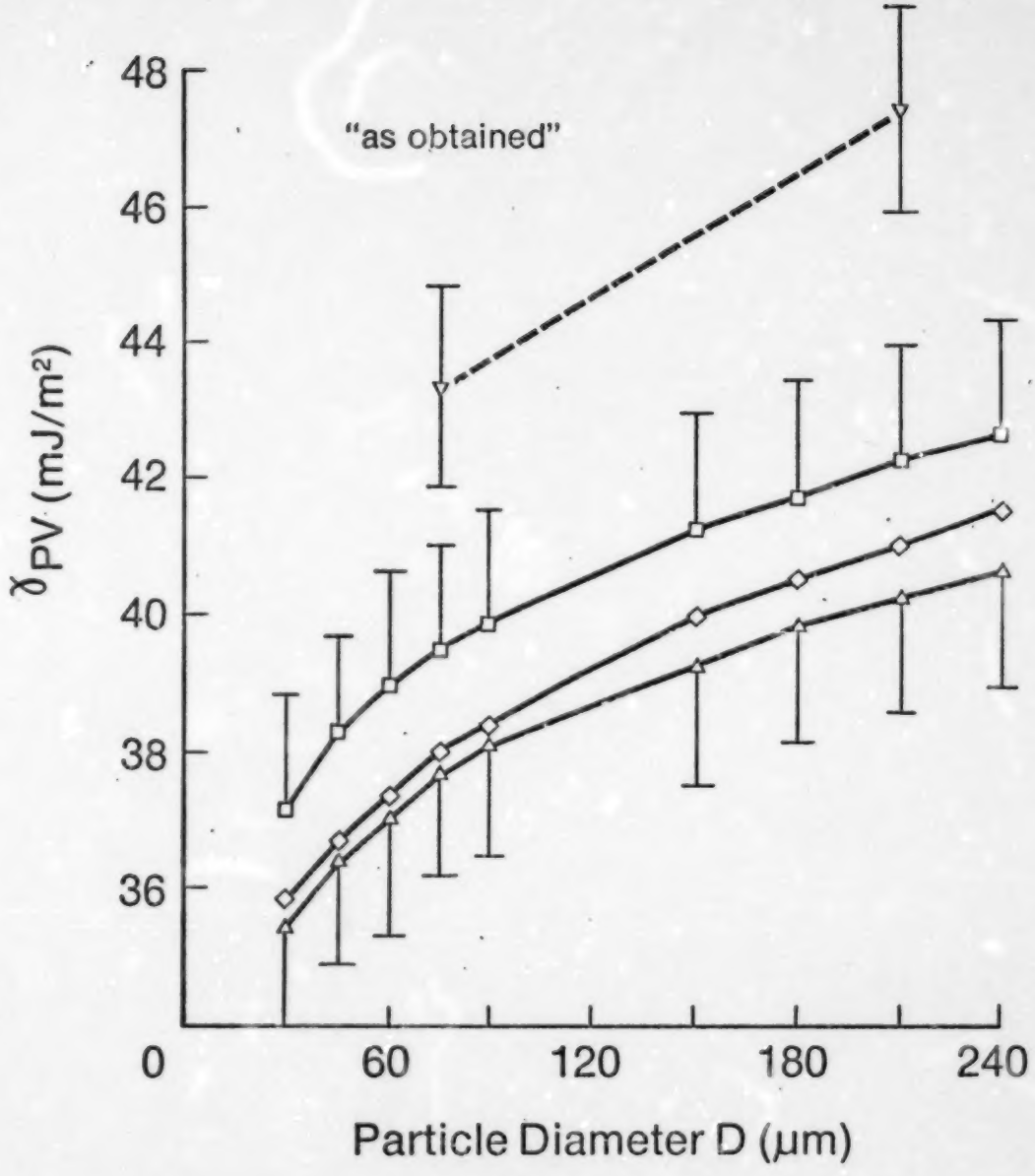
48
46
44
42
40
38
36
"as obtained"
γ_{PV} (mJ/m²)
0
60
120
180
240
Particle Diameter D (μm)

Figure 4

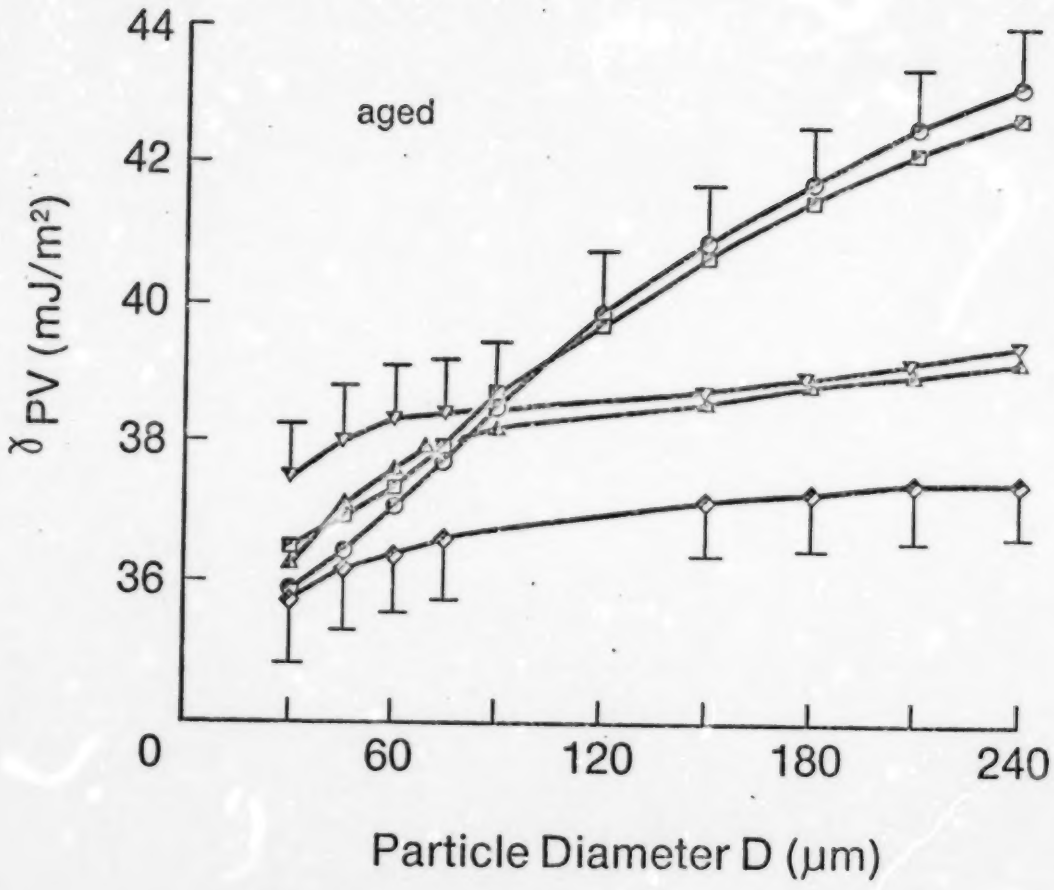
44
42
40
38
36
0
60
120
180
240
aged
γ_{PV} (mJ/m²)
Particle Diameter D (μm)

Figure 5

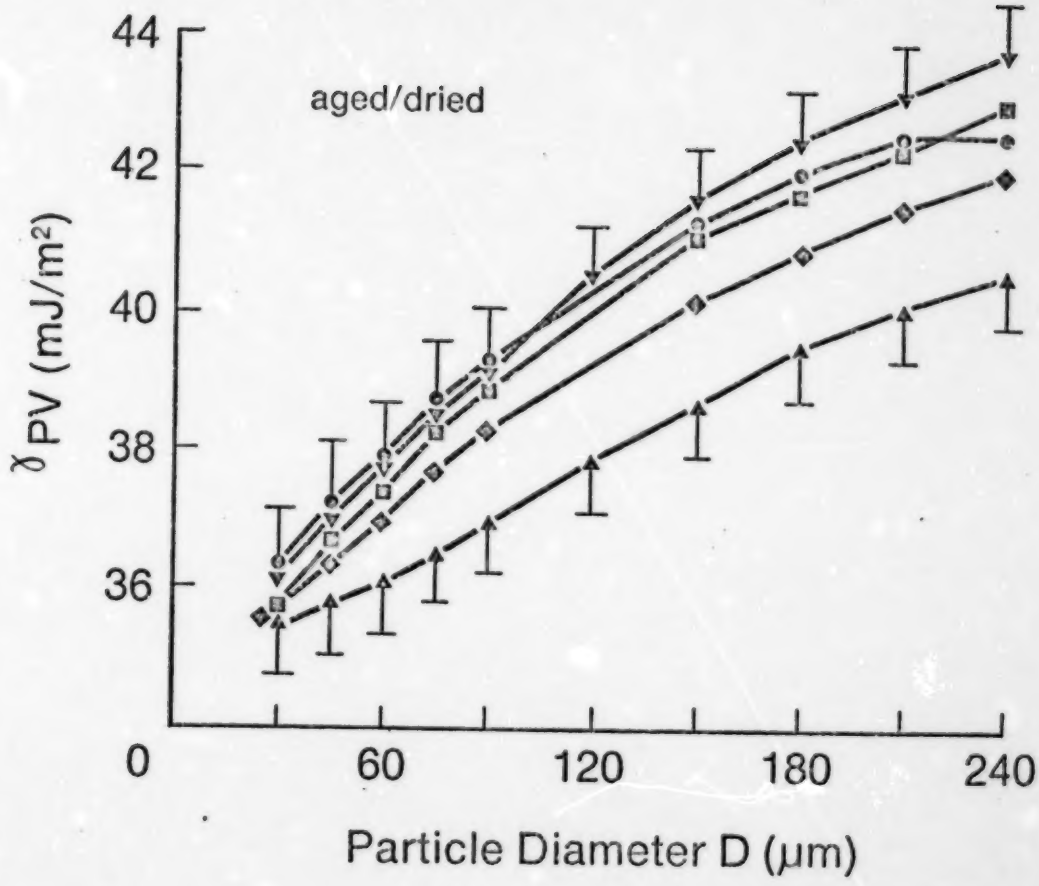
aged/dried
γ_{PV} (mJ/m²)
44
42
40
38
36
0
60
120
180
240
Particle Diameter D (μm)

Figure 6

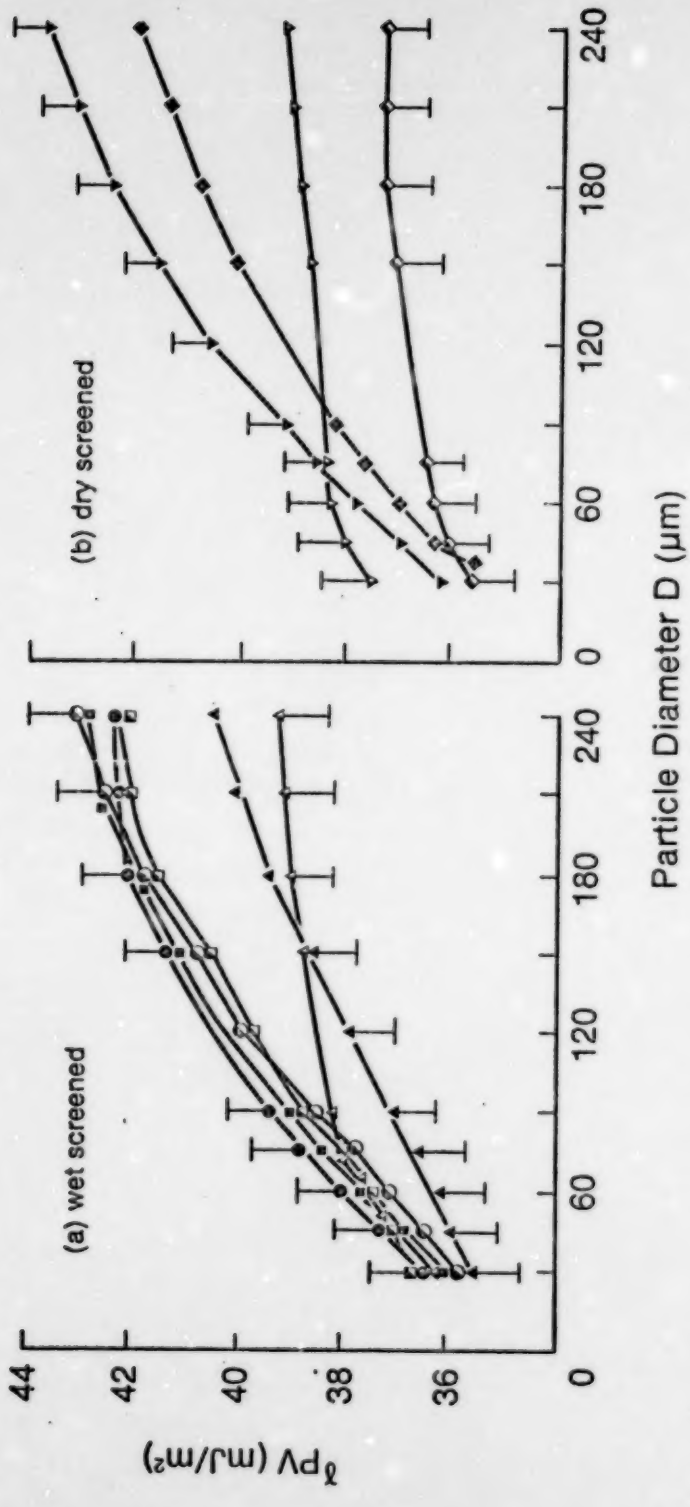
(a) wet screened
(b) dry screened
η_{PV} (mJ/m²)
Particle Diameter D (μm)
44
42
40
38
36
0
60
120
180
240

Figure 7

KEY WORDS

Coal powder; freezing front technique; surface tension of coal; storage of coal; aging of coal.

APPENDIX No. 2

FUEL

the science and technology of Fuel and Energy

Published by Butterworth

Determination of specific heats of coal powders by differential scanning calorimetry

Eva I. Vargha-Butler, Michael R. Soulard, Hassan A. Hamza* and A. Wilhelm Neumann

University of Toronto, Department of Mechanical Engineering, 5 King's College Road, Toronto, Ontario M5S 1A4, Canada

* *EMR, Western Research Laboratory, CANMET, Edmonton, Alberta, Canada*

(*Received* 5 *August* 1981; *revised* 27 *January* 1982)

Specific heats (C_p) of bituminous and subbituminous coals were investigated in the temperature range 300–360K by differential scanning calorimetry (DSC). To establish the validity of the procedure, specific heats of glass beads and graphites in powdered and bulk form were determined. Good agreement was obtained with the values for the specific heats of glass and graphites in the literature, and it was established that the specific heats were not dependent on the degree of diminution of these materials. Specific heats of coal samples were found to depend upon mesh size, temperature, rank, moisture content and whether the coal powder was wet- or dry-screened. However, there were only minor differences in C_p between bituminous and subbituminous coals.

(Keywords: coal; specific heat; instrumental methods of analysis)

Studies on the specific heats of coal powders were motivated by work on the wettability of coal particles using a freezing front technique.[1-3] The quantitative determination of contact angles on coal particles from this technique requires specific heat data. As such data for coal in a powdered form are not available it was decided to test the possibility of determining specific heats of coal powders by differential scanning calorimetry.

Coal consists of two main components: an organic (carbon) matrix and inclusions of inorganic mineral matter. There is an extensive network of pores which usually contains water. This water is thought to originate from thermal decomposition of oxygen-containing functional groups in the coal or it may be water of hydration as well as adsorptively-bonded water[4]. Most of the water is pesent as free water in the mined coals. As the specific heat of water is approximately four times that of coal, it is apparent that the specific heat of coal will be affected by the moisture content. Therefore, C_p determinations with dried coal samples are generally the most significant[4,5]. Specific heat measurements with both dried coals and coals having different moisture contents were performed.

To evaluate the suitability of the DSC technique for the measurement of specific heats of particulate matter, the specific heats of several films of polymers and polymer powders were studied[6]. A comparison of these results with literature data showed that the agreement is satisfactory and no differences in specific heat were found between the powdered and bulk forms of polymers[6].

As a further test of the validity of the procedure, the specific heats of glass beads with different particle sizes were determined in the present study. The specific heats of various carbonaceous materials other than coal (graphites from different origins) were studied also.

EXPERIMENTAL

Materials

The following materials were investigated: glass beads, graphite and coal.

Glass beads. The glass micro-beads were soda-lime glass products (Polysciences Inc.) with three different particle size ranges: 40–62, 75–100 and 150–210 μm in diameter. These particle sizes correspond to a range from 65 to 325 US mesh.

Graphite. Four graphites were studied; two of them were commercial graphite powders obtained from the Fisher Scientific Co. and have the designations G-64 and G-67. The G-64 sample is a natural graphite powder with particle size <100 US mesh whereas the G-67 sample is synthetic graphite (Acheson 38), with particles <325 US mesh size. The other two graphite samples were in bulk form: a molded ATJ type synthetic graphite (Union Carbide Corp.) and an electrode graphite (Nortel Mfg. Ltd., Toronto). Powders of these graphites were prepared by grinding the bulk form in an agate mortar. The mean particle size was 7.6 μm for ATJ and 3.2 μm for the electrode graphite.

Coal. Three coals (No. 1, No. 2 and No. 3) from Western Canada, each consisting of six fractions identified by a US mesh range, $<60>100$, $<100>150$, $<150>200$, $<200>325$, $<325>400$ and <400, were studied. The coals were provided by CANMET, Western Research Laboratory, Edmonton, Alberta. All of the coals had been ground, wet-screened and dried at room temperature. A portion of coal No. 3, which was dry-screened after grinding, was also studied. Coals No. 1 and 2 were medium-volatile bituminous coals; sample No. 1 was from

0016-2361/82/050437-06$3.00
©1982 Butterworth & Co (Publishers) Ltd.

the Quintette Area, Northeastern British Columbia and sample No. 2 from the Mountain Park Area, near Hinton, Alberta. Coal No. 3 was subbituminous coal from the Judy Creek Area, Northern Alberta.

The coals were stored at room temperature in closed bottles away from exposure to light or heat until use, to avoid chemical changes of the coal surface. A portion of each fraction of all the coals was oven-dried at 105°C until the weight of the portion was constant, and kept in a desiccator prior to the specific heat measurements. The specific heats of both the original and the dried coals were determined.

Method

Differential scanning calorimetry was used to measure the specific heats. In this technique the material is subjected to a linear temperature programme and the rate of heat flow into the material is continuously measured. This rate is proportional to the instantaneous specific heat of the material. Basically, two miniature sample holders (one for the material being investigated, the other for the inert reference material) are kept at the same temperature by supplying different amounts of electrical power to each holder. The differential power input is recorded together with time and temperature signals. The instrument used was a Perkin-Elmer Model DSC-2 calorimeter. A detailed discussion of the Perkin-Elmer differential scanning calorimeter and the specific heat measurement using DSC has been published by the manufacturer[7,8,9].

In preliminary calibrations all the controls were adjusted so that over the temperature range of 300–360 K the power recording remained on the scale. The rates of heating and cooling were set at 10 K min^{-1}, the chart speed at 20 mm min^{-1}, the chart range at 5 mV and the range control at 21 mJ s^{-1} (5 mcal s^{-1}). These settings were chosen on the recommendation of Perkin-Elmer for C_p measurements. Lower rates give poor sensitivity, higher rates provide greater sensitivity but poorer temperature accuracy. Dry nitrogen gas of 99.99% minimum purity was used for purging the sample holders.

After establishing a stable baseline the following three series of measurements were performed: (1) the empty reference aluminium capsule (pan) was tested against another empty pan of known weight; (2) after optimizing the baseline linearity, a weighed and encapsulated synthetic sapphire standard (α-Al_2O_3) with a weight of 8.21 mg was tested for calibration (the specific heat of sapphire is available in the literature[10]); (3) finally, the glass, graphite or coal samples (weighed and encapsulated) were put into the calorimeter, maintaining all prevailing experimental conditions.

The specific heat of the samples, C_p(sample), can be calculated following calibration with the sapphire disc (ratio method),[9,10] using the formula:

$$C_p(\text{sample}) = \frac{W(\text{sapphire})}{W(\text{sample})} \times \frac{D(\text{sample})}{D(\text{sapphire})} \times C_p(\text{sapphire}) \quad (1)$$

where: C_p(sapphire), specific heat of the standard (cal g^{-1} K^{-1}); W(sapphire) and W(sample), weights of the standard and of the sample, respectively (mg); D(sapphire) and D(sample), ordinate displacements of the standard and the sample, respectively (mm). Finally, the specific heat data were expressed in kJ kg^{-1} K^{-1}.

Small differences in the weights of the aluminium pans can be corrected for by using the following formula:

$$\Delta D = \frac{\Delta W \times C_p(\text{Al}) \times S}{R} \quad (2)$$

where: ΔD, ordinate displacement correction (mm) caused by the ΔW difference in pan weights (mg); C_p(Al), specific heat of the pan material (in this case, aluminium) (cal g^{-1} K^{-1}); S, scan rate (K s^{-1}); R, setting of the range control for full scale divided by the chart span (mcal s^{-1} mm^{-1}). The ordinate displacement correction (ΔD) was added to the displacement (D) of the material tested in the lighter pan. ΔW values vary from 0.01 to 2.00 mg which, if not corrected, could cause errors in C_p values up to 25%.

As the baseline is very sensitive to the exact position of the platinum lid on the sample holder, when changing the sample, the platinum lid should be removed, and then replaced very carefully and the initial position of the lid must be maintained always, if baseline linearity is to be preserved.

The specific heat data persented here are the arithmetic mean values of at least three measurements. The standard deviation and the population mean were calculated from the sample mean assuming a t-distribution. The errors given are 95% confidence limits.

RESULTS AND DISCUSSION

The specific heat values *versus* temperature for three fractions of glass beads and the specific heat values *versus* particle diameter of the glass beads at one selected temperature (300 K), are plotted in *Figure 1*. As expected for a chemically homogeneous material, there is no particle size dependence at any temperature and the specific heat values increase only slightly with increasing temperature. A comparison of these results with data in the literature for soda-lime glass (0.862–0.871 kJ kg^{-1} K^{-1} at 366 K[11] and 0.871 kJ kg^{-1} K^{-1} at 360 K) shows that the agreement is satisfactory.

The temperature dependence of specific heat values of

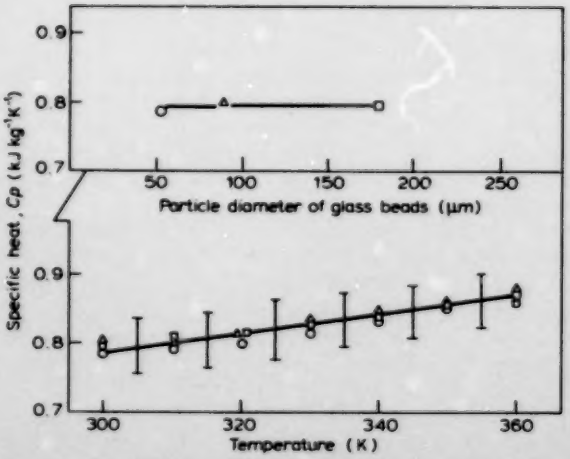

Figure 1 Specific heat of glass beads as a function of temperature and particle diameter (at 300 K). Particle diameter: ○, 40–65 μm; △, 75–100 μm; □, 150–210 μm

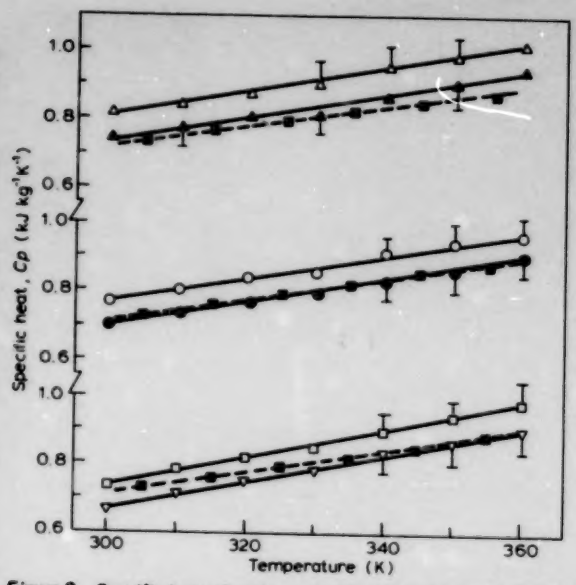

Figure 2 Specific heat of various graphites in bulk and powdered form as a function of temperature. ATJ graphite: △, powder; ▲, bulk. Electrode graphite: ○, powder; ●, bulk. Commercial graphite powders: □, G-64 type; ▽, G-67 type; ■, literature data[12]

various graphite powders and of graphites in bulk form are shown in *Figure 2*. The temperature dependence of the average value of the specific heat of graphite from the literature[12] is indicated by dotted lines in *Figure 2*. These values represent the best fit of the measured and/or calculated C_p values of numerous types of natural and manufactured graphites. No specification as to the state of diminution was given. De Sorbo and Tyler[13] measured a C_p value of 0.716 kJ kg^{-1} K^{-1} at 300 K for bulk graphite. The data presented in this Paper, at 300 K, are compatible with these results (*cf. Figure 2*).

The powders have slightly higher C_p values than the bulk samples for ATJ and electrode graphite. However, the G-67 graphite powder with its smaller particle size (≤325 US mesh) has a lower specific heat value than the G-64 graphite (≤100 US mesh).

The specific heat data of the oven-dried coals are summarized in *Tables 1–4*. The C_p values as a function of temperature for both the dried and the original, untreated coals, No. 1, No. 2, and No. 3 wet- and No. 3 dry-screened, are plotted in *Figure 3* for the <60>100 US mesh fractions. The specific heats of the dried coals increase with increasing temperature and can be approximated by a single straight line. For the original, untreated coals the temperature dependence of the specific heat is no longer rectilinear. The specific heat values are higher than those

Table 1 Specific heats of coal No. 1 fractions (wet-screened, dried)

Temperature (K)	Specific heats, C_p, at different mesh sizes of coal fractions (kJ kg^{-1} K^{-1})					
	<60 >100	<100 >150	<150 >200	<200 >325	<325 >400	<400
300	0.98 ± 0.02	1.02 ± 0.01	1.03 ± 0.05	1.06 ± 0.01	1.04 ± 0.06	1.04 ± 0.02
310	1.01 ± 0.03	1.08 ± 0.03	1.10 ± 0.07	1.09 ± 0.02	1.06 ± 0.04	1.06 ± 0.05
320	1.06 ± 0.06	1.12 ± 0.04	1.16 ± 0.03	1.15 ± 0.06	1.14 ± 0.04	1.13 ± 0.02
330	1.10 ± 0.06	1.17 ± 0.02	1.19 ± 0.02	1.22 ± 0.06	1.16 ± 0.06	1.14 ± 0.03
340	1.13 ± 0.03	1.17 ± 0.00	1.22 ± 0.05	1.22 ± 0.06	1.19 ± 0.06	1.20 ± 0.02
350	1.18 ± 0.04	1.21 ± 0.03	1.25 ± 0.02	1.28 ± 0.04	1.28 ± 0.06	1.27 ± 0.01
360	1.21 ± 0.01	1.24 ± 0.03	1.29 ± 0.02	1.34 ± 0.08	1.30 ± 0.03	1.30 ± 0.01

Table 2 Specific heats of coal No. 2 fractions (wet-screened, dried)

Temperature (K)	Specific heats, C_p, at different mesh sizes of coal fractions (kJ kg^{-1} K^{-1})					
	<60 >100	<100 >150	<150 >200	<200 >325	<325 >400	<400
300	1.03 ± 0.03	1.04 ± 0.05	1.06 ± 0.01	1.08 ± 0.08	1.13 ± 0.02	1.08 ± 0.02
310	1.07 ± 0.00	1.08 ± 0.01	1.11 ± 0.01	1.11 ± 0.07	1.17 ± 0.05	1.13 ± 0.01
320	1.10 ± 0.01	1.11 ± 0.06	1.16 ± 0.05	1.17 ± 0.07	1.19 ± 0.01	1.15 ± 0.00
330	1.14 ± 0.06	1.16 ± 0.01	1.20 ± 0.03	1.22 ± 0.05	1.24 ± 0.04	1.19 ± 0.02
340	1.19 ± 0.02	1.20 ± 0.04	1.23 ± 0.03	1.26 ± 0.02	1.26 ± 0.01	1.23 ± 0.00
350	1.21 ± 0.05	1.22 ± 0.02	1.25 ± 0.02	1.27 ± 0.05	1.27 ± 0.02	1.26 ± 0.01
360	1.25 ± 0.05	1.26 ± 0.03	1.29 ± 0.01	1.28 ± 0.02	1.29 ± 0.01	1.29 ± 0.01

Table 3 Specific heats of coal No. 3 fractions (wet-screened, dried)

Temperature	Specific heats, C_p, at different mesh sizes of coal fractions (kJ kg^{-1} K^{-1})					
	<60 >100	<100 >150	<150 >200	<200 >325	<325 >400	<400
300	1.04 ± 0.03	1.07 ± 0.05	1.06 ± 0.07	1.05 ± 0.05	1.01 ± 0.04	0.97 ± 0.05
310	1.09 ± 0.04	1.12 ± 0.03	1.14 ± 0.07	1.09 ± 0.01	1.06 ± 0.03	1.03 ± 0.03
320	1.13 ± 0.04	1.15 ± 0.06	1.16 ± 0.03	1.11 ± 0.04	1.10 ± 0.02	1.05 ± 0.01
330	1.16 ± 0.02	1.19 ± 0.03	1.19 ± 0.03	1.15 ± 0.02	1.12 ± 0.02	1.07 ± 0.02
340	1.22 ± 0.04	1.23 ± 0.00	1.24 ± 0.06	1.21 ± 0.02	1.19 ± 0.04	1.11 ± 0.03
350	1.22 ± 0.01	1.24 ± 0.05	1.25 ± 0.06	1.25 ± 0.01	1.20 ± 0.05	1.14 ± 0.04
360	1.24 ± 0.02	1.28 ± 0.05	1.33 ± 0.05	1.32 ± 0.03	1.27 ± 0.06	1.20 ± 0.01

Table 4 Specific heats of coal No. 3 fractions (dry-screened, dried)

Temperature (K)	Specific heats, C_p, at different mesh sizes of coal fractions (kJ kg^{-1} K^{-1})					
	<60 >100	<100 >150	<150 >200	<200 >325	<325 >400	<400
300	1.09 ± 0.04	1.10 ± 0.02	1.05 ± 0.03	1.02 ± 0.05	1.04 ± 0.03	1.07 ± 0.03
310	1.15 ± 0.04	1.13 ± 0.04	1.09 ± 0.02	1.07 ± 0.03	1.08 ± 0.02	1.10 ± 0.04
320	1.17 ± 0.06	1.18 ± 0.03	1.13 ± 0.04	1.09 ± 0.02	1.10 ± 0.03	1.13 ± 0.02
330	1.21 ± 0.08	1.21 ± 0.02	1.16 ± 0.03	1.13 ± 0.04	1.15 ± 0.01	1.17 ± 0.02
340	1.26 ± 0.01	1.25 ± 0.04	1.19 ± 0.01	1.20 ± 0.03	1.19 ± 0.03	1.22 ± 0.03
350	1.28 ± 0.02	1.27 ± 0.02	1.23 ± 0.01	1.23 ± 0.01	1.24 ± 0.02	1.25 ± 0.01
360	1.31 ± 0.04	1.32 ± 0.01	1.26 ± 0.03	1.28 ± 0.05	1.27 ± 0.03	1.30 ± 0.02

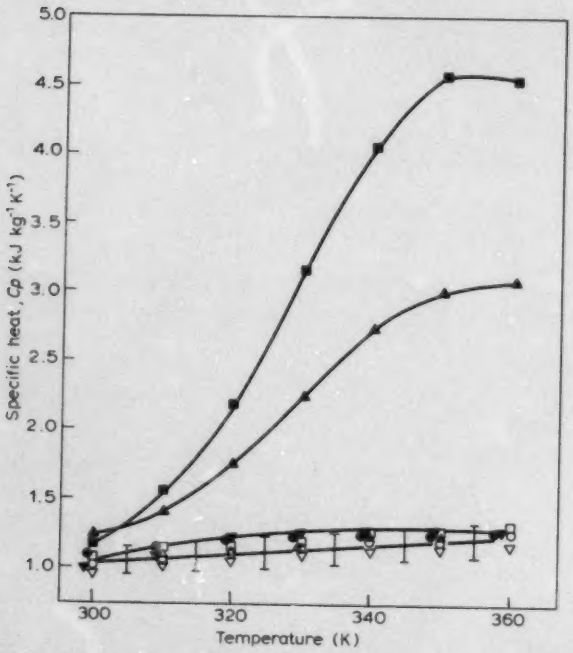

Figure 3 Specific heat of untreated and dried coals as a function of temperature (<60 >100 US mesh fraction). Coal No. 1 wet-screened: ▽, dried; ▼, untreated. Coal No. 2 wet-screened: ○, dried; ●, untreated. Coal No. 3 wet-screened: △, dried; ▲, untreated. Coal No. 3 dry-screened: □, dried; ■, untreated

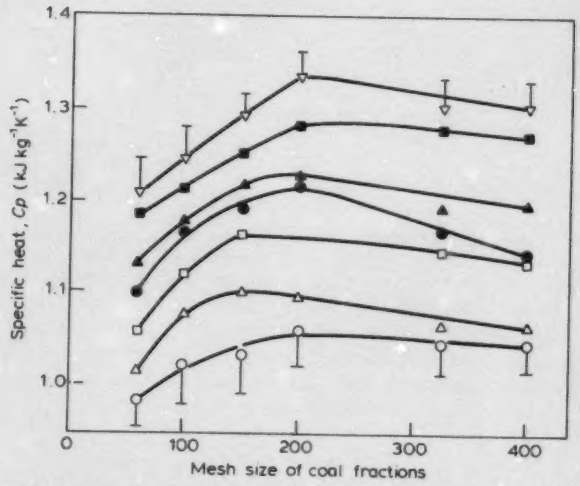

Figure 4 Specific heat of coal No. 1 (wet-screened, dried) as a function of particle size. ○, 300 K; △, 310 K; □, 320 K; ●, 330 K; ▲, 340 K; ■, 350 K; ▽, 360 K

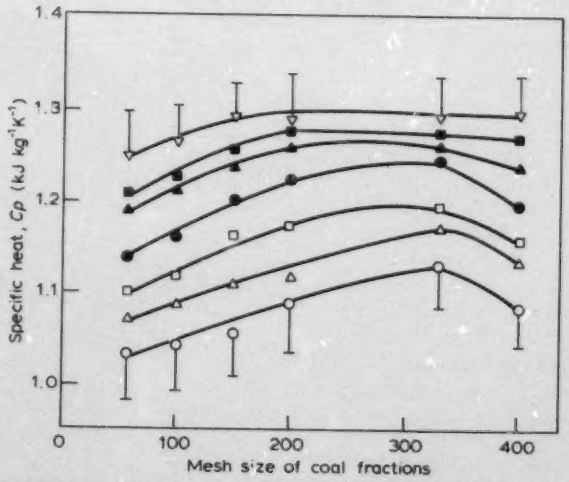

Figure 5 Specific heat of coal No. 2 (wet-screened, dried) as a function of particle size. ○, 300 K; △, 310 K; □, 320 K; ●, 330 K; ▲, 340 K; ■, 350 K; ▽, 360 K

of the corresponding dried coals and depend on the moisture content of the coal. At higher moisture content a considerable portion of the water may not be bound chemically but it may be present as free water and the specific heat value, as a result, will be much higher than that of the moisture-free coal[14]. The presence of water, which has larger specific heat than coal, seems to increase the measured specific heat of the moist sample[15].

So far, no explanation can be given of the non-rectilinear relation between the specific heat and the temperature of the original samples. However, it cannot be caused by loss of water during the measurements because the weight of the samples was unchanged at the end of the experiment.

The results show that the difference in specific heats between bituminous and subbituminous coals is due to their different water content rather than their rank (see *Figure 3* and *Tables 1–4*).

The specific heat values of the dried coals *versus* mesh size at different temperatures are plotted in *Figures 4–7*. The apparent change of C_p value with particle size is slightly outside the error limits. The particle size dependence of specific heat is attributed to the heterogeneous character of coal. During the grinding and screening processes various constituents in the coal undergo a selective size reduction and distribution according to their relative hardness. Minerals with lower hardness will be enriched in fractions with smaller particle

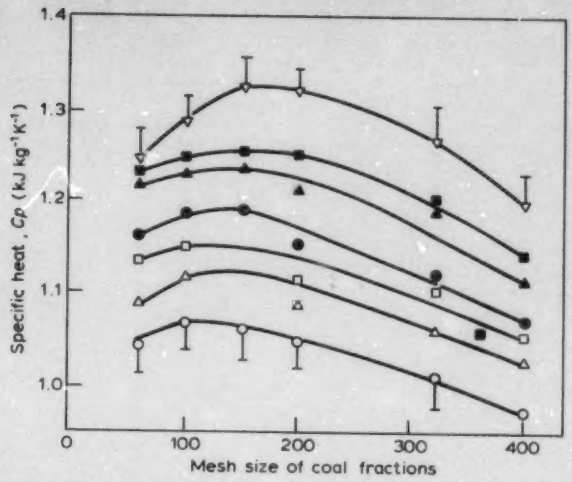

Figure 6 Specific heat of coal No. 3 (wet-screened, dried) as a function of particle size. ○, 300 K; △, 310 K; □, 320 K; ●, 330 K; ▲, 340 K; ■, 350 K; ▽, 360 K

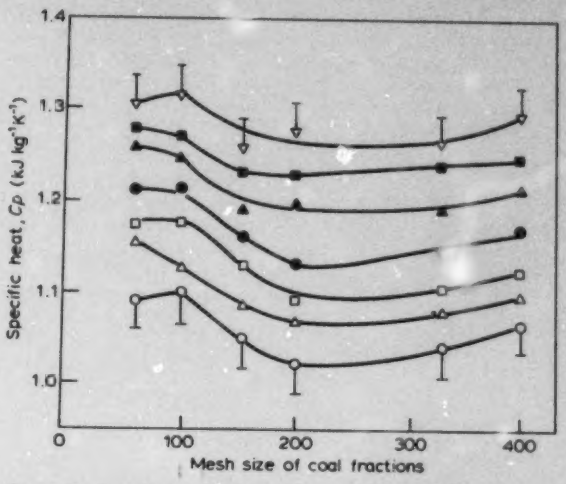

Figure 7 Specific heat of coal No. 3 (dry-screened, dried) as a function of particle size. ○, 300 K; △, 310 K; □, 320 K; ●, 330 K; ▲, 340 K; ■, 350 K; ▽, 360 K

sizes. The degree of oxidation and hydration of the coal particles depends on the particular chemical composition of each fraction and so does the specific heat. In addition, the pretreatment can influence the chemical composition of the coal fractions. The wet-screened coals show similar behaviour (*Figures 4–6*), the specific heat values of the fine fractions are generally lower than those of the intermediate fractions, and tend toward the C_p values of graphites. During the wet-screening process, the water-soluble inorganic contamination may be washed out and lead to a modification of the specific heat values. The surface tension and contact angle data determined by the freezing front techniques[1–3] for coal No. 2 showed that the hydrophobic character of the surface of coal particles increased with decreasing particle size. This result supports the previous interpretation.

The particle size dependence of C_p values for the dry-screened coal No. 3 differs from the wet-screened coal (*Figure 7*). However, the results of ash yield and trace element analysis also show different behaviour between the wet- and dry-screened fractions[16].

Singer and Tye[15] determined the specific heat of undried and predried Pittsburgh seam coal at 30, 65, 100 and 150°C (and at higher temperatures) by adiabatic calorimetry. The C_p values of the undried coal are 0.860, 0.920, 1.220 and 1.580 kJ kg^{-1} K^{-1}, whereas the predried coal has lower specific heat values, i.e. 0.850, 0.920, 0.990 and 1.060 kJ kg^{-1} K^{-1} at these temperatures. The specific heat values *versus* temperature plot of the undried Pittsburgh coal shows the same S-type curve as the curves for the original (undried) coal in *Figure 3*. The plot of the predried Pittsburgh coal is rectilinear in the temperature range 30–150°C, similar to the dried coal in *Figure 3*. The C_p data of the dried Pittsburgh coal are approximately 15–20% lower than the specific heat values of coal discussed in this Paper at the same (30 and 65°C) temperatures. The C_p meaurements were performed with small blocks of Pittsburgh coal (the samples were 63 mm square and of 12 mm depth) whereas the coals measured here were in powdered form with different particle sizes. Considering the particle size dependence of the C_p values of coal (C_p decreases with increasing particle size; see *Figures 4–6*) the agreement is satisfactory.

Agroskin and Goncharov[17] give a C_p value of 1.35–1.40 kJ kg^{-1} K^{-1} at 100°C for gas coal. The mean values in the present Paper, referring to the four dried coals (*Figure 3*), extrapolated to 373 K, are 1.275 kJ kg^{-1} K^{-1} for the $<60>100$ and 1.330 kJ kg^{-1} K^{-1} for the $<325>400$ US mesh fractions (not shown here). Agroskin and Goncharov[17] also indicate that the specific heat of coal increases continuously with increasing temperature until the temperature of decomposition (the metaplast state between 350 and 550°C) is reached.

It is concluded that differential scanning calorietry is an appropriate technique for determining the specific heats of coals. The technique is applicable to powders and sensitive to slight differences in C_p values due to 'as-mined' impurities, water content or pretreatment.

ACKNOWLEDGEMENTS

The work was supported by Energy, Mines and Resources, CANMET, Canada through contract No. 20SU·23440-0-9021.

REFERENCES

1 Vargha-Butler, E. I., Soulard, M. R., Hamza, H. A. and Neumann, A. W. *CIM Bulletin* 1981, **79**, 59
2 Soulard, M. R. *M.A.Sc. Thesis*, University of Toronto, Toronto, Canada, 1980
3 Soulard, M. R., Vargha-Butler, E. I., Hamza, H. A. and Neumann, A. W. (submitted for publication)
4 Karr, C. Jr. (Ed.) 'Analytical Methods for Coal and Coal Products', Vol. I, Academic Press, New York, 1978, p. 248–49, 255
5 Berkowitz, N. 'An Introduction to Coal Technology', Academic Press, New York, 1979, p. 80
6 Vargha-Butler, E. I., Hamza, H. A. and Neuman, A. W. (submitted for publication)
7 O'Neil, M. J. *Anal. Chem.* 1964, **36**, 1238
8 Watson, E. S., O'Neill, M. J., Justin, J. and Brenner, N. *Anal. Chem.* 1964, **36**, 1233
9 O'Neill, M. J. *Anal. Chem.* 1966, **38**, 1331

10 Ginnings, D. C. and Furukawa, G. T. *J. Am. Chem. Soc.* 1953, **75**, 522
11 Touloukian, Y. S. and Buyco, E. H. 'Thermophysical Properties of Matter', Vol. 5, IFI/Plenum, New York, 1970
12 Mantell, C. L. 'Carbon and Graphite Handbook', Wiley/Interscience, New York, 1968, p. 359
13 De Sorbo, W. and Tyler, W. W. *J. Chem. Phys.* 1953, **21**, 1660
14 van Krevelen, D. V. 'Coal', Elsevier, Amsterdam, 1961, p. 418
15 Singer, J. M. and Tye, R. P. *US Bur. Mines Rep. Invest.* 1979, No. 8364, p. 13
16 Hancock, R. G. V., Vargha-Butler, E. I., Hamza, H. A. and Neumann, A W. (unpublished)
17 Agroskin, A. A. and Goncharov, E. I. *Coke and Chem., USSR* 1965, **11**, 16

APPENDIX No. 3

Design of a New Solidification Chamber

The redesign of the experimental set-up for the freezing front technique was completed.

In the original apparatus one end of the cell was heated electrically and the other was cooled by circulating water. Control of the advance of the solidification front was difficult, since it was dependent on the amount of heating at one end and the amount of cooling at the other, both of which being varied during the experiment. It was difficult to obtain any particular velocity of the solidification front and to maintain a constant velocity for any period of time. It was also difficult to control the shape of the solidification front.

The apparatus was redesigned to allow for improved control of the advance of the solidification front. In the redesigned cell the thermoelectric devices replace the heating transformer

and cooling water. This allows for more precise control of the heating and cooling of the copper cell. The rate of advance of the solidification front can be maintained constant at any chosen value. The shape of the solidification front can also be controlled.

The apparatus consists of the following components:

- copper cell;
- thermoelectric devices 2;
- Cambian Bipolar Controller 2;
- temperature programmer;
- thermistor 2;
- aluminum heat sink;
- teflon box;
- heating coil;
- power source.

The freezing front experiment is performed in the copper cell. The matrix material and particles are placed in the copper cell and are covered by a glass microscope slide. During the experiment the solidification front moves horizontally.

In order to perform the experiment two conditions must be satisfied. Firstly, there must be a horizontal temperature gradient in the matrix material, so that there is a sharp solidification front. Secondly, the temperature of the matrix material must be lowered, causing the solidification front to move. These two things are done by heating or cooling each end of the copper cell by means of thermoelectric devices. The amount of heat transfer by each thermoelectric device is determined by a

feedback controller. The temperature at each end is measured by a thermistor. This is compared to the programmed value, producing an error signal which is amplified by the Bipolar Controller which in turn powers the thermoelectric device. This is done independently for each end of the copper cell. Water circulating through the aluminum heat sink removes heat from the thermoelectric devices.

A temperature gradient in the copper, and therefore in the matrix material is caused by maintaining a constant temperature difference between each end of the copper cell. The maximum temperature gradient is 10°C/cm.

The solidification front is caused to move by lowering the temperature of both ends of the copper cell, and therefore the matrix material. The maximum rate of cooling is 0.1°C/sec. The velocity of the solidification front is given by the rate of cooling divided by the temperature gradient.

One of the problems of previous apparatus was that is was difficult to control the solidification front velocity. With the current apparatus the velocity of the solidification can easily be controlled since, once the temperature gradient has been fixed, the velocity varies directly with the rate of cooling. The value of the temperature gradient and rate of cooling are set digitally. The experiment can be repeated with the same velocity by using the same settings for the temperature gradient and the rate of cooling.

Another problem of previous apparatus was that the vertical profile of the solidification front could not be controlled.

Often the solidification front at the top of the matrix would advance ahead of the front at the bottom making observations difficult. This occurred because the glass slide was cooler than the matrix material. In the current apparatus the copper cell is contained inside a teflon box. The glass slide is heated by drawing warm air over it. The temperature of the glass slide, and therefore the shape of the profile of the solidification front, is controlled by varying the temperature of the air. This is done by varying the current, from the power source, through the heating coil. The warm air, after it has passed over the glass slide is removed by a fan. This also removes any vapours of the matrix material which may be present.

Freezing Front Apparatus

Preliminary Instruction Sheets

A. Start-up Procedure

1. Turn on cooling water.
2. Set controls to initial values

   Switches - set ,
   - down ,
   - output off ;

   Rate - 0.099 ;

   Low - 20 ;

   High - 20 ;

   Diff. - 00 .
3. Turn on programmer.
4. Check the program value and T_1 and T_2.
   - The program value should be 20. If it is not switch the up-down switch to the up position, then the down position. If it then does not reach 20, seek assistance.
   - Both T_1 and T_2 should be a little less than 20. If they read 0, then thermistors are broken, and seek assistance. If they read above 20, check the cooling water.
5. Turn on bipolar controllers.
6. Set output switch to on.

7. Check the values of T_1 and T_2.
   - Both T_1 and T_2 should go to 20. If they do not, check to see if the program is 20. If the program value is not 20, set it to 20 using the up-down switch. If the program value is 20, and the temperatures are not 20, set the output switch to off, turn off the bipolar controllers, and seek assistance.
8. Place matrix material and particles in copper cell.
9. Melt matrix material.
   - Set high to a value 1 or 2 degrees higher than the melting point of the matrix material.
   - Set the up-down switch to up.
   - Check the program value. It should be equal to the high value.
   - Check T_1 and T_2. They should rise to the high value.
   - If the matrix does not melt, increase the high value by 1 or 2 degrees.
10. Set the temperature difference.
   - Set difference to a value of approximately 10-30.
   - Check T_2, and it should rise to a value equal to high plus difference.
11. Start solidification.
   - Set the set switch to <u>stop</u>.
   - Set the up-down switch to <u>down</u>.
   - Rate should be 0.099.
   - Set the set switch to <u>run</u>.

- Check the value of T_1. Once it reaches a value below the melting point of the matrix material, set the switch to stop.
- Introduce a crystal of the matrix material into the notch. Solidification should begin.
  - If the crystal melts, the temperature is above the melting point. Lower temperature by setting switch to run for a minute, then to stop and introduce another crystal.
- Once solidification begins observe through microscope. The front should initially move quickly, then slow down and stop.
- Once the front has stopped, the experiment can be started.

B. Experiment

- The velocity of the front is given by

$$V = \frac{(\text{rate } ^\circ C/\text{sec})}{(\text{diff. } ^\circ C)}(5 \times 10^4 \ \mu m)$$

- To adjust the velocity, change the rate value to the necessary value.
- Set the switch to run, down.
- If it is necessary to stop, set the switch to stop. To resume experiment, set the switch to run.
- To change the velocity, change the rate value.

During the experiment, have the selector on T_1 or T_2. Check frequently. If T_1 or T_2 start to rise, turn the output to off, and check the cooling water.

- If it is necessary to increase the temperature, set switches to run, up, and set rate value to appropriate value.
- In order to control the shape of the front, it may be necessary to heat the glass slide using the hair dryer.

Important Points

(1) Protect Bipolar Controllers.

- Only turn bipolar controllers on with the output switch off.
- Only turn the output switch on when the program value is close to T_1 and T_2.

(2) Protect Thermoelectric Devices

- The maximum temperature of these devices should be less than 100°C.
- Sum of high and diff. should be less than 100.
- Check T_1 and T_2 frequently. If the temperature rises unexpectedly, turn output to off, and check cooling water.

C. Shut-down Procedure

1. After experiment, it may be necessary to re-melt matrix material. Set diff. to 00 and switches to set, up. The program value should read a value equal to the high setting, and T_1 and T_2 should approach this value.

2. After cleaning cell of matrix material, set the switch to set, down, and T_1 and T_2 should go to 20.
3. Turn output off, then turn off bipolar controllers.
4. Set all switches and controls to initial values.
5. Turn off programmer.
6. Turn off cooling water.

Remember to protect the bipolar controllers and the thermoelectric devices. If anything goes wrong, turn output to off, and turn off bipolar controllers and ensure that cooling water is running.